Biobased Chemistry and Technology

BSc Thesis Biosytems Engineering

Modelling the production of duckweed in combination with economic possibilities

Bart van Marrewijk

7 February 2017

WAGENINGEN
UNIVERSITY & RESEARCH

Modelling the production of duckweed in combination with economic possibilities

Name course	:	BSc Thesis Biosystems Engineering
Number	:	YEI-80324
Study load	:	24 ects
Date	:	7 February 2017

Student	:	Bart van Marrewijk
Registration number	:	960414 545 090
Study programme	:	BAT
Report number	:	062BCT

Supervisor(s)	:	Dr. ir. R.J.C van Ooteghem
Examiners	:	Dr. ir. A.J.B. van Boxtel
Group	:	Biobased Chemistry and Technology (BCT)
Address	:	Bornse Weilanden 9 6708 WG Wageningen The Netherlands

Preface

In September 2016 I started my bachelor thesis. The result of this research is shown in this report. Of my close family members a lot are working in the horticulture sector. The same holds for me, although I only work during the weekends and holidays at my fathers and uncle rose nursery. Since I have a lot of interest in the greenhouse sector and wanted to combine technology. I have chosen to study in Wageningen to become a biosystem engineer. Finding a topic for my bachelor thesis was difficult, since a lot of options are possible, but I wanted to learn something new. Besides, the interest in processes that occur in a greenhouse I wanted to do some mathematics, because in the future, modelling will become more important. Without the basic knowledge about mathematics of processes, modelling will become difficult. Therefore, I chose estimating the production of duckweed with a photosynthetic model in combination with the economic possibilities. With this topic I had the opportunity to learn more about plant science, since I do not have a lot of experience with plants and might be valuable in the nearby future.

In this report, I tried to improve the photosynthetic model for estimating the production of duckweed. The result of this model is used to determine the maximum production with given harvest strategy and climate conditions. The developed model can be used for further research and elaborated were needed. I want to thank Rachel van Ooteghem for supporting my project. The feedback and discussions we had encouraged me to think about other influences that could affect the result of the model. I would also like to thank Adrie van der Werf for his opinion and expertise on cultivating duckweed. As last, I want to thank my family that always supported and gave me the opportunity to study at the university.

I hope you will enjoy reading this thesis.

Bart van Marrewijk
Wageningen, 7 February 2017

Abstract

In the Netherlands, a lot of protein rich soy is imported from South-America. This soy is mostly used for animal feed. Unfortunately, this process is not environmentally friendly, since a lot of energy is needed to transport all this soy. As a result, some companies started to cultivate protein rich duckweed as a replacement for soy. One of these companies is ECOFERM; who build a greenhouse on top of a rosé stable to grow duckweed. However, in 2016 the cultivation of duckweed stopped, since it was not economic profitable. The main reasons were firstly that the costs were too high and secondly that the duckweed did not reach the production output as expected. In previous research, a photosynthetic model was developed to predict the production at ECOFERM. Although the output of duckweed in certain months could be estimated accurately, the model did not explain the discrepancy between the yield found in literature and the low amount of duckweed harvested at ECOFERM. New companies started this summer to cultivate duckweed and the sustainable potential is promising. It is favourable to improve this model and be able to estimate the production with given inputs and determine if cultivating duckweed has economic possibilities.

The previous model used the water temperature for the photosynthetic model. As this model is based on the characteristics of a leaf, the temperature of duckweed is calculated. The result showed that the duckweed temperature is almost equal to the water temperature. On average, the duckweed temperature was lower, because evapotranspiration of water requires a lot of energy. Moreover, during the night, the temperature of a greenhouse decreases and there is no irradiation from the sun. Consequently, the temperature of duckweed is on average lower than the water temperature.

While trying to improve the photosynthetic model, the nitrogen and phosphorus consumption rates were calculated. The consumption rates were higher than the amount of N and P added by thin fraction, consequently the duckweed was cultivated in nutrient deficit conditions. Furthermore, the photosynthetic model was adapted for a changing mat density and leaf area index. The model output was sensitive to the initial mat density. Only during one month the mat density was measured, leading to a limiting amount of data to validate the model. The difference between the model and actual harvested data was 7.4% or 133 kg fresh weight (FW). The estimated parameters in this month were used to compare the model from July to September with the harvested data. By determining the initial mat density, an accurate result was obtained with only a deviation fit of 3.1%. Future research on this model can focus on finding a more accurate description of duckweed growth as a response to low CO_2 concentrations.

The optimal production was calculated with the photosynthetic model and a model of Lasfar (2007). The yield increased from 14,430 kg FW to 33,590 kg FW. This production could have been realised when more thin fraction would have been added to the water, to obtain an optimal concentration of N and P. Besides this, the optimal model had a mat density which was 4 times as high as measured. With the optimal model, a profit in one year of €416 was obtained. A similar result was obtained with a model from literature. Although the total production was almost the same, the months with an elevated photoperiod had a big difference. For rosé calves, cultivating duckweed is not economically profitable if all cost for cultivating duckweed are considered. Pigs however have less strict feed requirements and can eat more fresh duckweed. Consequently, a semi-closed loop of duckweed and pigs seems to be more promising for a sustainable and economic profitable business.

Table of contents

1 Introduction

1.1 Background

Currently there are 7,453 million people in the world ('WorldofMeters', 2016). Take a look one month later and this number is increased with 6.8 million. It is a well-known fact that the world population is increasing rapidly. Unfortunately, this is not without consequences. One of the biggest problems is global warming. There are many processes in the world that can be improved to alleviate this problem. One of these is the production of protein by animals.

Firstly, a lot of water is needed to obtain protein rich food; 1 kg beef requires 15,000 L water ('IME', 2013). Protein rich food for the livestock is mainly based on soy, however 96.3% of soy needs to be imported from outside Europe (Gelder and Herder, 2012). Furthermore, 34% of global warming is caused by livestock, of which 21% is caused by manure management (Tuomisto and Teixeira de Mattos, 2011).

Moreover, the manure is rich in nitrogen (N) and phosphorus (P). In the Netherlands, the total number of cattle increased in 2015 with 3.5%, which was partly caused by the abolition of the milk quota on April 1, 2015. As a consequence, in 2015 the maximum European phosphorus ceiling was exceeded with 7.2 million kg P ('CBS', 2016). Not all manure can be used for the land due to eutrophication. The surplus needs to be processed or transported. In the last 10 years 10% of all phosphorus could not be used on own land (Kroes et al., 2016). Given these numbers and the increasing world population, changes are needed to improve the situation.

ECOFERM is a company that uses the manure from rosé calves for the production of electricity, heat, and duckweed. This reduces transport cost and manure emissions. Moreover, soy could be partly replaced by duckweed. Unfortunately, the expenses for maintaining duckweed in a greenhouse were too high. As a result, the company had to stop the production of duckweed. However, with a protein percentage of 43% (Kroes et al., 2016) compared to soy 36% ('USDA', 2016), still a lot of things are possible. ABC Kroos is a company that wants to produce protein on large-scale in 2017, where the production is to a certain extent based on duckweed. Since growing duckweed is still expensive, models that can predict and therefore optimize the production cycle can reduce costs significantly.

1.2 Problem description

Already a few models have been made to predict the amount of harvested duckweed. In previous research, a model of the photosynthesis process has been developed (Rooijakkers, 2016). This model was based on a combination of Farquhar's (1980) photosynthetic model to calculate the CO_2 assimilation and Goudriaan's (1994) light efficiency model. This combination was made by Van Ooteghem (2007). This model had to be adapted to make it more suitable for duckweed. One of these adaptions was the light distribution on the leaves. Unfortunately, there was a minimum deviation of 9% between the model and measured values. The production of only 3 months could be accurately estimated. Some assumptions have been made to make this model. The water temperature is used for the photosynthesis model, because it has a high correlation with photosynthesis (Filbin and Hough, 1985). However, the leaf surface temperature might be different, due to irradiation. In the photosynthetic model, the dark respiration rate is assumed constant for day and night, although according to Fuhrer (1983) light can reduce the dark respiration rate.

In the models, it is assumed that carbon fixation is primarily caused by CO_2 uptake from air. However, carbon fixation by dissolved carbon components is also possible. Furthermore, at ECOFERM, low concentrations of oxygen caused inhibition of growth (Kroes et al., 2016). On the other hand high dissolved oxygen concentrations can also decrease photosynthesis (Landolt and Kandeler, 1987). However, this effect is not taken into account.

The area of duckweed is assumed homogenous, although there was a standard deviation of 50 g fresh weight (FW) m^{-2} with an average of 350 g FW m^{-2} (Kroes et al., 2016). Moreover, after harvesting, the area distribution is certainly not homogenous. Therefore, the model should be adapted for a changing LAI after harvesting. Furthermore, this model assumed that the nutrient concentrations in the pond were optimal. However, nutrient deficit conditions can decrease the growth rate (Lasfar et al., 2007). Besides this, the nutrient concentration in the pond is unknown. As a result, it is unknown if the current model is based on optimal concentrations or on nutrient deficit conditions. As last, the semi-closed loop at ECOFERM was not profitable, yet new companies started this summer. The economic possibilities are still unknown. In order to make duckweed the new protein source, it should be commercial attractive.

1.3 Aim

In the current situation, the photosynthetic model could not predict the duckweed yield year round. The objective is to improve the model in order to get a better prediction. A small economic analysis will be made to estimate the possibilities for commercial companies.

1.4 Research questions

What improvements of the photosynthetic model developed by Rooijakkers (2016) have to be made, to get an accurate estimation of the production? Secondly, what are the economic possibilities for growing duckweed in the Netherlands?

Sub questions:

- What is the temperature of duckweed compared with the water temperature?
- Which parameters are estimated correctly, and which can be improved?
- Which nutrients have a high influence on duckweed growth?
- What is the influence of harvesting on the distribution of duckweed in the pond and the LAI?
- What is the accuracy of the model simulated with inputs from literature?
- What are the economic possibilities for cultivating duckweed in the Netherlands?

1.5 Approach

- Improve parameters of photosynthetic model and add variables if necessary
- Investigate the influence of the CO_2 and O_2 concentration in water
- Use a dynamic area in the model
- Economic analysis of possibilities in the Netherlands

From previous research (Rooijakkers, 2016) parameters of the model were estimated. A literature study will be done, to determine if these parameters are theoretically possible. Moreover, in the model the influences of the nutrients are not taken into account. The available nutrient models will be included in the model. The influence of the surface temperature and area after harvesting will be taken into account, namely in previous research it was assumed that the water temperature was equal to the temperature of duckweed. However, at high irradiance the leaf surface temperature will probably be much higher. The effect of this temperature will be investigated.

The nitrogen and phosphorus uptake will be determined. Then the nutrient concentration in the pond can be calculated, if the conditions are not optimal for plant growth then the photosynthetic model will be adapted. The uptake rates will be combined with the optimal growth rate to establish the optimal nutrient concentration for duckweed. The results will be compared with the optimal situation. With calculating the nutrient consumption, the total amount of thin fraction needed can be calculated. From the total production and the amount of thin fraction added, the profit or loss will be determined and compared with the optimal situation.

A comparison between crop algae or duckweed will not be made. Moreover, depreciation and labour costs will not be taken into account for the economic analysis. Only a comparison will be made between the electricity costs and profits for cultivating duckweed.

2 Literature

2.1 Dissolved components

2.1.1 Uptake of dissolved carbon dioxide

In the photosynthetic model, no effects of dissolved components are taken into account. However, it might be possible that that these components can affect the growth rate. Dissolved substances are taken up by the roots in almost all plants. Duckweed species can also use the lower epidermis below the fronds. With a Hutner solution, the uptake from the medium was determined (Landolt and Kandeler, 1987). This solution does not contain carbonate; an exact composition is given in appendix 10.2. Sucrose was added during the experiment; otherwise the duckweed would not have survived. The conclusion was that uptake of carbon is mainly via gaseous exchange (Landolt and Kandeler, 1987). Carbon uptake in water partly depends on the pH. A pH larger than 6.5 results in the conversion of carbon dioxide to bicarbonate. Experiments with different pH values showed that at a pH of 8, 86% of all carbon uptake is from aqueous inorganic carbon. In contrary with a pH of 6.8 and a carbonate free medium, uptake was reduced to 37% (Filbin and Hough, 1985). This conclusion is surprising, because according to Eshel (1986) no direct effect of pH was detected. For *Spirodela polyrhiza*, 1% of all carbon used for assimilation is derived from water at a pH of 5.9 (Eshel and Beer, 1986). This is in agreement with another research, namely aqueous carbon sources are barely utilized by the fronds (Bowker and Denny, 1980). At higher pH values, more bicarbonate is available. Photosynthesis was inhibited, because uptake of bicarbonate costs more energy than CO_2 uptake (Shelp and Canvin, 1980). Therefore, lower pH ranges are preferred. Moreover, the CO_2 concentration in the air influences the total aqueous carbon uptake. In Table 1, the assimilation of carbon from air and liquid is given. As mentioned by Filbin the data shows increased carbon assimilation from aqueous medium at increasing pH levels.

Table 1. Assimilation rate of carbon from gas and liquid phase at different pH values (Eshel and Beer, 1986).

pH	Dissolved C_i (mM)	Assimilation rate nmol C g FW min^{-1} from gas phase	Assimilation rate nmol C g FW min^{-1} from liquid phase
4.9	0.01	478.8±72.6	Not measured
5.9	0.03	494.9±27.8	5.6±0.99
7.2	0.15	600.1±115.3	22.7±3.94
8.0	0.96	518.2±62.7	24.8±0.89
8.1 Light	1.10	733.5±164	53.5±10.60
8.1 Dark	1.10	4.7±0.27	2.7±1.01

Although the table shows a small increase in carbon uptake from the water with increasing pH values, the maximum aqueous carbon uptake was 5%. The difference between the results is caused by the concentrations of carbon. The maximum concentration inorganic (C_i) of Eshel was 1.1 mM, Filbin used a Hutners' solution with addition of 1.0 g/L glucose, which is 2.2 mM C. Besides, the experiments are done in different growth conditions. As a result, different pH levels in both experiments can cause different assimilation rates. Because most experiments above showed little aqueous carbon uptake, the effect on the photosynthetic model is therefore not significant.

2.1.2 *Uptake of carbohydrates*

Besides the uptake of inorganic carbons, dissolved carbohydrates have carbon atoms, which can be taken up by duckweed. Unfortunately, not all carbohydrates are suitable for carbon uptake. In appendix 10.1, a list is given for substances with all carbon sources that cannot be used by *Lemnaceae* species. At low light intensities the plant uses sucrose as energy source, especially for hexoses (Landolt and Kandeler, 1987). Sucrose concentrations between 0.5 – 2.5% gives optimal growth at 18.5 µmol m^{-2} s^{-1}. However, at saturated light intensities sucrose inhibits growth. Additionally, at low pH values aqueous carbon uptake is mainly through sugars. In short, carbon uptake from carbohydrates does not seems to be important, as already at low concentrations sucrose starts to inhibit growth. Therefore, the influence of carbohydrates is not simulated in the model.

2.1.3 Dissolved oxygen

In the report of ECOFERM the duckweed did not survive at low oxygen concentrations (Kroes et al., 2016). A blower was applied to increase the O_2 concentration, however this blower increased the O_2 concentration to 85 mg L^{-1}. Filbin and Hough (1985) discovered that dissolved oxygen and photosynthesis have a high correlation of r=0.88. For photorespiration the correlation was even higher namely 0.98. This is not surprising, namely higher O_2 concentrations result in more oxidation and less carboxylation of rubisco. In paragraph 2.3, more information is given about these processes. More important than the correlation factor is the inhibition of photosynthesis by oxygen. In table 2, the influence of the oxygen concentration on the photosynthesis rate is given. At concentrations higher than 21 mg L^{-1} oxygen, net photosynthesis was inhibited by 38%. Even higher concentrations caused an increase of the light and dark respiration, namely the respiration almost doubled (table 3). Another experiment showed that 20 days old *Lemna minor* had more organic C loss at an increased oxygen concentration. However, this increase was only measured in lighted environment, at low light intensities no difference was found (Filbin and Hough, 1985). Although the oxygen concentration has effect on the photorespiration, still CO_2 loss in light was never bigger than 4% of the total photosynthesis (Filbin and Hough, 1985). Thus, experimental enhancement of photorespiration with oxygen was never as great as the inhibition of photosynthesis. Unfortunately, no models have been made that describe the net photosynthetic rate as a function of the dissolved oxygen concentration. However, from table 2 concentrations higher than 8 ppm O_2 should be prevented. In other words, the O_2 concentration at ECOFERM are limiting the net photosynthesis rate.

Table 2. Influence of dissolved oxygen concentration for *Lemna minor* on photosynthetic rate (Filbin and Hough, 1985).

Dissolved oxygen $mg\ L^{-1}$	Net photosynthesis rate $mg\ g^{-1}h^{-1}$
0.6	2.20±0.22
8.48	2.01±0.14
21.20	0.77±0.49

Table 3. Respiration of *Lemna minor* at different oxygen concentrations (Filbin and Hough, 1985).

Dissolved oxygen $mg\ L^{-1}$	Light respiration (% total C)	Dark respiration (% total C)	L:D ratio
7.4	1.7	3.2	0.5
28.5	6.1	5.4	1.1

2.1.4 Influence CO_2 concentration on growth rate

The CO_2 concentration at ECOFERM ranged between 1000 and 2100 ppm (Rooijakkers, 2016). CO_2 concentrations between 300 to 1000 ppm and a constant light intensity did not affect growth rate for *Lemna minor* (Loats et al., 1981). From an another research at increased CO_2 concentrations, there is an increase of organic matter at light intensities between 800 and 1200 µmol m^{-2} s^{-1}, but the growth rate was unaffected at 350 ppm and 1500 ppm CO_2 (Björndahl and Nilsen, 1985). The table below gives a summary of the growth rates with given CO_2 concentrations. Obviously, the growth does not differ much for duckweed species.

Table 4. Relative growth rate at 2% oxygen for *Lemna gibba* with different CO_2 concentrations (Andersen et al., 1985).

µL CO2 L^{-1}	RGR mg g^{-1} d^{-1} days 0-4	RGR mg g^{-1} d^{-1} days 4-6
350	235±31	265±109
750	323±4	271±23
1500	331±14	288±39

2.2 Nitrogen and phosphorus kinetics

In the previous photosynthetic model, it was assumed that the nutrients were optimal throughout the year. In the paragraphs below the kinetics of nitrogen and phosphorus are given to gain insight into the N and P consumption rates. There are four processes in a duckweed pond that cause a reduction of nitrogen and phosphorus concentration, namely:

1. Ammonia volatilization
2. Denitrification
3. Uptake by duckweed
4. Sedimentation

Especially sedimentation, denitrification and uptake by duckweed were most significant in nitrogen reduction. Duckweed was responsible for the consumption of 10 to 27% of all available nitrogen (Zimmo et al., 2004).

2.2.1 Nitrogen uptake kinetics

The main sources of nitrogen are nitrate and ammonium. The uptake capacity of ammonium is 3-11 times higher than nitrate uptake (Cedergreen and Madsen, 2002). This difference is caused by the lower minimum concentration for uptake of NH_4^+ and pH dependency. Moreover, nitrate reductase is inhibited by ammonium (Xu and Shen, 2011), further ammonium assimilation causes a high strain on the plasma membrane proton pump. Consequently, for proton-NO_3^- cotransport is reduced (Ingemarsson et al., 1984). Increased nitrogen concentrations resulted in an elevated N consumption, however this increase was not always caused by duckweed, but also by the other processes mentioned before (Zimmo et al., 2004).

From literature, a lot of different nitrogen uptake rates can be found. Zhang (2014) developed a model for the ammonium uptake rate as a function of the concentration, this model can be found in appendix 10.1. A consumption rate of 446 mg N m^{-2} d^{-1} was obtained at a mat density of 350 g FW m^{-2} and a N concentration of 12 mg N L^{-1}. In this experiment, the medium was refreshed each 3 days to minimize the effect of algae and the 4 processes mentioned before. In the figure below the N consumption by duckweed as a function of nitrogen concentration and mat density. If the mat density became larger than 600 g FW m^{-2} then the model overestimates the N consumption rate, because already at normal nitrogen concentrations the consumption rate is more than 665 mg N m^{-2} d^{-1}.

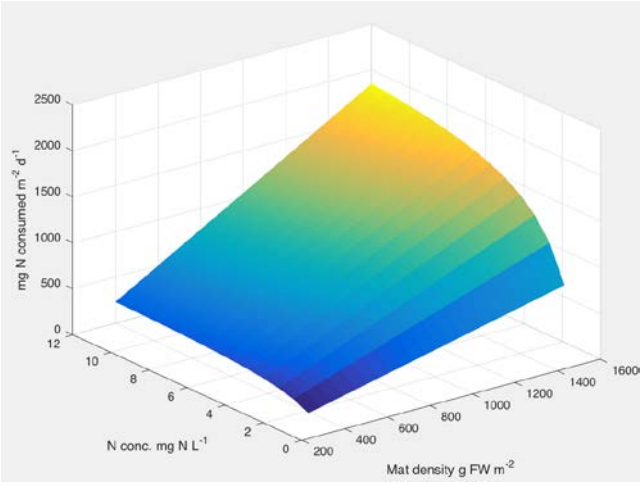

Figure 1. Nitrogen consumption as a function of the concentration and mat density (Zhang, 2014).

Zimmo (2004) found a maximum nitrogen uptake by duckweed of 547±136 mg N m^{-2} d^{-1}. However, this was solely 42% of the total N consumption. According to another research the N uptake depends on the nitrogen concentration, chemical oxygen demand (COD), mat density and hydraulic retention time (Krishna and Polprasert, 2008). N-consumption by duckweed was estimated at 72% at an uptake rate of 620 mg N m^{-2} d^{-1}. According to Landolt (1987)

concentrations higher than 8.4 mg N L^{-1} did not increase N content of fronds, increased concentrations would result in more N loss through other processes (Figure 2).

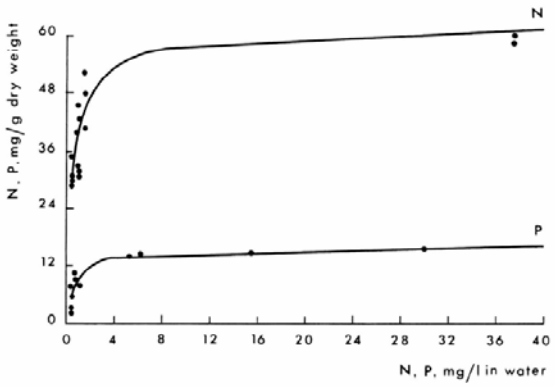

Figure 2. N and P content as function of the nutrient concentration (Landolt and Kandeler, 1987).

Furthermore, another research found a maximum uptake rate of 100 and 480 mg N m^{-2} d^{-1} (Al-Nozaily et al., 2000). The different values of all researchers mentioned are probably caused by different climate conditions. Additionally, the processes described by Zimmo are situation dependent and therefore influence the maximum N uptake by duckweed. Furthermore, N-loss through washing can cause differences of 9% (Al-Nozaily et al., 2000). Due to the fact that the total N consumption by duckweed found by Krishna was 72% and the result of Zimmo was 42%, it seems that the total N consumption is system dependent. Therefore, only N reduction by duckweed is taken into account. Besides, the differences are caused by the fact that the consumption rates depends on the previous N concentrations (Cedergreen and Madsen, 2002). Concentrations higher than 10 mg N L^{-1} did not increase the uptake anymore (Zhang et al., 2014). The intrinsic growth is constant for 7 to 30 mg N L^{-1} (Lasfar et al., 2007), however other research concluded that 1 to 5 mg N L^{-1} results in a constant growth rate (Zhang et al., 2014). To optimize the N consumption, the concentration should be higher than 9 mg N L^{-1}, otherwise growth and also consumption rates are not optimal (Lasfar et al., 2007; Landolt and Kandeler, 1987). After the N consumption is determined, the amount of thin fraction required to obtain optimal concentrations can be calculated.

2.2.2 Influence of depth

In research of Zimmo (2004) it was mentioned that the depth of a pool might have influence on the total N consumption. A higher consumption of N and P was measured at increased depth (Xu and Shen, 2011). Moreover, at increasing depths the production and protein content also increased. However during this research the conditions were not *ceteris paribus*, because no extra N or P were added during measurements. Consequently, at low depth less N and P was available after 20 days. The area of the pool is more important than the reactor depth. Despite this the P consumption was elevated at increasing reactor depth (Al-Nozaily et al., 2000). Unfortunately, no models are available that describe the influence of the depth.

2.2.3 Phosphorus uptake kinetics

Lemna minor accumulates a lot of phosphorus compared to other vascular plants; only some algae have a higher accumulation (Landolt and Kandeler, 1987). Phosphorus is mostly taken up as phosphate (PO_3^{4-}). Compared to nitrogen, much lower values are needed for optimal growth (Lasfar et al., 2007). Analysis showed that 0.03 to 2.8% of dry matter is phosphorus, in contrary the nitrogen content is between 0.8 and 7.8% (Landolt and Kandeler, 1987). Phosphorus in manure mainly exists in the form of diphosphorus pentoxide (P_2O_5). An exothermic reaction with H_2O converts diphosphorus pentoxide to phosphate**.** The uptake mechanism is $H^+/H_2PO_4^-$ cotransport, in which phosphate-induced membrane depolarization is linked to phosphate uptake. In Figure 3 the electrical membrane potential of *Lemna gibba* is given at different pH levels. From this figure it can been seen that at extremely low or high pH levels depolarisation is reduced. As a result there is less phosphate uptake and growth is inhibited (Ullrich-Eberius et al., 1984).

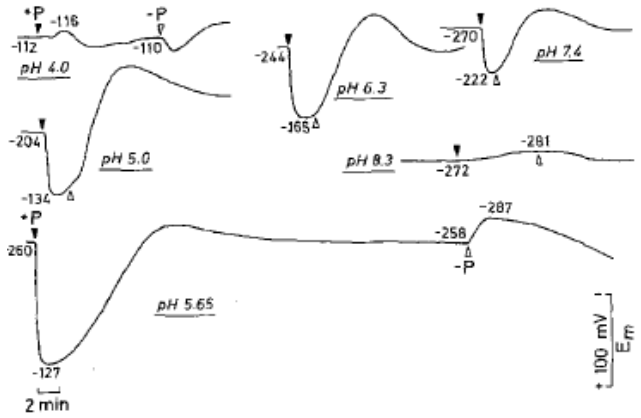

Figure 3. Membrane potential at different pH levels for *Lemna gibba* (Ullrich-Eberius et al., 1984).

Optimal growth occurs when the phosphorus concentration is between 4 and 22 mg P L^{-1} (Lasfar et al., 2007). *Lemna* minor has a phosphorus uptake of 200 mg m^{-2} d^{-1} (Cheng et al., 2002). However from another research an uptake rate between 13 to 58 mg P m^{-2} d^{-1} was found, which depends on the nitrogen concentration and the depth of the pond (Al-Nozaily et al., 2000). The nitrogen concentration influences the phosphorus uptake, namely at concentrations higher than 34 mg N L^{-1} phosphorus uptake was inhibited; at 20 mg N L^{-1} optimal phosphorus uptake was detected.

At 5 mg P L^{-1} the phosphorus content in the fronds did not increase anymore with increasing phosphorus concentrations (Landolt and Kandeler, 1987). Therefore, it seems that the optimal concentration of phosphorus is between 5 and 22 mg P L^{-1}. Unfortunately, no kinetic Michaelis-Menten equations are available for phosphorus uptake. In an experiment of Frédéric (2006), the phosphorus consumption rates as a function of P content in the fronds were calculated. The consumption rates were ±125 mg P m^{-2} d^{-1}; these are high compared to the result of Al-Nozaily. However, this result was obtained at a relatively high mat density of 783.3 g FW m^{-2}. From the values above, clearly a lot of different values are found in literature for N and P consumption rate. Consequently, it is better to use the P content of duckweed for determining the consumption rates, because this represents the minimum amount of P taken up by the duckweed.

2.2.4 Nitrogen from the air

During the production season, thin fraction was added to increase the N concentration. The total amount of N added in one year was 4.88 kg. Given the N uptake kinetics mentioned earlier and considering a normal nitrogen content of 3.9% nitrogen per kg DM; with a yearly production of 865 kg DM, it seems that there are other mechanisms that cause an increase in the nitrogen concentration. The air of the stable is transported to the greenhouse; a small fraction of the ammonia in this air is removed by the bio bed. The remaining part can dissolve in water, because an ammonia molecule has three polar bonds. These bonds create a dipole molecule, and because water is also a dipole molecule, ammonia can dissolve. After dissolution in water the following equilibrium reaction can takes place:

$$NH_3 + H_2O \leftrightarrow NH_4^+ + OH^{-1}$$

Undoubtedly, ammonium is not only used by duckweed, but also by other physicochemical or biological processes. The biological processes are nitrification and ammonification plant uptake. Physicochemical are sedimentation, ammonia stripping and ion exchange (Lee et al., 2009). Sedimentation with NH_4^+ is unlikely, because all salt reactions of ammonium are soluble in water. To determine the amount of dissolved gas, the law of Henry's is used. The concentration of dissolved gas is proportional to its partial pressure in the gas phase.

$$K_H = \frac{c_a}{p_g} \qquad [M\ atm^{-1}] \qquad 2.1$$

K_H is temperature dependent (Sander, 1999) and can be calculated using $\ln(K_H) = \frac{4092}{T_g} - 9.70$ (Dasgupta and Dong, 1986). This variable is constant for infinite time, provided that the temperature is constant. As a result, volatilization and dissolution rates are in equilibrium. The lowest non-limiting N concentration is 7 mg N L^{-1} (Lasfar et al., 2007), which is approximately 8.52 mg NH_3 L^{-1}. If no manure is added than at equilibrium between air and water exchange this would require an air NH_3 concentration of 9 ppm. The average ammonia emission of calves is ±522 mg h^{-1}, which causes a maximum concentration of 8 ppm NH_3. Concentrations higher than 25 ppm are harmful and can cause health problems (Koerkamp et al., 1998). It is unlikely that in combination with the bio bed the concentration is more than 8 ppm. At optimal concentrations the ammonia content in the air is lower than the N concentration in the water. As a consequence, the ratio of volatilization and dissolution is not in equilibrium, which results in a transport of ammonia from the water to the air.

If there is no nitrogen in the water and the concentration in the air is 6 ppm NH_3, then according to Henry's law, at 25°C the concentration in water will increase to 4.7 mg N L^{-1}. At this concentration growth is limited. In ECOFERM pond, the surface is almost fully covered with duckweed, which reduced the dilution rate. Besides this, it is unlikely that the NH_3 concentration will be larger than 6 ppm due to the fact there is a bio bed. In other words, the concentration in the air is too low for optimal growth. However, the ammonia in the air can increase the concentration. Therefore, nitrogen from the air cannot be neglected in the model.

2.2.5 Influence nutrients on parameters photosynthetic model

As mentioned in the uptake kinetics of N and P, low nutrient concentrations can inhibit growth. Unfortunately, a model that describes the influence of nutrients on the parameters of the photosynthetic model has not been made so far. Probably because measuring the photosynthetic parameters, for example the maximum carboxylation rate ($V_{c\ max}$) and the maximum electron transport rate (J_{max}), is difficult and time consuming (Walcroft et al., 1997). Nitrogen and phosphorus have a strong influence on photosynthetic parameters. High nutrient concentration caused an increase of at least 35% for $V_{c\ max}$, J_{max} and T_p. A decreasing concentration caused an increase in stomatal resistance (Bown et al., 2007). Walcroft (1997) found similar results, where the N-content of leaves have a linear relationship with $V_{c\ max}$ and J_{max}. At increasing N concentrations, $V_{c\ max}$ and J_{max} increased (Walcroft et al., 1997). Besides, the activation energy for the electron transport rate and carboxylation are also N concentration dependent. Both researchers shared this result for *Pinus radiate*.

According to other research the internal conductance is N concentration dependent. Both $V_{c\ max}$ and J_{max} increased with increasing nutrient supply from 0.5 mM to 4.0 mM N. Unfortunately, this was not for measured *Lemnaceae* species but *Eucalyptus globulus* seedlings (Warren, 2004). Obviously, at low N & P concentrations the parameters have a different value. Despite this fact, there are no models available that describe the influence of the N and P content on the parameters. The photosynthetic model is based on optimal nutrient concentrations, with the growth rate as function of the N and P concentration it is possible to multiply the output of model with a correction factor.

2.2.6 Electric conductivity

The electric conductivity (EC) indicates the conductance of a liquid. This conductance represents the amount of nutrients or salinity. Distilled water is almost an insulator and water with a high salinity conduct electricity more easily. At ECOFERM the thin fraction digestate has a EC of 46 mS cm^{-1} (Kroes et al., 2016), which means that the thin fraction should be diluted to make it suitable as fertilizer. Optimal growth is observed at an EC of 1.2 mS cm^{-1}, with a tolerable range between 0.6 and 1.4 mS cm^{-1} (Wendeou et al., 2013). Throughout the year the EC was on average 1.27, consequently no correction for the EC is needed.

2.3 Rubisco

Ribulose-1,5-biphosphate carboxylase/oxygenase (rubisco) is one of the main enzymes of plants; without this enzyme photosynthesis is impossible. The photosynthetic model is developed by the characteristics of rubisco, especially the carboxylation and regeneration of ribulose-1,5-biphosphate (RuBP). Rubisco catalyses the addition of gaseous carbon dioxide to RuBP. Rubisco is active in the Calvin cycle; in this cycle rubisco is carboxylated. The ATP and NADPH used in these reactions are mainly provided by the light reactions. One molecule CO_2 generates two molecules of 3-phoshoglycerate (3-PGA) (Wostrikoff and Stern, 2009). The PGA is in 3 main reactions converted to triose phosphate. The triose phosphate is partly converted to other sugars and used for plant growth. This part is relatively small and it is transported to the cytosol. To generate 1 free triose phosphate, 3 carbon molecules are needed. The 5 other produced triose phosphates remain in the chloroplasts and are used to regenerate rubisco (Heldt and Piechulla, 2011a). It is possible that rubisco reacts with oxygen, this unavoidable reaction produces 3-PGA and 2-PGA. This process is called photorespiration.

2.3.1 Rubisco limitations

The photosynthetic rate is limited by 2 main processes: RuBP carboxylation or RuBP regeneration. However, RuBP regeneration could also be limited by triose-phosphate utilization (TPU) (Farquhar, 2001). This limitation is not included and becomes limiting for high CO_2 concentrations and high light intensities (Sage, 1990). As a result, higher photosynthetic rates can arise then presumed. It depends on the environmental conditions, which process limits photosynthesis. The predominant limitation causes the non-limiting processes to be regulated downward. The synthesis rate of sucrose is also adapted, which results in less generation of biomass. At low CO_2 concentrations carboxylation of RuBP limits photosynthesis, at high CO_2 RuBP is not saturated and the photosynthesis is inhibited through RuBP regeneration (Hikosaka et al., 2006). This specie specific limitation depends on temperature, CO_2 concentration and nutrient status. Nutrient status was one of the main causes for the inaccuracy of the previous model.

2.3.2 Triose phosphate use

In the Calvin cycle carbon needs to be exported. However, at high CO_2 concentrations the carboxylation of rubisco produces too much carbon, and the export of these carbons is too slow compared to the production. In other words the rate for making starch and sucrose from triose phosphates is slower than rubisco carboxylation and regeneration (Yang et al., 2016). As a result, the photosynthesis is inhibited by TPU. In contrary to the conclusion of Sage (1990), TPU inhibition is also possible at normal CO_2 concentrations (Hikosaka et al., 2006). This was confirmed by Yang (2016), namely TPU limitation was found at sensitive CO_2 concentrations. Due to the fact that TPU can inhibit the photosynthesis, the CO_2 assimilation rate should be adapted at TPU limiting conditions.

2.4 Dark respiration

There are two respiration mechanism in plants: dark respiration and photorespiration. Both use their own substrate and have different processes (Mangat et al., 1974). It is important to distinguish these processes, because dark respiration is partly positive, in contrary to photorespiration. Dark respiration generates energy, which can be used for making 3-PGA.

Dark respiration is an important parameter in the model, since the net assimilation rate is determined by subtracting the dark respiration from the gross assimilation (van Ooteghem, 2007). Dark respiration can therefore influence the photosynthetic model a lot. It is also referred to as mitochondrial respiration (R_d) and works continuously (Sharkey et al., 2007). During illumination R_d is between 25 to 100% of respiratory activity in darkness (Wang et al., 2001). Oxidation of carbon compounds is performed by the tricarboxylic acid (TCA) cycle and takes place in the stroma. This cycle releases CO_2 and provides redox equivalents. This reducing agent creates a proton gradient across the inner mitochondrial membrane, which results in synthase of ATP. This process is also called oxidative phosphorylation (Kromer, 1995). Generally plants have a lower dark respiration at increased light intensities (Mangat et al., 1974). Moreover, at elevated CO_2 concentrations the dark respiration is higher, due to the fact that more biomass is created at

increased concentrations. Consequently more energy is needed, which is partly derived from respiration (Wang et al., 2001). Besides influence of CO_2, Filbin and Hough (1985) found higher dark respiration rates for increasing dissolved oxygen concentration. In fact the dark respiration is also controlled by ATP (Mangat et al., 1974). Figure 4 shows the decrease of dark respiration of *Lemna minor* for increasing light intensities (Fuhrer, 1983). In the current model the dark respiration was assumed constant, however according to the figure this seems to be questionable. Therefore, in the new model the dark respiration will not be assumed constant.

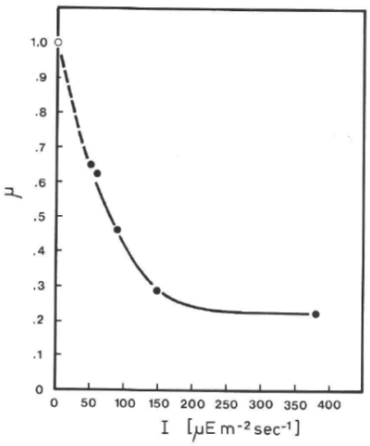

Figure 4. Fraction of dark respiration inhibited by light (Fuhrer, 1983).

2.5 Mat density

A lot of research has been done to determine the optimal biotic and abiotic factors. The optimal ranges of nutrients, temperature, CO_2 and light intensities all have been researched. These processes determine the intrinsic growth rate (r_i), with the intrinsic growth rate it is possible to calculate the mat density as a function of time. This can be used to determine the optimal mat density at given climate conditions. Increased mat density results in less light available for each frond. An advantage is that there is less transmission of light in the water, consequently there is less growth of bacteria and algae (Xu and Shen, 2011). Körner (1998) assumed that the mat density could inhibit duckweed growth. In his experiments the coverage of the reactor was 90% at a mat density of 558 g FW m^{-2}. In another research the percentage of the water covered with duckweed is linear up to 250 g FW m^{-2}. Extrapolating resulted in 457 g FW m^{-2} at a fully covered pond (Jupsin et al., 2005). The amount of g FW duckweed at a fully covered surface is important for determining the leaf area index (LAI), because then the fraction m^2 [leaf] m^{-2} [soil] can be calculated.

A model was made that determined the mat density at given initial mat density and intrinsic growth rate (Frédéric et al., 2006). The maximum non limiting mat density was reached at ±176 g DM m^{-2} (Driever et al., 2005). Higher mat densities resulted in a negative growth rate. In Figure 5A the increase in dry matter is given for different harvesting strategies as a function of the initial mat density. Harvesting less duckweed at shorter intervals favoured nutrient consumption and total biomass production (Xu and Shen, 2011). The output of the model in Figure 5B shows indeed higher biomass production at increased harvest frequency. In other words, the formula of Frédéric confirms Xu's conclusion. In the previous model the effect of the mat density and LAI was not taken into account. The assumption was made that the pond was always fully covered with duckweed, even after harvesting. Further, the mat density did not have any influence on the growth rate. However, Figure 5 shows obviously that high mat densities can inhibit growth, low densities are also not favourable to obtain a maximum production. In the ECOFERM pond, the average mat density was ±350 g FW m^{-2} on Augustus 24, 2015 (Kroes et al., 2016). According to the harvest strategy the surface must always be fully covered with duckweed, but pile up of duckweed should be prevented. However, at 350 g FW m^{-2} there is no pile up; besides the LAI is not even 1. Moreover, Figure 5B indicates that the increase in dry weight is 13.3 g DM m^{-2} at an

optimal mat density of 82 g DM m^{-2} (Frédéric et al., 2006), however with 350 g FW m^{-2} or 24.5 g DM m^{-2}, solely a maximum production of 7.0 g DM m^{-2} is possible. Therefore, in the new model it might be a good idea to make the LAI dynamic.

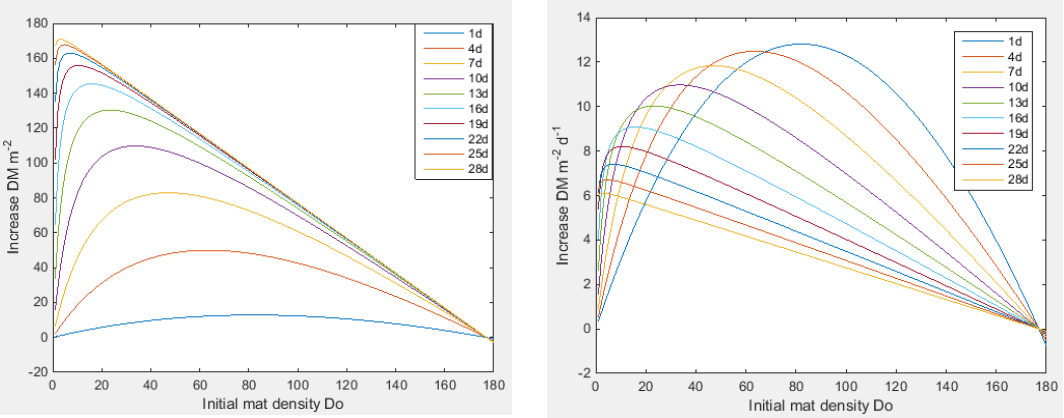

Figure 5A & B. Left the increase in mat density at given initial mat density and harvesting strategy. Right the increase in mat density per day.

2.6 Temperature

Previous photosynthetic model could not predict the months July and Augustus accurately (Rooijakkers, 2016). These months had a relatively high light intensities and temperatures compared to April and October. The model was based on the water temperature, in which the optimal temperature was set to 26°C. The figures below give the growth rate as function of the temperature. Figure 6 shows an optimal range between 25 and 27°C (Lasfar et al., 2007).

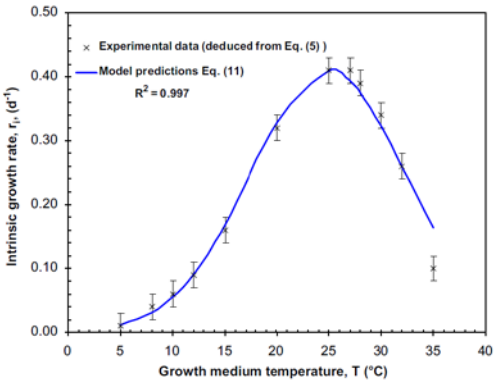

Figure 6. Intrinsic growth rate as a function of the water temperature (Lasfar et al., 2007).

However, from the figures below, a higher temperature seems to be possible before limiting the growth rate.

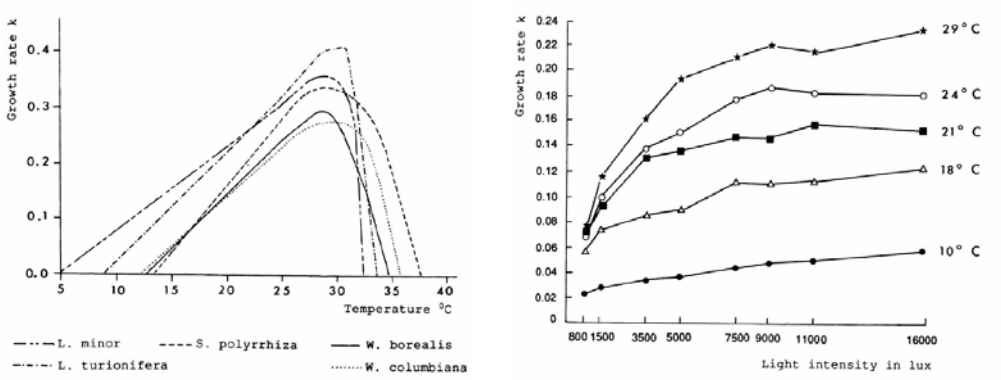

Figure 7. Different graphs for water temperature dependency of Lemnaceae. Left (Docauer, 1983) and right (Ashby and Oxley, 1935).

Moreover, the photosynthetic model is in fact based on the plant temperature. The temperature of duckweed has been compared with the air temperature. At 1.5 cm above the surface a temperature difference of ±2.5 degrees was measured (Dale and Gillespie, 1976). The difference between water and surface temperature is smaller, although at 2 cm below the fronds already temperature differences were detected. The effect of mat thickness was not considered, because the net radiation had more influence between successive days (Dale and Gillespie, 1976). From other research the frond temperature is on average 1 to 3°C higher during irradiation than the water temperature (Landolt and Kandeler, 1987). Another research showed at 92.5 µmol m^{-2} s^{-1} the water temperature was 2.7°C lower than the upper frond temperature (Casperson, 1956). At ECOFERM measurements were taken between the roots, where the average lengths of the roots are 3 to 6 cm (Landolt and Kandeler). According to these facts, it might be better to calculate the temperature of the duckweed to prevent modelling errors.

2.6.1 Evapotranspiration

The fronds of the duckweed can evaporate water; as a result, energy is removed from the plant. Consequently, the plant temperature decreases. The evapotranspiration is not plant density dependent, since the amount of fronds exposed to the atmosphere remains constant (DeBusk et al., 1983). For most plant species the opening of the stomata depends on seasonal conditions, in contrary *Lemna minor* has a fixed canopy, in other words the opening of the stomata is climate independent. Consequently, the evapotranspiration only depends on meteorological and physiological factors. There are a lot of models available for calculating the evapotranspiration rate (Ilahi, 2009). These models were compared for plants in a greenhouse. The FAO Penman model (FPE) had relatively good estimations and it is recommended for plastic greenhouses (Ilahi, 2009). This model used the canopy cover coefficient method (CCC); to determine the actual evapotranspiration the result must be multiplied with a crop coefficient (K_c). The determination of the K_c value depends on biological and environmental conditions. Therefore, K_c is location dependent and consequently not an good option to determine the evapotranspiration.

For uniform wetland surfaces, the Penman equation (PE) can work well (Drexler et al., 2004). However, the Penman-Monteith (PM) model is probably better, because for *Lemna minor* the PM model has an inaccuracy of 5 to 10% (Al Nozaily, 2000). Although different models are available, only the inaccuracy of the PM model for duckweed is known. Therefore, this model seems to be the best choice for determining the vaporization by duckweed.

2.7 Feed requirements rosé calves

For an economic analysis it is useful to implement the effect of the nutrient composition for rosé calves, because with adding duckweed the feed composition changes. For optimal health and growth the following nutrient variables are important for rosé calves; VEVI, DVE, OEB, DVLYS, DVMET, NDF, P and starch (CVB, 2012) (Kroes et al., 2016). In Table 5 more information about

these variables is given. Obviously, not only the protein percentage is important, but also the composition of these proteins.

Table 5. Summary of important parameters for cattle feed composition.

Parameters	Description
VEVI	Net available energy
DVE	Indicates the amount of proteins that is digestible
OEB	Indicator of the availability of protein and energy in the rumen. These should be in balance, OEB>0 more protein available than energy. OEB<0 too little protein available.
DVLYS	Digestible amount of lysine
DVMET	Digestible amount of methionine
NDF	Neutral Detergent Fibre, represents the quantities of fibre parts. Gives also information about the ratio of cell wall and cell content
P	Phosphorus
Starch	-

Each raw material has a different nutrient composition, therefore for the replacement of soy by duckweed this different composition must be taken into account. In Table 6 the compositions of duckweed and soy are given. The replacement of soy without any adaptions to the total feed composition will probably result in less growth and increased global warming, because in the stomach and intestines of the cattle fermentation takes place. Further the CH_4 emission is strongly related to the amount of feed fermented in the rumen, which depends on feed intake and composition (Hatew, 2015). In the report of ECOFERM already a few calculations were done, and the cattle feed was mixed to satisfy the feed requirements (Kroes et al., 2016). In this model it was assumed that rosé calves eat 6 kg dry matter a day. For minimalizing the cost this might cause problems, because fresh duckweed has a low dry matter content. Duckweed was given fresh to the calves, however according to research it is better to dry or ferment the duckweed (Hoving et al., 2012). Squeezing it is also possible, but this causes losses of valuable nutrients and the dry weight content increases only slightly. According to Hoving (2012) drying did not have any effect on the aroma. Experiments with cows and a duckweed+corn diet of ratio 2:1 had a higher growth rate than a control group with corn, crude protein concentrate and access to grass pasture. At this diet some cows had bloat symptoms, because a large amount of fresh plant was ingested (Rusoff et al., 1980). The percentage of fresh duckweed in total feed composition was relatively low, as a result no problems occurred at ECOFERM. However, for larger quantities problems might arise. These minimum requirements are given in Table 14.

Table 6. Comparison of nutrient characteristics of soy and duckweed. The last row shows the requirements for rosé calves.

	DM %	VEVI units / kg DM	DVE	OEB	DVLYS	DVMET	NDF	P	Starch
Duckweed	5.2	871	140	236	7.8	1.3	231	10.4	15
Soy 60 RC	88.0	1242	267	213	17.4	4.4	145	7.3	10
Minimum requirements rosé calves	>24.8	1030	79.1	0	5.5	2.1	265	265	4.5

2.8 Literature comparison estimated parameters

In previous research the maximum electron transport ($J_{max\ 26}$), stomatal resistance (R_s), CO_2 compensation points (Γ), degree of curvature (θ) and the cuticular resistance (R_{cut}) were estimated, because these parameters had a relatively high sensitivity (Rooijakkers, 2016). The parameters were determined with the lowest sum of squared error mechanism. Some initial parameters values were from different plants, consequently it is questionable if these parameters are correct for duckweed. In the following paragraphs the value from previous research of these parameters is compared with literature.

2.8.1 Maximum electron transport rate

The electron transport rate is related to the assimilation rate or in other words photosynthesis. The basis process of photosynthesis is well known; light, water and carbon dioxide produces sugars and oxygen. Two processes during photosynthesis are the light and dark reaction. Light reaction takes place in the thylakoids. In these thylakoids pigments work together in pigment-protein complexes (LHCs). The most common pigments are chlorophyll a (Chl a) and b (Chl b*)*. These chlorophyll pigments absorb the complete light spectrum except 500 to 550 nm.

Sometimes the energy of the light exceeds the maximum energy use by photosynthesis. Under these circumstances, regulation of light harvesting is necessary to balance the absorption and utilization of light energy (Müller et al., 2001). The energy of excited Chl pigments, can be used for 3 processes.

1. Fluorescence
2. Photochemical quenching (qP)
3. Non-photochemical quenching (NPQ)

In some plants, the excess of energy can also be used for production of $^1O_2$. Chl fluorescence mainly originates from PS(II). In this process, light is re-emitted by chlorophyll from excited to non-excited chlorophyll. At energy, surplus excited Chl can also be converted to its ground state by NPQ. In this process de-excitation takes place by emission of heat, this process affects the Chl fluorescence. In Figure 8 all processes that cause the de-excitation of Chl pigments are given.

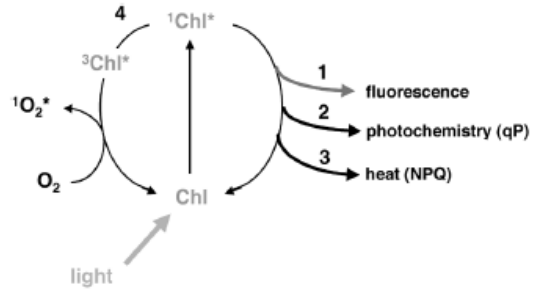

Figure 8. All processes of activation and deactivation of Chl pigments (Müller et al., 2001).

Chl quenching can be measured with a fluorimeter. From this measurement, the fluorescence yield can be calculated. With changing the light intensity the maximum, minimum and steady state fluorescence can be determined (Müller et al., 2001). The quantum yield of non-cyclic electron transport is proportional to the product of photochemical fluorescence quenching and efficiency of photosystem(II) in reaction centres (Genty et al., 1989). At high light intensities, the quantum yield is less accurate, because energy state quenching (qE), causes an energy drain in PS(II). As a result a non-linear relationship between photochemical quenching (qP) and quantum yield can arise (Genty et al., 1989). The equations to determine the quantum yield are given below.

$$photochemical\ fluorescence\ quenching = \frac{F_{m\prime} - F_s}{F_v} \quad [-] \qquad 2.2$$

$$efficiency\ PH(II) = \frac{F_v}{F_{m\prime}} \quad [-] \qquad 2.3$$

$$Quantum\ yield\ \phi_{PSII} = \frac{F_{m\prime} - F_s}{F_{m\prime}} \rightarrow \frac{\Delta F}{F_{m\prime}} \quad [-] \qquad 2.4$$

In the model the parameter J_{max26} had an initial value of 467 µmol m^{-2} s^{-1}; this parameter is temperature and quantum flux dependent (Nolan and Smillie, 1976). The initial value was derived from chloroplasts of *Hoderum vulgare*, which is a barley specie. The quantum flux is influenced by CO_2/O_2 specificity of rubisco, in other words the CO_2 compensation point.

From the quantum yield, the electron transport rate can be calculated. Accurate estimates depend on validity of $\Delta F/F_{m'}$ and excitation distribution between PS(I) and PS(II) (Laisk and Loreto, 1996). Weiss (Weiss et al., 2000) calculated the effective quantum yield for *Lemna minor*, which includes a small change in the formula. Namely, the steady state-fluorescence yield (F_s) was replaced by F_t. F_t is the transient yield of chlorophyll during irradiation. The effective quantum yield is an indicator of the ability to move electrons beyond PS(II). A maximum relative electron transport rate of 73.1±1.4 µmol m^{-2} s^{-1} was found.

$$ETR = Irradiance * \frac{\Delta F}{F_{m'}} * 0.5 * Absorbance \qquad [\mu mol\ m^{-2}\ s^{-}] \qquad 2.5$$

$$RETR = Irradiance * \frac{\Delta F}{F_{m'}} \qquad [\mu mol\ m^{-2}\ s^{-}] \qquad 2.6$$

A fraction of 0.5 is applied because only 50% of the quantum yield is absorbed by PH(II). The standard absorbance coefficient is 0.84; for *Wolffia arrhiza*, the absorbance is 0.872 (Ritchie and Mekjinda, 2016). According to the formulas above, the maximum electron transport rate of Weiss was 32.6 µmol m^{-2} s^{-1}. Research for 6 different C_3 plants resulted in a maximum range of 75 to 272 µmol m^{-2} s^{-1} (Laisk and Loreto, 1996), so the result of Weiss is relatively low. Another research found a maximal quantum efficiency in light of 0.73 at 200 µmol m^{-2} s^{-1}. With equation 2.5 the maximum electron transport rate is 63.7 µmol m^{-2} s^{-1} (Frankart et al., 2003). The difference is caused by the fact that Weiss calculated the F_t instead of the F_s. The figure below shows the maximum electron transport rate as a function of the temperature. Obviously in previous research the J_{max} was overestimated and therefore has to be adapted to 63.7 µmol m^{-2} s^{-1}.

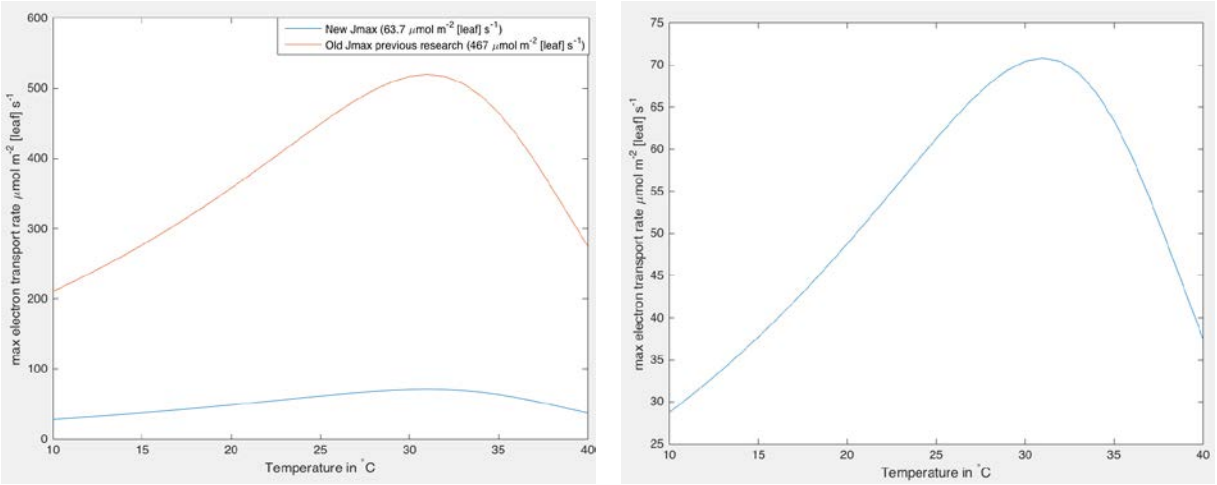

Figure 9A & B. Maximum electron transport rate J_{max} as a function of the temperature compared with the new value according literature and the value used in previous research. The image right shows the temperature dependency with an J_{max26} of 63.7 µmol m^{-2} s^{-1}.

2.8.2 CO_2 compensation point (Γ)

The CO_2 compensation point gives information at which CO_2 concentration the rate of photosynthesis is equal to the rate of respiration. In most plants, this occurs in limited light conditions. In previous research a constant compensation point of 36.5 µmol mol^{-1} was used (Rooijakkers, 2016). In fact Γ depends on the Michaelis-Menten equation of rubisco carboxylation and oxygenation and therefore it is temperature dependent (van Ooteghem, 2007). The increase of Γ with temperature seems to be greater for lower irradiances, which suggest that the light intensity influences the dark respiration (Farquhar et al., 1980). The CO_2 compensation point is also nutrient, chlorophyll and time of the day dependent (Bauer and Martha, 1981). Therefore, it might be better to make the compensation point dynamic. Farquhar (1980) developed a dynamic model that determined the compensation point including the influence of dark respiration. Calculations with equation 2.7 resulted at maximum and minimum dark respiration a compensation point Γ of 78.3 and 42.0 µmol mol^{-1}. The parameters in this equation can be found in appendix 10.1.

$$\Gamma = \frac{\frac{K_c * O * k_o}{2 * K_o * k_c} + K_c * \left(1 + \frac{O}{K_o}\right) * \frac{R_d}{V_{c\,max}}}{1 + \frac{R_d}{V_{c\,max}}} \qquad [\mu mol\ mol^{-1}] \qquad 2.7$$

According to literature, *Lemna minor* has a compensation point of 10.3 ppm at a dissolved oxygen concentration of 1% (Fuhrer, 1983). Increased dissolved oxygen elevated the compensation point. Other experiments with *Lemna minor* showed a CO_2 compensation point of 0.95 ppm (Filbin and Hough, 1985). The formula therefore seems not suitable for duckweed species. Normally plants with a high respiration have a relatively high CO_2 compensation point (Bauer and Martha, 1981). Moreover, a low respiration would be remarkable due to the fact that plants with high growth rate have in generally a high respiration rate (Van der Werf et al., 1992). However, *Lemna minor* is floating on water and the opening of stomata is climate independent. Therefore, there is no CO_2 build up, which probably results in a low CO_2 compensation point (Filbin and Hough, 1985).

2.8.3 Degree of curvature

The degree of curvature (θ) represents the shape of the light-response curve. The curvature ranges between 0 and 1 (Goudriaan and Van Laar, 1994). Values close to one indicate a sensitive plant for the given parameters. The curvature depends on CO_2 partial pressure gradient, light absorption and photosynthetic capacity of the leaf (Evans et al., 1993). The estimated curvature was 1.018, which is theoretically not possible. This would suggest that the photosynthesis is unlimited increasing. Therefore, the maximum curvature was set to 1.0.

2.8.4 Total CO_2 resistance

There are a lot of formulas available for calculating the total resistance. The resistance from the intercellular cells to the outside depends on the boundary resistance and a parallel system of the stomatal and cuticular resistance (Bot, 1983). For determining the total resistance, the diffusion from intercellular cells to the chloroplast should also be included, since the carboxylation of RuBP takes place in the stroma (Heldt and Piechulla, 2011b). In previous research the model was based on a parallel system and the carboxylation resistance (Rooijakkers, 2016). Although the model uses the carboxylation resistance, calculations were done with the mesophyll resistance. This resistance for *Lemna minor* is light intensity dependent (Fuhrer, 1983). The total CO_2 resistance was calculating with following formula (Rooijakkers, 2016);

$$R_{totCO_2} = \frac{R_{cut} * R_s}{(R_{cut} + R_s)} + R_{c\,CO2} \qquad [s\ m^{-1}] \qquad 2.8$$

The stomatal resistance (R_s) was estimated at 62.04 s m^{-1} and did not differ much from theoretically value of 62.5 s m^{-1} (Fuhrer, 1983). Unfortunately, in this research the value was found by unpublished research. The R_s determines opening of the stomata. An open stoma allows the diffusion of CO_2 from the atmosphere into the intercellular gas space of the leaf, at the same time water vapour escapes from the leaf to the atmosphere. Normally, the opening and closing is caused by biochemical reactions (Heldt and Piechulla, 2011c, 2011b). However, for duckweed, the stomata are always open. Therefore, the R_s can be assumed constant. Experiments with different C_3 plants showed a stomatal resistance range of 48 to 500 s m^{-1} (Whiteman and Koller, 1967). In other words, the current value is theoretically possible compared to literature.

The cuticular resistance for CO_2 diffusion in the cuticular membranes R_{cut} was $236.48*10^3$ s m^{-1} (Rooijakkers, 2016). This initial value was obtained from a research based on submerged leaves. However the R_{cut} is overestimated, namely in a normal photosynthetic model the R_{cut} is 2000 s m^{-1} (van Ooteghem, 2007). In another experiment the cuticle resistance in dark was measured for a lot of plants, the average value was 2835 s m^{-1} (Whiteman and Koller, 1967). Moreover, the cuticle is on the surface of water, therefore it is better to compare R_{cut} with floating plants. Unfortunately, no values are known for duckweed species, however compared to other research the cuticular resistance was too high. Coincidentally, as the parallel system of Bot was used, the error in the total resistance was reduced.

The mesophyll resistance is influenced by many environmental conditions. Fuhrer (1983) calculated the mesophyll resistance as a function of the light intensity and oxygen concentration. The R_m is very dynamic and depends on many environmental aspects like; salinity, nitrogen concentration, altitude, water logging, plant temperature, aging, CO_2 concentration and light intensity (Flexas et al., 2008). As a result, it might be better to calculate the mesophyll resistance, instead of using the light dependent mesophyll values from Fuhrer (1983). The mesophyll resistance is calculated with the carboxylation resistance and adding a constant factor of 15 s m^{-1}. The carboxylation resistance can be calculated with the effective Michaelis-Menten constant (K_m) and the maximum carboxylation rate ($V_{c\ max}$) (Farquhar et al., 1980; Goudriaan and Van Laar, 1994).

$$R_{c\,CO_2} = \frac{K_m}{V_{C\,max}} * \frac{\rho CO_{2T}}{M_{CO_2}} \qquad [s\,m^{-1}] \qquad 2.9$$

The figure on the next page shows a decreasing mesophyll resistance for an increasing temperature. The maximum resistance was ±2280 s m^{-1}, which is low compared to the maximum resistance of 11794 s m^{-1} at 0 µmol m^{-2} s^{-1} (Fuhrer, 1983). All equations and parameters used for this calculation can be found in appendix 10.1.

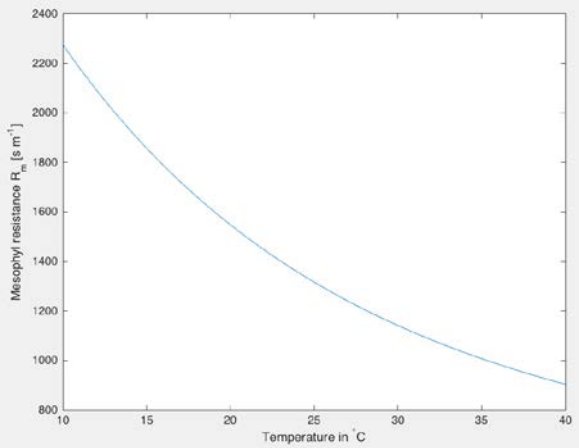

Figure 10. Mesophyll resistance as a function of the temperature.

Angiosperms have a relatively low mesophyll conductance compared to other plants (Flexas et al., 2008). Maxwell (2000) did research on *K. daigremontiana*. The total conductance of this angiosperm plant can be calculated with the following formula;

$$g_m = \frac{A}{(C_i - C_c)} \qquad [\mu mol\ m^{-2}\ s^{-1}\ bar^{-1}] \qquad 2.10$$

A is the net photosynthetic flux at steady state (4.8 µmol m^{-2} s^{-1}), g_m is the mesophyll conductance, C_i and C_c are the CO_2 concentrations in internal cavity and the chloroplasts. After calculation of g_m, the mesophyll resistance can be calculated, since the resistance is the inverse of the conductance. R_m was equal to 2976 s m^{-1} and it is relatively low compared to the max R_m of Fuhrer; 11764 s m^{-1}. This was expected because Maxwell's calculations were at a light intensity of 650 µmol m^{-2} s^{-1}. The mesophyll resistance of *Lemna minor* at 380 µmol m^{-2} s^{-1} was 1313 s m^{-1}. Therefore, the currently used mesophyll resistance values are possible.

The total resistance is equal to the sum of the successive resistances (Gaastra, 1959). Supported by Gaastra, the total resistance for the photosynthetic model is the sum of individual resistances $R_s+R_b+R_c$ (van Ooteghem, 2007).

Instead of using the R_c, it better to replace the carboxylation resistance by the mesophyll resistance (R_m). Namely, the R_m represents the total resistance from intercellular cells to the carboxylation site. In other words R_m describes the complete pathway, instead of the carboxylation resistance (Figure 11) (Willmer and Fricker, 1996).

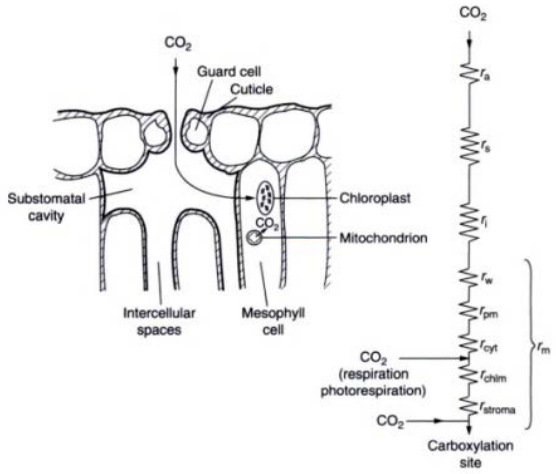

Figure 11. Complete pathway of CO_2 diffusion from outside to the carboxylation site (Willmer and Fricker, 1996).

Moreover, Goudriaan (1994) mentioned the total leaf resistance depends on a parallel system, but the CO_2 limited rate for net photosynthesis was calculated with equation 2.11 .

$$R_{tot} = R_s + R_b + R_m \qquad [s\ m^{-1}] \qquad 2.11$$

Therefore, for calculating the total resistance the equation above has the best characteristics. Unfortunately, no values for the boundary resistance of duckweed are known, however this resistance can be calculated with a standard boundary resistance equation (van Ooteghem, 2007). Due to the fact that the results of equation 2.9 were different than the measured values by Fuhrer (1983) it might be better to simulate the model with the value of the mesophyll resistance found in literature and calculate the total resistance with equation 2.11.

3 Current photosynthetic model

Photosynthesis is the most important process for plants; without the conversion of CO_2 to sugars no growth is possible. In previous research a photosynthetic model was used to determine the production of duckweed with given inputs. All equations of this model are given in this chapter. The model is based on the uptake of carbon. The uptake rate is determined by biological processes, for example; CO_2 diffusion, electron transport rate, carboxylation and regeneration of rubisco. The origin of the model was derived from experiments with the gas exchange between air and plants (Farquhar et al., 1980). In these equations the uptake rate could be determined with the CO_2 concentration, light intensity and the temperature. Small changes were made to make this model more suitable for estimating the production of duckweed (Rooijakkers, 2016). The LAI was assumed to be constant, this means that the mat density is constant, in other words m^{-2} [leaf] is equal to m^{-2} [soil].

In paragraph 2.3, information was given about the carboxylation and regeneration of rubisco. These two processes determine the maximum net assimilation rate. In the model, these processes are represented as CO_2 limited rate for photosynthesis (P_{nc}) and maximum endogenous photosynthetic capacity (P_{mm}).

3.1 CO_2 limited photosynthesis rate

The CO_2 limited photosynthesis rate (P_{nc}) represents the capacity of rubisco, which is decreased in low CO_2 and light conditions. P_{nc} is calculated with the total CO_2 diffusion resistance. The carboxylation resistance is normally determined by the maximum carboxylation allowed by the rubisco enzyme ($V_{c\,max}$). However, in the formula the carboxylation resistance is replaced by the mesophyll resistance, which depends partly on the carboxylation resistance (Wilmer, 1996).

$$P_{nc} = \frac{\rho_{CO_2} T}{R_{tot\_CO_2}} * (\mathrm{CO_{2a}} - \Gamma) \qquad [mg\ CO_2\ m^{-2}\ leaf\ s^{-1}] \qquad 3.1$$

The density of CO_2 is temperature dependent; the formula is given below.

$$\rho_{CO_2} T = \rho_{CO_2} * \frac{T_0}{T_c} \qquad [kg\ m^{-3}] \qquad 3.2$$

The total resistance is given as a parallel system and the mesophyll resistance. The parallel resistance depends on the cuticular and stomatal resistance (Bot, 1983). The mesophyll resistance is light dependent and interpolated during integration. In paragraph 2.8.4 some remarks are given about this formula.

$$R_{totCO_2} = \frac{R_{sCO_2} * R_{cut}}{R_{sCO_2} + R_{cut}} + R_{mCO_2} \qquad [s\ m^{-1}] \qquad 3.3$$

3.2 Maximum endogenous photosynthetic capacity

The maximum endogenous photosynthetic capacity (P_{mm}) is derived from the regeneration of RuBP. This regeneration is determined with the temperature dependent electron transport rate (J_{max}). The capacity of the thylakoid reactions determine the ability to regenerate RuBP (Sage, 1990). The capacity is influenced by the electron transport rate and calculated with equation 3.4.

$$P_{mm} = \frac{M_{CO_2}}{4} * J_{max} \qquad [mg\ CO_2\ m^{-2}\ leaf\ s^{-1}] \qquad 3.4$$

The electron transport rate is required for the production of NADPH and ATP, without these energy carriers photophosphorylation of ADP does not takes place. The carboxylation of rubisco requires energy; therefore the electron transport rate is an important process in assimilation.

$$J_{max} = J_{max26} * e^{E_j * X} * D \qquad [\mu mol\ e^-\ m^{-2}\ s^{-1}] \qquad 3.5$$

On the next page two formulas are given for calculating the electron transport rate, *S* and *H* are constants for the temperature dependency J_{max}.

$$X = \frac{T_c - T_{opt}}{T_c * R_g * T_{opt}} \qquad [mol\ J^{-1}] \qquad 3.6$$

$$D = \frac{1 + e^{\frac{S*T_{opt} - H}{R_g * T_{opt}}}}{1 + e^{\frac{S*T_c - H}{R_g * T_c}}} \qquad [-] \qquad 3.7$$

3.3 Net maximum assimilation rate

Both processes P_{nc} and P_{mm} calculate the mg CO_2 uptake per square meter. The lowest assimilation rate determines the actual maximum assimilation rate (Sage, 1990) (Hikosaka et al., 2006). With a Blackman response equation, the net assimilation rate can be determined (Goudriaan and Van Laar, 1994). If the curvature theta is equal to zero, the shape represents a regular rectangular hyperbola and close to one it represents a Blackman curve. Although the negative exponential curve of the Blackman response does not have a mechanistic justification, it gives the best description for plants (Goudriaan and Van Laar, 1994). At a curvature of one, the result is similar to the theory mentioned by Sage and Hikosaka.

$$P_{n\,max} = \frac{P_{mm} + P_{nc} - \sqrt{(P_{mm} + P_{nc})^2 - 4 * \theta * P_{mm} * P_{nc}}}{2 * \theta} \qquad [mg\ CO_2\ m^{-2}\ leaf\ s^{-1}] \qquad 3.8$$

The maximum gross leaf assimilation ($P_{g\ max}$) is determined by adding the leaf dark respiration rate and the net maximum assimilation rate.

$$P_{g\,max} = P_{n\,max} + M_{CO2} * r_{dul} \qquad [mg\ CO_2\ m^{-2}\ leaf\ s^{-1}] \qquad 3.9$$

In the model the dark respiration is assumed constant; r_{dul}=1.36 µmol m^{-2} s^{-1}.

3.4 Light use efficiency

As mentioned there are two sorts of respiration, dark respiration produces energy in exchange for the emission of CO_2. Photorespiration does not produce energy; it consumes energy. Under high light intensities, this process is not a problem. However, under low light intensities a part of the light will be used for oxygenation of rubisco. Oxygenation requires two times more energy than carboxylation (Goudriaan and Van Laar, 1994). Below the formula for the light efficiency by photorespiration is given. The number of electrons (e^-) fixed per CO_2 is 4.

$$\epsilon = \psi * \frac{M_{CO2}}{4} * \frac{\max(CO_{2a}, \Gamma) - \Gamma}{\max(CO_{2a}, \Gamma) + 2\Gamma} \qquad [mg\ CO_2\ J^{-1}] \qquad 3.10$$

To convert the amount of µmol e^- to J a conversion factor ψ is used. The parameter F_p represents the amount of radiation absorbed by non-photosynthetic tissues. ζ is the conversion factor for µmol photons to joule, and since 1 photon can absorb 2 e^-, the formula is divided by two.

$$\psi = \frac{1 - F_p}{2} * \zeta \qquad [\mu mol\ e^-\ J^{-1}] \qquad 3.11$$

3.5 Gross and net assimilation rate

The gross leaf assimilation is calculated with the light efficiency and maximum gross assimilation.

$$P_{g\,L} = P_{g\,max}\left(1 - e^{\frac{-\epsilon * I_A}{P_{g\,max}}}\right) \qquad [mg\ CO_2\ m^{-2}\ leaf\ s^{-1}] \qquad 3.12$$

I_A represents the absorbed radiation; in the model however, the measured light intensity in the greenhouse is assumed equal to the absorbed irradiation. Due to the fact that the LAI is constant, the unit of the gross assimilation in equation 3.12 is equal to $mg\ [CO_2]\ m^{-2}\ [soil]$.

The net assimilation has to be calculated, otherwise the model would assume that respiration causes an increase in biomass. The dark respiration was assumed constant. Furthermore, a correction for the optimal pH is applied based on equation 3.14.

$$P_{g\,N} = (P_{g\,L} - r_{DuL} * M_{CO2}) * pH_{corr} \qquad [mg\ CO_2\ m^{-2} soil\ s^{-1}] \quad 3.13$$

$$pH_{corr} = \frac{-1.0082 + 0.59297 * pH - 0.10831 * pH^2 + 0.00948 * pH^3 - 0.00034 * pH^4}{0.27} \qquad [mg\ CO_2\ m^{-2} soil\ s^{-1}] \quad 3.14$$

Table 7. All parameters and values used in photosynthetic model

P_{nc}	CO_2 limited rate photosynthesis	eq 3.1	$[mg\ CO2\ m^{-2}\ leaf\ s^{-1}]$
Γ	CO_2 compensation point	36.5	$[ppm]$
$\rho_{CO_2}T$	Density CO_2 at temperature T_{dw}	eq 3.2	$[kg\ m^{-3}]$
ρ_{CO_2}	Density CO_2 at standard T_0	1.98	$[kg\ m^{-3}]$
T_0	Standard temperature	273.15	$[K]$
T_{opt}	Optimum temperature for duckweed	299.15	$[K]$
R_sCO_2	Stomatal resistance CO_2	62.5	$[s\ m^{-1}]$
R_{cut}	Cuticular resistance CO_2	2.39E+05	$[s\ m^{-1}]$
R_mCO_2	Mesophyll resistance CO_2	model	$[s\ m^{-1}]$
$R_{tot}CO_2$	Total CO_2 resistance	eq 3.3	$[s\ m^{-1}]$
P_{mm}	Maximum endogenous capacity	eq 3.4	$[mg\ CO2\ m^{-2}\ leaf\ s^{-1}]$
R_g	Gas constant	8.314	$[J\ mol^{-1}\ k^{-1}]$
ρ_{chl}	Superficial chlorophyll density	0.46	$[g\ m^{-2}]$
J_{max}	Maximum electron transport rate at given T_{dw}	eq 3.5	$[umol\ e^-\ m^{-2}\ s^{-1}]$
J_{max26}	Maximum electron transport rate at 298.15K	467 ρ_{chl}	$[umol\ m^{-2}]$
X	Variable temperature dependency J_{max}	eq 3.6	$[mol\ J^{-1}]$
D	Variable temperature dependency J_{max}	eq 3.7	$[-]$
S	Constant temperature dependency J_{max}	710	$[J\ mol^{-1}\ K^{-1}]$
H	Constant temperature dependency J_{max}	220000	$[J\ mol^{-1}]$
$P_{n\,max}$	Maximum net assimilation rate	eq 3.8	$[mg\ CO2\ m^{-2}\ leaf\ s^{-1}]$
$P_{g\,max}$	Maximum gross leaf assimilation	eq 3.9	$[mg\ CO2\ m^{-2}\ leaf\ s^{-1}]$
ϵ	Light use efficiency	eq 3.10	$[mg\ CO2\ J^{-1}]$
ψ	Conversion e^- to J^{-1} and adapted for non-photosynthetic tissue	eq 3.11	$[umol\ e^-\ J^{-1}]$
F_p	Amount of radiation absorbed by non-photosynthetic tissue	0.3	$[-]$
ζ	Conversion e^- to J^{-1}	4.59	$[umol\ e^-\ J^{-1}]$
$P_{g\,L}$	Gross leaf assimilation rate	eq 3.12	$[mg\ CO2\ m^{-2}\ leaf\ s^{-1}]$
$P_{g\,n}$	Net leaf assimilation rate	eq 3.13	$[mg\ CO2\ m^{-2}\ leaf\ s^{-1}]$
r_{Dul}	Dark respiration rate	1.36	$[mg\ CO2\ m^{-2}\ leaf\ s^{-1}]$
pH_{corr}	Correction value for pH	model	$[-]$
E_j	Activation energy electron transport rate	3700	$[J\ mol^{-1}]$
θ	Degree of curvature	1	$[-]$
A_{pond}	Surface of the pond	880	$[m^{-2}]$

4 Improvements model

4.1 Development temperature model greenhouse and crop

In previous photosynthetic models, it was assumed that the water temperature is equal to the duckweed temperature. This temperature was used to calculate the assimilation rate. According to the literature study in chapter 2.6, this assumption is probably not correct. Namely, irradiation can result in higher temperatures. Moreover the variables in the model are crop temperature dependent (van Ooteghem, 2007). Furthermore, wind and radiation cause temperature differences between the water and the duckweed. Therefore, it is better to simulate the model with the crop temperature instead of the water temperature. Unfortunately, this temperature has not been measured. Therefore, the temperature will be estimated with physics. The following formulas are mostly based on the processes described by Van Ooteghem and Van den Top (2014). No models of the water and greenhouse temperature were made, since these were both measured.

4.1.1 Temperature of the duckweed

The duckweed temperature (T_{dw}) is established with an energy balance given in equation 4.1. The formula takes the convection with the greenhouse and the water into account. Furthermore, transfer of energy by radiation is an important factor, namely shortwave radiation from the sun and longwave radiation between the roof and duckweed takes place. Evapotranspiration causes a decrease in temperature, since vaporization of water requires energy.

$$\frac{dTdw}{dt} = \frac{Qdw_{rlw} + Qdw_{rd} + Qdw_{cg} + Qdw_{w} - Qdw_{H2O}}{\rho_{dw} * Cp_{dw} * V_{dw}} \quad [K\ s^{-1}] \quad 4.1$$

Longwave radiation between roof and duckweed (Qdw_{rlw}) mainly depends on the emission coefficients and the view factor. The view factor is relatively low, since only a part of the greenhouse is covered with duckweed. The area covered with duckweed is divided by the total area.

Formula for view factor duckweed to roof;

$$Fro_{dw} = (1 - \tau_{dw\,lw}) * Fro_{sk} * LAI_t * \frac{A_{pond}}{A_{tot}} \quad [-] \quad 4.2$$

The longwave transmittance ($\tau_{dw\,lw}$) and emission coefficient (E_{dw}) of duckweed is determined with following formulas;

$$\tau_{dw\,lw} = e_t^{-kc_{lw} * LAI_t} \quad [-] \quad 4.3$$

And the emission coefficient;

$$E_{dw} = 1 - \tau_{dw\,lw} \quad [-] \quad 4.4$$

With equation 4.2, 4.3 and 4.4, Qdw_{lr} can be calculated;

$$Qdw_{rlw} = A_r * E_r * E_{dw} * Fro_{dw} * \sigma * (T_r^4 - T_{dw}^4) \quad [W] \quad 4.5$$

Shortwave radiation absorption of sunlight by duckweed (Qdw_{rd}) depends on the measured light intensity (I_m) and the absorption coefficient, which can be assumed equal to the shortwave emission coefficient (van Ooteghem, 2016).

$$Ab_{dw} = 1 - \tau_{dw\,sw} \quad [-] \quad 4.6$$

$$Qdw_{rd} = A_{pond} * LAI_t * Ab_{dw} * I_m \quad [W] \quad 4.7$$

There is heat transfer between water and duckweed (Qdw_w). The heat transfer coefficient ($\alpha_{dw\,w}$) is 50 W m^{-2} K^{-1} and describes the energy transfer through convection.

$$Qdw_w = A_{pond} * LAI_t * \alpha_{dw\,w} * (T_w - T_{dw}) \quad [W] \quad 4.8$$

Then there is convection between the greenhouse air and duckweed (Qdw_{cg}). The greenhouse air temperature is an input in the model. The heat transfer coefficient ($\alpha_{dw\,g}$) is determined with the boundary resistance for heat transfer and the heat capacity of the air. First, the heat transfer coefficient is calculated.

$$\alpha_{dw\,g} = \frac{\rho_a * c_{p,air}}{R_{b\,heat}} \qquad [W\,m^{-2}\,K^{-1}] \qquad 4.9$$

Then the boundary resistance is calculated, which depends on the leaf width (l_w) and the airflow (V_{windG}) in the greenhouse.

$$R_{b\,heat} = \frac{1174 * \sqrt{l_w}}{\left(lw * \left|T_{dw} - T_g\right| + 207 * V_{windG}^2\right)^{0.25}} \qquad [W\,m^{-2}\,K^{-1}] \qquad 4.10$$

By combining equations 4.10 and 4.9, convection between the duckweed and the greenhouse is calculated.

$$Qdw_{cg} = A_{pond} * LAI_t * \alpha_{dw\,g} * (T_g - T_{dw}) \qquad [W] \qquad 4.11$$

The final energy process is evapotranspiration. A Penman-Monteith model was used, since experiments with this model had an accuracy of 5 to 10% for *Lemna minor* (Al Nozaily, 2000). First, the resistance to diffusion of water for the boundary layer has to be determined.

$$R_{b\,H2O} = Le^{\frac{2}{3}} * R_{b\,heat} \qquad [W\,m^{-2}\,K^{-1}] \qquad 4.12$$

The resistance for evaporation is the sum of the boundary resistance and the stomatal resistance (Caicedo et al., 2000). The stomatal resistance of CO_2 for *Lemna minor* is converted to H_2O resistance by division by 1.6 (Bot, 1983). Further, there is an aerodynamic resistance (r_a); normally this variable is crop height dependent. However, the height of duckweed is very small, therefore it is allowed to calculate r_a as in the case of open water (Al Nozaily, 2000).

$$r_a = \frac{245}{0.5 * V_{windG} + 0.5} \qquad [s\,m^{-1}] \qquad 4.13$$

The vapour pressure deficit (VPD) has to be calculated to determine how much water can be evaporated. Vapour pressure saturation is calculated with equation 4.16 and holds if the duckweed temperature T_{dw} > 273.15 (van 't Ooster, 2016);

$$p_s = \frac{\left(610.5 * 10^{\frac{7.5*(T_{dw}-273.15)}{237.3+(T_{dw}-273.15)}}\right)}{1000} \qquad [kPa] \qquad 4.14$$

$$p_v = p_s * \frac{RH}{100} \qquad [kPa] \qquad 4.15$$

$$VPD = p_s - p_v \qquad [kPa] \qquad 4.16$$

The slope of the saturation vapour pressure (Δ) depends on the saturation pressure and the crop temperature.

$$\Delta = \frac{4098 * p_s}{\left((T_{dw} - 273.15) + 237.3\right)^2} \qquad [kPa\,K^{-1}] \qquad 4.17$$

The psychometric constant (y) is calculated with equation 4.18.

$$y = 0.665 * 10^{-3} * atmkPa \qquad [-] \qquad 4.18$$

The net radiation (R_n) is the difference between incoming net shortwave radiation (R_{ns}) and outgoing net longwave radiation (R_{nl}) (Allen et al., 1998). R_{nl} cannot be calculated easily, because it depends on maximal possible sunshine and actual sunshine. It is possible to calculate R_n with the uptake of light by duckweed; however, this has never been done in literature. As an alternative, R_n is calculated using the following formula (Valdés-Gómez et al., 2009):

$$R_n = (1 - R_{dw}) * I_m + E_{sky} * E_{dw} * (T_g^4 - T_{dw}^4) \quad [W] \quad 4.19$$

Finally the heat of evapotranspiration can be calculating using formulas: 4.12, 4.13, 4.14, 4.17, 4.18 and 4.19. The amount of water evaporated is independent of the mat density and therefore not taken into account (Busk, 1983).

$$\lambda E = \frac{\left(\Delta * R_N + \frac{\rho_{air} * Cp_{air} * VPD}{r_a}\right)}{\Delta + \gamma\left(1 + \frac{r_c}{r_a}\right)} * A_{pond} \quad [W] \quad 4.20$$

4.1.2 Temperature of the roof

In the previous paragraph, the equation for longwave radiation absorption by duckweed from the roof was mentioned. However, the temperature of the roof has not been measured and therefore has to be determined with the following energy balance.

$$\frac{dTr}{dt} = \frac{Qr_{oc} + Qr_{olw} + Qr_{dwl} + Qr_{wlw} + Qr_{sw} + Qr_{gc} + Qr_{slw} - Qr_{H_2O}}{\rho_r * Cp_r * V_r} \quad [K\ s^{-1}] \quad 4.21$$

First, the convection between outside air and roof is determined.

$$Qr_{oc} = A_r * \alpha_{wind} * (T_{out} - T_r) \quad [W] \quad 4.22$$

α_{wind} represents the heat transfer coefficient, which is airflow dependent. If the airflow (V_{wind}) is smaller than 4 m s^{-1}, then the following formula can be used;

$$\alpha_{wind} = 1.2 * V_{wind} + 2.8 \quad [W\ m^{-2}\ K^{-1}] \quad 4.23$$

If V_{wind} is bigger than 4 m s^{-1} then equation 4.24 is used. An increasing airflow results in an increasing heat transfer coefficient and thus more transfer of energy.

$$\alpha_{wind} = 2.5 * V_{wind}^{0.8} \quad [W\ m^{-2}\ K^{-1}] \quad 4.24$$

Secondly, longwave radiation between outdoor air and roof (Qr_{olw}) is calculated with;

$$Qr_{olw} = A_r * E_r * E_{sky} * Fro_{sk} * \sigma * (T_{sky}^4 - T_r^4) \quad [W] \quad 4.25$$

The sky temperature (T_{sky}) is calculated with the assumption that the clouded fraction c_{Tsky} is constant over the whole month. $E_{sky\ clear}$ represents the fictive emission coefficient of a clear sky.

$$T_{sky} = \left(\left(1 - c_{Tsky}\right) * E_{sky\ clear} * T_{out}^4 + c_{Tsky} * \left(T_{out} - \frac{9}{\sigma}\right)\right)^{0.25} \quad [K] \quad 4.26$$

Longwave radiation from duckweed to indoor air is similar to Qdw_{rlw}; eq. 4.5.

$$Qr_{dwl} = -1 * Qdw_{rlw} \quad [W] \quad 4.27$$

Besides longwave radiation from duckweed, there is also longwave radiation from the water to the roof (Qr_{wlw}). The formula is almost similar to Qr_{olw} only the view factor is different.

$$Qr_{wlw} = A_r * E_r * E_{sky} * Fro_w * \sigma * (T_w^4 - T_r^4) \quad [W] \quad 4.28$$

With the view factor for water to roof (Fro_w);

$$Fro_w = (1 - \tau_{w\,sw}) * Fro_{sk} * (1 - LAI_t) * \frac{A_{pond}}{A_{tot}} \quad [W] \quad 4.29$$

The shortwave radiation absorption is determined with the absorption coefficient by the roof and the outdoor irradiation. The absorption coefficient is 1 minus the transmittance ($Trans_r$).

$$Qr_{sw} = A_r * (1 - Trans_r) * I_{tot} \quad [W] \quad 4.30$$

Below the convection of the greenhouse to the roof (Q_{rgc}) with heat transfer coefficient α_g is calculated.

$$Qr_{gc} = A_r * \alpha_g * (T_g - T_r) \quad [W] \quad 4.31$$

Longwave radiation between the soil and the roof (Qr_{slw});

$$Qr_{slw} = A_r * E_r * E_{soil} * Fro_s * \sigma * (T_s^4 - T_r^4) \quad [W] \quad 4.32$$

The last process is condensation of water on the roof (Qr_{H2O}). First the mass transfer coefficient has to be determined ($k_{as\ ri}$). $k_{as\ ri}$ depends on the heat transfer coefficient ($\alpha_{as\ ri}$) of the roof and the air in the greenhouse.

$$\alpha_{as\ ri} = 3 * |T_g - T_r|^{\frac{1}{3}} \quad [W\ m^{-2}K^{-1}] \quad 4.33$$

Then the mass transfer coefficient is determined

$$k_{as\ ri} = \frac{\alpha_{as\ ri}}{\rho_{air} * Cp_{air} * Le^{\frac{2}{3}}} \quad [W\ m^{-2}K^{-1}] \quad 4.34$$

After calculating the mass transfer coefficient, the water flow rate ($\phi r_{H_2O\ flux}$) is determined. The mass flow depends on the vapour saturation concentration of the roof temperature ($CsT_{r\ H2O}$) and vapour concentration at greenhouse temperature ($CT_{g\ H2O}$). The maximum function corrects for a negative mass flow.

$$\phi r_{H_2O\ flux} = \max(A_r * k_{as\ ri} * (CT_{g\ H_2O} - CsT_{r\ H_2O}), 0) \quad [kg\ H_2O\ s^{-1}] \quad 4.35$$

The evaporation energy (R_w) is the energy needed for evaporation of water. Qr_{H2O} is the total energy loss by condensation of water.

$$Qr_{H_2O} = R_w * \phi r_{H2O\ flux} \quad [W] \quad 4.36$$

4.1.3 Temperature of the soil

A part of the greenhouse is not covered with duckweed; therefore, a new differential equation for the temperature of the soil is made. It is assumed that the soil contains mainly sand with a small amount of water and air. The area of the footpath is added to the soil area, as an extra differential equation for only the footpath would increase computation time significantly and the benefit is relatively small.

$$\frac{dTsoil}{dt} = \frac{Qs_{sw} + Qs_{cg} + Qs_{rlw} + Qs_{stc}}{(0.7 * \rho_{sand} * Cp_{sand} + 0.2 * \rho_{H_2O} * Cp_{H_2O} + 0.1 * \rho_{air} * Cp_{air}) * V_s} \quad [K\ s^{-1}] \quad 4.37$$

Shortwave radiation from the sun is absorbed by the soil (Qs_{sw}). The absorption coefficient is based on formulas developed by Van Ooteghem (2007); a few changes were made because the total radiation absorbed is not inhibited by plants or screens. Therefore, the absorption coefficient (Ab_s) is 1 minus the shortwave radiation reflection by the soil.

$$Qs_{sw} = A_{soil} * Ab_s * I_m \quad [W] \quad 4.38$$

The heat transfer coefficient for convection between T_g and T_s depends on which temperature is higher. If $T_g < T_s$ then equation 4.39 is used, otherwise eq. 4.40.

$$\alpha_{a\ s} = 1.7 * |T_g - T_s|^{\frac{1}{3}} \quad [W] \quad 4.39$$

$$\alpha_{a\ s} = 1.3 * |T_g - T_s|^{0.8} \quad [W] \quad 4.40$$

The heat transfer through convection between greenhouse air and soil:

$$Qs_{cg} = A_{soil} * \alpha_{a\ s} * (T_g - T_s) \quad [W] \quad 4.41$$

Longwave radiation of soil and roof (Qs_{rlw}) is already determined with equation 4.32:

$$Qs_{rlw} = -Qr_{slw} \quad [W] \quad 4.42$$

The last process is conduction from the stable roof to the soil (Qs_{stc}):

$$Qs_{stc} = A_{soil} * U_s * (T_{stable} - T_s) \quad [W] \quad 4.43$$

4.1.4 Temperature of the stable

The stable has a small influence on the total energy balance, since there is only conduction from stable to soil. The stable temperature is determined from the ventilation rate, heat production of the animals and heat loss of the building by convection. The model is derived from Van den Top (2014). Because only small changes were made a summary of the equations is given below.

$$\frac{dT_{stable}}{dt} = \frac{Qst_{fv} + Qs_p + Qs_{cw} + Qst_{sc}}{\rho_{air} * Cp_{air} * V_{stable}} \quad [K\ s^{-1}] \quad 4.44$$

Table 8. Summary of the energy transfer processes in a stable.

Process	Description	Equations	
Qst_{fv}	Heat transfer forced ventilation	$Qst_{fv} = \phi_{fans} * \rho_{air} * Cp_{air} * (T_{out} - T_{stable})$	4.45
Qsp	Heat production by rosé calves	$Qs_p = Q_t * F * k_s(0.8 - 1.85 * 10^{-7} * (T_{stable2} + 10)^4)$	4.46
Qscw	Conduction stable and water	$Qs_{cw} = A_{pond} * U_{s\,w} * (T_w - T_{stable})$	4.47
Qstsc	Conduction stable and soil	$Qst_{sc} = -Qs_{stc}$	4.48

Table 9. All variables and parameters for determining T_{dw}, T_r, T_s and T_{st}.

LAI_t	Leaf area index for temperature model; fraction of pond covered with duckweed	0.9	$[-]$
E_r	Emission coefficient roof	0.41	$[-]$
E_{dw}	Emission coefficient duckweed	0.44	$[-]$
A_{tot}	Total surface greenhouse	4800	$[m^2]$
A_{pond}	Area of the pond	880	$[m^2]$
A_r	Area roof	4958	$[m^2]$
kc_{lw}	Extinction coefficient longwave by canopy	0.64	$[-]$
kc_{sw}	Extinction coefficient shortwave by canopy	0.48	$[-]$
$\tau_{dw\,lw}$	Longwave transmittance	0.56	$[-]$
$\tau_{dw\,sw}$	Shortwave transmittance	0.65	$[-]$
Ab_{dw}	Absorption coefficient of duckweed	0.35	$[-]$
Fro_{sky}	View factor roof to sky	cos(14.5)	$[-]$
Fro_{dw}	View factor roof to duckweed	0.07	$[-]$
σ	Stefan Boltzmann constant	5.67E-08	$[W\ m^{-2}\ K^{-1}]$
$\alpha_{dw\,w}$	Heat transfer coefficient duckweed and water	50	$[W\ m^{-2}\ K^{-1}]$
$\alpha_{dw\,g}$	Heat transfer coefficient duckweed and greenhouse	eq. 4.9	$[W\ m^{-2}\ K^{-1}]$
$atmkPA$	Atmospheric pressure	input	$[kPa]$
VPD	Vapour pressure deficit	eq 4.16	$[kPa]$
ρ_{air}	Density air	in model	$[kg\ m^{-3}]$
Cp_{air}	Heat capacity air	1000	$[J\ kg^{-1}\ K^{-1}]$
$R_{b\,heat}$	Boundary resistance	eq 4.10	$[s\ m^{-1}]$
$R_{s\,H2O}$	Stomatal resistance for water	39.1	$[s\ m^{-1}]$
r_c	Resistance for evapotranspiration	R_{bheat} $_+RsH_2O$	$[s\ m^{-1}]$
$VwindG$	Airflow in greenhouse	0.09	$[m\ s^{-1}]$

Le	Lewis number for water vapour in air	0.89	$[-]$
l_w	leaf width	4.00E-03	$[m]$
$Trans_r$	Transmission roof	0.59	$[-]$
ρ_{dw}	Density duckweed	950	$[kg\ m^{-3}]$
Cp_{dw}	Specific heat duckweed	3980	$[J\ kg^{-1}\ K^{-1}]$
V_{dw}	Volume of duckweed	0.3242	$[m^3]$
r_{sH_2O}	Stomatal resistance water	39.1	$[s\ m^{-1}]$
r_c	Resistance evapotranspiration	eq 4.12 + $r_{s\ H2O}$	$[s\ m^{-1}]$
r_a	Aerodynamic resistance	eq 4.13	$[s\ m^{-1}]$
p_s	Vapour pressure at saturation	eq 4.14	$[kPa]$
p_v	Vapour pressure unsaturated air	eq 4.15	$[kPa]$
Δ	Slope saturation vapour pressure	eq 4.17	$[kPa\ K^{-1}]$
R_{dw}	Albedo of duckweed	0.25	$[-]$
R_n	Net radiation	eq 4.19	$[W]$
γ	Psychometric constant	eq 4.18	$[-]$
E_{soil}	Emission coefficient soil	0.7	$[-]$
$E_{sky\ clear}$	Emission coefficient fictive clear sky	eq 10.7	$[-]$
E_w	Emission coefficient water	1	$[-]$
E_{sky}	Emission coefficient sky	1	$[-]$
C_{Tsky}	Clouded fraction	0.5	$[-]$
poH_2O	Vapour pressure outside	eq 10.8	$[-]$
$Vwind$	Airflow in greenhouse	0.09	$[m\ s^{-1}]$
Fro_w	View factor water to roof	0.016	$[-]$
Fro_s	View factor soil to roof	0.9096	$[-]$
α_{wind}	Heat transfer coefficient convection T_{out} and T_r	eq 4.23 or 4.24	$[W\ m^{-2}\ K^{-1}]$
α_g	Heat transfer coefficient convection T_g and T_r	4	$[W\ m^{-2}\ K^{-1}]$
$\alpha_{as\ ri}$	Heat transfer coefficient condensation roof	eq 4.33	$[W\ m^{-2}\ K^{-1}]$
$k_{as\ ri}$	Mass transfer coefficient	eq 4.34	$[m\ s^{-1}]$
R_w	Energy of evaporation of 1 kg water	2.22E+06	$[J\ kg^{-1}]$
$\rho_r *$	Density roof	2	$[kg\ m^{-2}]^*$
Cp_r	Heat capacity roof	1256	$[J\ kg^{-1}\ K^{-1}]$
$V_r *$	Volume roof	A_r	$[m^{-2}]^*$
ρ_{sand}	Density sand	1600	$[kg\ m^{-3}]$
Cp_{sand}	Specific heat sand	800	$[J\ kg^{-1}\ K^{-1}]$
ρ_{H_2O}	Density water	998	$[kg\ m^{-3}]$
Cp_{H_2O}	Specific heat water	4186	$[J\ kg^{-1}\ K^{-1}]$
V_s	Volume of duckweed	0.32	$[m^3]$
E_{soil}	Emission coefficient soil	0.7	$[-]$
β_s	Reflection of soil	0.58	$[-]$
Ab_s	Absorption coefficient soil $= (1 - \beta_s)$	0.42	$[-]$
$\alpha_{a\ s}$	Heat transfer coefficient indoor air and soil	eq 4.39 or 4.40	$[W\ m^{-2}K^{-1}]$
A_{soil}	Area of soil	3920	$[m^2]$
U_s	Conduction stable and soil	1.6	$[W\ m^{-2}K^{-1}]$

ϕ_{fans}	Fan speed	[-]	$[m^3\ s^{-1}]$
$T_{stable2}$	Temperature of stable in °C	273.15-Tst	$[°C]$
$U_{s\,w}$	Thermal conductance Tw and Tstable	2.48	$[W\ m^{-2}\ K^{-1}]$
Q_t	Heat production rose calves based on weight	Input	$[W]$
F	Correction factor temperature stable	[-]	$[-]$
k_s	Correction factor for wet floors	0.9	$[W]$
*[1] The density was given in kg m^{-2}; consequently, the volume is replaced by the area of the roof.			

4.2 Improvements photosynthetic model

In previous model some assumptions are made, which can result in different outputs. As a consequence, the new model described in the paragraphs below includes a dynamic LAI and nutrient concentration. Gaussian integration is applied for the gradual extinction of light at high mat densities. Furthermore, some small changes have been made to make the model more suitable for duckweed species.

4.2.1 Correction estimated parameters

The parameters in the previous model were mainly based on characteristics of a tomato plant. Therefore, some parameter values were not in range when comparing these values with duckweed species. In Table 10 a summary of the literature study in paragraph 2.8 is given.

Table 10. Parameters of previous research compared to the values found in literature.

Parameters	Old value	Estimated	Literature
ETR [µmol m^{-2} s^{-1}]	467	470.79	65.1
R_s [s m^{-1}]	62.5	62.04	62.5
Γ [ppm]	36.5	37.04	0.95
θ [-]	0.71	1.018	Max=1
R_{cut} [s m^{-1}]	239*10^3	236.48*10^3	superfluous

4.2.2 Leaf area index

The leaf area index (LAI) is a variable that gives an indication for the m^2 [leaf] m^{-2} [soil]. In previous model the LAI was assumed to be constant, however while harvesting it is possible that the mat density becomes lower than one. Therefore, it is not correct to assume a constant mat density. At a mat density of 558 g FW m^{-2}, 90% of the water is covered with duckweed (Körner and Vermaat, 1998). The simulations were done with Runge-Kutta and not with ode45, due to the fact that the inputs are changing over time. For example, the old mat density (Mat_{old}) and the produced biomass (Δx) changes during integration. The parameter Harvest represents the amount of duckweed harvested at time t.

$$Mat_{new} = Mat_{old} - \frac{Harvest(ZB)}{A_{pond}} + \frac{\Delta x}{A_{pond}} \qquad [g\ FW\ m^{-2}] \qquad 4.49$$

$$LAI = \frac{Mat_{new}}{FullA} \qquad [-] \qquad 4.50$$

At increasing LAI, the duckweed starts to pile up. As a consequence, less light is available for each frond. Furthermore, there is an uneven distribution of light caused by the non-linear photosynthetic light response curve (Goudriaan and Van Laar, 1994). As a result, the gradual extinction of light is taken into account with a three-point Gaussian integration. If the extinction coefficient of leaves multiplied with the LAI exceeds the value of 3, a five-point Gaussian integration is applied, since then the three-point is not accurate enough (Goudriaan and Van Laar, 1994).

In the calculation, two counters are used. One counter is used for integration over the canopy depth. It describes the gradual extinction of light at different layers. These depths are

symmetrically selected, in which the central point has the greatest weighing factor. The other counter is needed for light correction. This light correction depends on if the leaf is sunlit or shaded at the given canopy depth level.

Table 11. Values depth and weight for Gaussian integration.

Depth X_g	0.112702	0.5	0.887298
Weight W_g	0.277778	0.4444	0.277778

$$l_1 = [1;2;3], l_2 = [1;2;3]$$

The LAI at depth L is determined by multiplying the LAI calculated earlier with the depth factor.

$$LAI_l = LAI * X_g(l_1) \qquad [m^2\ leaf\ m^{-2} water] \quad 4.51$$

The gross leaf assimilation rate is determined by the shaded and sunlit fraction. $P_{g\ sun}$ depends on both counters (l_1 and l_2) and the sum of the light efficiency part.

$$P_{g\ sun}(l_1) = P_{g\ max} \sum_{l_2=1}^{3} W_g(l_2) \left(1 - e^{\frac{-\epsilon * I_{A\ sun}(l_1,l_2)}{P_{g\ max}}}\right) \qquad [mg\ CO_2\ m^{-2}\ leaf] \quad 4.52$$

A part of the fronds is in the shadow; as a result, the light absorption is different. Namely, these fronds do not have a perpendicular light flux ($I_{A\ ppd}$), which means no correction for $I_{A\ ppd}$ is needed. As a result, $P_{g\ shd}$ depends only on the canopy depth, in other words the second counter l_2 is neglected for fronds in the shadow.

$$P_{g\ shd}(l_1) = P_{g\ max} \left(1 - e^{\frac{-\epsilon * I_{A\ shd}}{P_{g\ max}}}\right) \qquad [mg\ CO_2\ m^{-2}\ leaf] \quad 4.53$$

Subsequently the sunlit and shaded parts are combined to determine the total gross leaf assimilation rate, with f_{SLA} is the fraction sunlit leaf area.

$$P_{g\ L}(l_1) = \sum_{l_1=1}^{3} W_g(l_1) \left(f_{SLA} * P_{g\ sun}(l_1) + (1 - f_{SLA}) * P_{g\ shd}(l_1)\right) \qquad [mg\ CO_2\ m^{-2}\ leaf] \quad 4.54$$

The shaded irradiation is in fact the diffuse radiation inside the greenhouse ($I_{A\ dif}$) and the difference between the mean total absorption ($I_{A\ tdir}$) and absorption of direct radiation of sunlit leaves ($I_{A\ dir}$) (Goudriaan and Van Laar, 1994). This difference represents the absorption of scattered radiation.

For the shaded and sunlit irradiation, the following equations are used:

$$I_{A\ sun}(l_1, l_2) = I_{A\ shd}(l_1) + I_{A\ ppd}(l_1) * X_g(l_2) \qquad [W\ m^{-2}\ soil] \quad 4.55$$

$$I_{A\ shd}(l_1) = I_{A\ dif}(l_1) + I_{A\ tdir}(l_1) - I_{A\ dir}(l_1) \qquad [W\ m^{-2}\ soil] \quad 4.56$$

Below a table is given for the calculation of the diffuse and direct radiation at different layers.

Table 12. Formulas for diffuse and direct radiation at layer depth l_1.

$I_{A\ dif}(l_1) = (1 - \beta_{dif}) * I_{P\ dif} * k_{dif} * \tau_{dif}(l_1)$	Diffuse radiation at leaf layer l_1	$[W\ m^{-2}\ leaf]$	4.57
$I_{A\ tdir}(l_1) = (1 - \beta_{dir}) * I_{P\ dir} * k_{dir} * \tau_{dir}(l_1)$	Total direct radiation at leaf layer l_1	$[W\ m^{-2}\ leaf]$	4.58
$I_{A\ dir}(l_1) = (1 - s) * I_{P\ dir} * k_{dirBL} * \tau_{dirBL}(l_1)$	Direct radiation at leaf layer l_1	$[W\ m^{-2}\ leaf]$	4.59
$I_{A\ ppd}(l_1) = \frac{1 - s}{sin\beta} * I_{P\ dir}$	Direct flux leaves perpendicular to direct beam	$[W\ m^{-2}\ leaf]$	4.60

$I_{P\ dif}$ and $I_{P\ dir}$ are the diffuse and direct light in greenhouse. These are calculated with the transmittance of the roof for diffuse (τ_{difR}) and direct (τ_{dirR}) light. The fraction diffuse or direct light is not constant throughout the year; each day the diffuse ($I_{P\ difO}$) and direct radiation ($I_{P\ dirO}$) is different. The formulas for the calculation of transmittance and the direct and diffuse light outside can be found in appendix 10.2, Table 30.

$$I_{P\ dif} = \tau_{difR} * I_{P\ difO} \qquad [W\ m^{-2}\ soil] \qquad 4.61$$

$$I_{P\ dir} = \tau_{dirR} * I_{P\ dirO} \qquad [W\ m^{-2}\ soil] \qquad 4.62$$

Below all extinction coefficients are given (k_x). The diffuse coefficients (k_{dif}, k_{difBL}) are constant in time and layer depth. The direct extinction coefficients (k_{dir}, k_{dirBL}) are also constant for each layer depth, but they depend on the position of the sun. The transmittance (τ_x) is calculated with the extinction coefficients and it is layer depth dependent. These equations can be found in appendix 10.2. The diffuse and direct extinction coefficients are calculated with following formulas and scattering coefficient (s):

$$k_{dif} = k_{difBL} * \sqrt{1-s} \qquad [-] \qquad 4.63$$

$$k_{dir} = k_{dirBL} * \sqrt{1-s} \qquad [-] \qquad 4.64$$

$$k_{dirBL} = \frac{slo}{sinB} \qquad [-] \qquad 4.65$$

The solar declination (δ_{sun}) is the angle between the horizontal plane and position of the sun.

$$\delta_{sun} = \text{asin}\left(sin\left(2\pi * \frac{23.45}{365}\right) * cos\left(2\pi * dayN + \frac{10}{365}\right)\right) \qquad [°C] \qquad 4.66$$

SinB is the sine of the solar elevation, which has to be calculated for each hour with the following formulas. Obviously, the position of the sun changes during the day, therefore the solar time corrected for the Middle European time is calculated.

$$SOL_{hr} = hour - \left(1 - \frac{long}{15}\right) \qquad [h] \qquad 4.67$$

$$sinB = \sin(lat) * \sin(\delta_{sun}) + \cos(lat) * \cos(\delta_{sun}) * \cos\left(2\pi * \frac{SOL_{hr} - 12}{24}\right) \qquad [-] \qquad 4.68$$

4.2.3 Triose phosphate use

As mentioned in the literature study in chapter 2, triose phosphate use (TPU) can inhibit photosynthesis at high light intensities and CO_2 concentrations. This inhibition occurs if the rate for making starch and sucrose from triose phosphates is slower than Rubisco carboxylation and regeneration. Due to the fact that TPU can inhibit the CO_2 assimilation rate the net max assimilation rate calculation (eq 3.8) is extended for TPU limitation. TPU is calculated with the carboxylation (V_c) and oxygenation rate (V_o). V_c can be calculated by using the maximum carboxylation rate, CO_2 concentration, Michaelis-Menten carboxylation (K_c) and oxygenation (K_o). The maximum carboxylation rate is derived from J_{max}, namely there is linear relationship between J_{max} and $V_{c\ max}$ (Walcroft et al., 1997). In the last divisor of equation 4.69 the oxygenation is multiplied with α_{TPU}, which represents the fraction of glycolate carbon not returned to the chloroplast (Von Caemmerer, 2000).

$$TPU = \frac{V_c}{3} - \frac{Foc * V_c}{6} - \frac{\alpha_{TPU} * Foc * V_c}{2} \qquad [\mu mol\ m^{-2}\ leaf\ s^{-1}] \qquad 4.69$$

V_c can be calculated using the electron transport rate at a given irradiance or by using carboxylation velocities (Farquhar et al., 1980; Von Caemmerer, 2000). Since the influence of light on J_{max} is unknown, V_c is determined with the carboxylation velocity.

$$V_C = V_{c\,max} * \frac{CO_2}{CO_2 + K_c * \left(1 + \frac{O}{K_o}\right)} \qquad [\mu mol\ m^{-2}\ leaf\ s^{-1}] \quad 4.70$$

After calculation of V_c and TPU, the maximum CO_2 assimilation rate by TPU can be calculated with equation 4.71. Normally the mitochondrial respiration (R_d) is subtracted. However, the minimum of P_{nc} and P_{mm} and A_p determines which process is limiting for CO_2 uptake. As a result, R_d is subtracted at the end of the model.

$$A_p = 3 * TPU * M_{CO_2} \qquad [mg\ CO_2\ m^{-2}\ leaf\ s^{-1}] \quad 4.71$$

4.2.4 Conversion mg CO_2 to biomass

In order to estimate the generated biomass, the CO_2 assimilation rate has to be converted to fresh weight. First the gross assimilation rate has to be converted to the net assimilation and multiplied with the correction factors.

$$P_{g\,N} = \left(P_{g\,L} * LAI - rD * MCO_2\right) * pH_{corr} * Mat_{corr} * N_{corr} \qquad [mg\ CO_2\ m^{-2}\ soil\ s^{-1}] \quad 4.72$$

Then CO_2 assimilation rate is converted to formaldehyde (CH_2O, c_{cs}), subsequently the amount of formaldehyde is converted to kg DM. Additionally the equation is divided by the DM percentage, since the production data is also in FW.

$$f_{w_{CO_2}} = \frac{c_{cs}}{ASRQ} * \frac{1}{DM} \qquad [kg\ FW\ kg^{-1}CO_2] \quad 4.73$$

Consequently, this is multiplied with the net assimilation rate ($P_{g\,N}$).

$$\frac{dFW}{dt} = f_{w_{CO_2}} * P_{g\,N} \qquad [kg\ FW\ m^{-2}\ soil\ s^{-1}] \quad 4.74$$

4.2.5 Modelling nutrients

4.2.5.1 Intrinsic growth rate

The photosynthetic model is made with the assumption that the nutrient concentration is always optimal. It might be possible that the nutrients become limiting, therefore a correction factor is applied. It is also possible to calculate the growth rate during integration and limit the growth rate if it is larger than the maximum growth rate at a given nutrient concentration. Due to the fact that the parameters of the photosynthetic model are affected at low concentrations (Walcroft et al., 1997), it is better to multiply the net assimilation rate with a factor.

The intrinsic growth rate as a function of nutrient concentration is determined with the following Michaelis-Menten models (Lasfar et al., 2007):

$$r_iN = \alpha_N * \frac{C_N}{(C_N + K_N)} * \frac{K_{IN}}{(K_{IN} + C_N)} \qquad [d^{-1}] \quad 4.75$$

And for phosphorus:

$$r_iP = \alpha_P * \frac{C_P}{(C_P + K_P)} * \frac{K_{IP}}{(K_{IP} + C_P)} \qquad [d^{-1}] \quad 4.76$$

Normally Michaelis-Menten models do not have parameters similar to K_{IN}, and K_{IP}, however high concentrations can inhibit growth. Therefore the last terms were added (Lasfar et al., 2007). After calculating r_iN and r_iP, the correction factor N_{corr} is calculated with equation 4.75 or 4.76.

$$N_{corr} = \min\left(\frac{e^{r_iN}}{e^{r_iNmax}}, \frac{e^{r_iP}}{e^{r_iPmax}}\right) \qquad [-] \quad 4.77$$

4.2.5.2 N & P consumption and addition of nutrients

For determining the concentration N and P as a function of time, the consumption rates have to be determined. The model of Zhang (2014) overestimated the consumption rate (Figure 1), since consumption rates higher than 665 mg N m^{-2} d^{-1} are unlikely. Unfortunately, there are no other models that describe the uptake of N as a function of the concentration. However, it is possible to determine the consumption rates based on generated biomass (Δx) and N or P content of the fronds. This method has been done for *Lemna minor,* which gave accurate results, as long there were no microalgae present (Frédéric et al., 2006).

$$N_{conc} = N_{conc\ Old} + \frac{tNk * N_{concL}}{Volume} + \frac{\Delta N_{air} * A_{pond}}{Volume} - \frac{\Delta x * N_{content} * DM * 10^6}{Volume} \qquad [mg\ N\ L^{-1}] \quad 4.78$$

The equation above describes the increase of N by adding thin fraction. $N_{conc\ Old}$, is the old concentration from previous integration. To calculate the increase in the N concentration the amount of litre thin fraction (tNk) added is multiplied with the N_{concL} and divided by the volume. Moreover, the concentration was influenced by ammonia in the air (paragraph 4.2.5.3). ΔN_{air} is the integral of equation 4.80 minus the integral of previous time step. According to the report some trace elements have been added, yet none of these trace elements contain phosphorus. However, iron nitrate and manganese nitrate contain nitrogen atoms. The concentrations were ±7.5 µmol L^{-1} Fe and ±5 µmol L^{-1} Mn. This means that if the trace elements are added the concentration N in the water increases with 0.18 mg N L^{-1} [1]. The last term in the formula represents the consumption rate as a function of generated biomass and the percentage N per DM ($N_{content}$). The $N_{content}$ of duckweed is concentration dependent. Points of Figure 2 are used to derive their logarithmic relationship (see equation 4.79). Furthermore, the generated biomass (Δx) is multiplied with the dry matter content, 10^6 is a conversion for kg to mg. The formula for P consumption rate is similar, only some parameters have different values.

$$N_{content} = \frac{12.59 * \ln(N) + 32.013}{1000} \qquad [\%] \quad 4.79$$

Equation 4.79 is only valid if N<9 mg N L^{-1}, otherwise the $N_{content}$ is equal to 5.7%.

4.2.5.3 Ammonia mass transfer coefficient

As mentioned in the literature study in chapter 2, it is possible that ammonia in the air dissolves in water. The rate depends on the mass transfer coefficients, Henry's law and concentrations in gas and liquid. During the calculations, it is assumed that the concentration in the air is constant.

$$\phi''_m = \frac{C^g_{m,b} - m_{gl} C^l_{m,b}}{\frac{m_{gl}}{k_l} + \frac{1}{k_g}} \ or \ \frac{\frac{C^g_{m,b}}{m_{gl}} - C^l_{m,b}}{\frac{1}{k_l} + \frac{1}{m_{gl} k_g}} \qquad [mg\ N\ m^{-2}\ s^{-1}] \quad 4.80$$

m_{gl} is determined with the inverse of Henry's law (inverse of H; equation 2.1), k_l and k_g are the mass transfer coefficients. Due to the fact that H/k_l is relatively small, the total mass transfer coefficient (K^2) is equal to k_g (Ibusuki and Aneja, 1984). K is temperature independent and constant from 0.02 to 0.12 µmol NH_3 L^{-1}. Unfortunately, no other values are found in literature, therefore it is assumed that K is also constant for higher concentrations.

4.2.6 Mat density limitations

The light use efficiency formula is based on tomato plants and takes into account the effect of light at increased mat densities. An increased mat density results in an elevated LAI. It is possible that the mat density becomes extremely high. However, mat densities higher than 177 g FW m^{-2} are theoretically not possible (Frédéric et al., 2006). The maximum growth rate is mainly at low mat densities and the maximum production is at 82 g FW m^{-2} (Frédéric et al., 2006). The increase in the mat density can be calculated with 4.81 and 4.82.

[1] Total N in Fe and Mn= 12.5 µmol L^{-1}

[2] $\frac{1}{K} = \frac{H}{k_l} + \frac{1}{k_g}\ cm\ s^{-1}$

$$r_i = \frac{\ln(x(1)) - \ln(Xold)}{\Delta t} \qquad [g\ FW\ m^{-2}\ soil] \quad 4.81$$

To determine the optimal mat density, equation 4.82 is calculated for all mat densities. Subsequently the optimal mat density is compared with the current mat density. The result of this comparison is converted to a fraction between 0 to 1. The assimilation rate is multiplied with this factor. However, this correction is only applied when current mat density was higher than the optimal density at given growth rate. Otherwise the assimilation rate is limited because the mat density is too low, which is not correct. Namely, the production is limited, because the mat density is not optimal, but the growth rate is not inhibited at low mat densities.

$$D = \frac{D_l * D_o}{(D_l - D_o)e^{(-r_i * h)} + D_o} \qquad [g\ FW\ m^{-2}\ soil] \quad 4.82$$

4.2.7 Dark respiration rate

The dark respiration rate (rD_{ul}) was previously assumed to be constant, although according to literature the dark respiration is light intensity dependent (Fuhrer, 1983). rD_{ul} is inhibited for increased light intensities. Unfortunately, no model exists for this inhibition, therefore a model has been made based on Table 13. The net assimilation rate ($P_{g\ N}$) is determined by subtracting rD from the gross leaf assimilation $P_{g\ L}$, with rD (rD_{ul}*LAI), since the $P_{g\ N}$ is in m^{-2} [soil] and not m^{-2} [leaf].

$$rD_{ul} = \left(0.23 + (1 - 0.23) * \mathrm{e}^{-1.6*10^{-4}*I_m*\zeta}\right) * rD_{ul}0 \qquad [\mu mol\ m^{-2}\ leaf\ s^{-1}] \quad 4.83$$

Table 13. Inhibition of dark respiration at given light intensities.

Light intensity [µmol m^{-2} leaf s^{-1}]	0	50	80	150	370	500
Fraction inhibition rDul	1	0.65	0.45	0.30	0.23	0.23

4.3 Correlation coefficient

The correlation coefficient matrix is determined to establish which parameter are correlated. First the Jacobian matrix is calculated. This matrix is the partial derivative of the output y divided by the change of the parameters. A summary of this formula is given below. The size of the matrix is determined by the amount of measurements N and the amount of parameters N_p ($N*n_p$).

[–] 4.84

$$J = \begin{bmatrix} \frac{\partial y(1|p)}{\partial p_1} & \frac{\partial y(1|p)}{\partial p_2} \\ \frac{\partial y(2|p)}{\partial p_1} & \frac{\partial y(2|p)}{\partial p_2} \\ \vdots & \vdots \\ \frac{\partial y(N|p)}{\partial p_1} & \frac{\partial y(N|p)}{\partial p_2} \end{bmatrix}$$

Then the covariance is determined:

$$cov = \frac{V}{N - n_p} * (J' * J)^{-1} \qquad [-] \quad 4.85$$

The diagonal of the covariance gives the variance (varP). Given the square root of the variance (stdp) and the covariance matrix, the correlation coefficient (cc) can be calculated.

$$cc = \frac{cov}{stdp * stdp'} \qquad [-] \quad 4.86$$

4.4 Lasfar's model

The result obtained with optimal management of the photosynthetic model is compared with the results of Lasfar's model (Lasfar et al., 2007). Already a part of this model is used in the photosynthetic model at nutrient deficit conditions and at high mat densities. The model is given below and it is photoperiod dependent. The model is simulated with the water temperature. Although the system is simulated with a time step of 0.05 day, the correction factor for the photoperiod is only determined once a day.

$$r_i L = R * f(T) * g(E) * \frac{C_N}{(C_N + K_N)} * \frac{K_{IN}}{(K_{IN} + C_N)} \frac{C_P}{(C_P + K_P)} * \frac{K_{IP}}{(K_{IP} + C_P)} \quad [d^{-1}] \quad 4.87$$

$$f(T) = \theta_1^{\left(\frac{T - T_{op}}{T_{op}}\right)^2} * \theta_2^{\frac{T - T_{op}}{T_{op}}} \quad [-] \quad 4.88$$

$$g(E) = \theta_3^{\left(\frac{E - E_{op}}{E_{op}}\right)^2} * \theta_2^{\frac{E - E_{op}}{E_{op}}} \quad [-] \quad 4.89$$

After the intrinsic growth rate ($r_i L$) is calculated, equation 4.82 is used to determine the increase in mat density. This increase is compared with the production of the photosynthetic model with similar inputs.

4.5 Modelling feed requirements

To determine the economic possibilities for duckweed the composition of the fodder should be taken into account. In Table 14 the requirements are given for cattle feed. For some cattle feed the maximum daily uptake is given (Table 15). In combination with the cost per ton of each raw material the reduced feed costs by cultivating duckweed can be calculated. Unfortunately, the maximum uptake of fresh duckweed is unknown. From the report of the company, daily water uptake was ±20.8 L d^{-1} per animal, which is in agreement with literature (Atkeson et al., 1934). It assumed that a maximum of 0.3 kg DM duckweed per animal per day is consumed, since it is unlikely that more than 25% of daily water requirement is taken up by eating duckweed. The rosé calves had a starting weight of 110 kg and an end weight of 400 kg; during a year the average weight was ±225 kg. The composition of the fodder changes during growth, however for modelling, it was assumed to be constant. The average weight of 225 kg is used in the model. At this weight one rosé calve eats 5 kg DM a day (CVB, 2012). Simulations were done with a yield of 9 ha grass and 36 ha maize, where each day the same amounts of grass and maize were given to the animals. At ECOFERM duckweed was not dried, but directly given to the animals. For each month, the daily average of the duckweed production is used. Simulations are done with the constraints given in Table 14 and Table 15.

Table 14. Feed requirements rosé calves; values 1030, 1170 and 79.1 from (CVB, 2012) all other values from Kroes (2016).

	Minimum	Maximum
VEVI units/kg DM	1030	1170
DVE g/kg DM	79.1	120
OEB kg/ton DM	0	65
dvLYS g/100g RE	5.5	9
dvMET g/ 100g RE	2.1	2.5
NDF kg/ton DM	265	500
P kg/ton DM	4.5	10
Starch kg/ton DM	140	350
DM per day at 225 kg	[-]	5

Table 15. Composition of all raw materials ('Forfarmers', 2016).

	Wheat straw	Duckweed	Grass sil.	Maize sil.	Soy60RC	Potatoes Parings	Turnip flakes	Sugar Beet pulp
DM	900	52	470	300	880	220	890	900
VEVI	336	871	913	950	1242	1248	1185	1014
DVE	-4	140	65	47	267	85	137	93
OEB	-17	236	63	-28	213	-60	152	-62
dvLYS	0.7	7.8	3.5	3.1	17.4	6.2	8.6	6.4
dvMET	0.3	1.3	1.3	1.2	4.4	2.1	3.2	2.1
NDF	745	231	499	390	145	75	261	366
P	1.1	10.4	4.2	2	7.3	1.9	11	0.8
Starch	0	15	0	304	10	695	22	0
Limit	30% kg tot.	0.3 kg DM	70% tot.	70% tot.	Max 2 kg	Max 10 kg	Max 2 kg	max 3 kg
€ / DMton	110	[-]	[-]	[-]	370	200	280	195
*tot.=total								

The feed requirement for pigs is different and based on the energy value (EW), phosphorus (P), calcium (Ca) and intestinal digestible amino acids (dv(MET+CYS), dvLYS, dvTHR and dvTRP). Compared to rosé calves, methionine and lysine are essential, due to the fact that these amino acids cannot produced by the pigs themselves (Gwaze and Mwale, 2015). 50% of the protein content in a soy diet for pigs can be replaced by duckweed (Le thi Men et al., 1997). The minimum requirements are given below. Unfortunately, the cysteine (CYS) content of some raw materials is unknown, however in dvMET+CYS a minimum of 55% methionine is required. Therefore, the system is simulated with dvMET=0.55*dv(MET+CYS).

Table 16. Requirements pig feed (Wertenbroek et al., 2013).

	Minimum	Maximum
EW	2.1	2.6
dvLYS g/EW	6.4	7.8
dvMET g/EW	2.4	2.8
P g/EW	1.9	2.3
Ca g/EW	5.7	6.9
DM per day at 225 kg	[-]	5

On the next page, a summary is given of the most important processes to determine the duckweed production. The circles with a light blue background colour are inputs. The light blue rectangles represent the output of an equation of which the arrows to the rectangles are inputs. The subscript numbers in these rectangles show in which paragraph more information can be found. The dark rectangles are integrated with Runge-Kutta. Furthermore, the circles with a white background colour are inputs in the model which change at each time step. These are calculated with the blue lines.

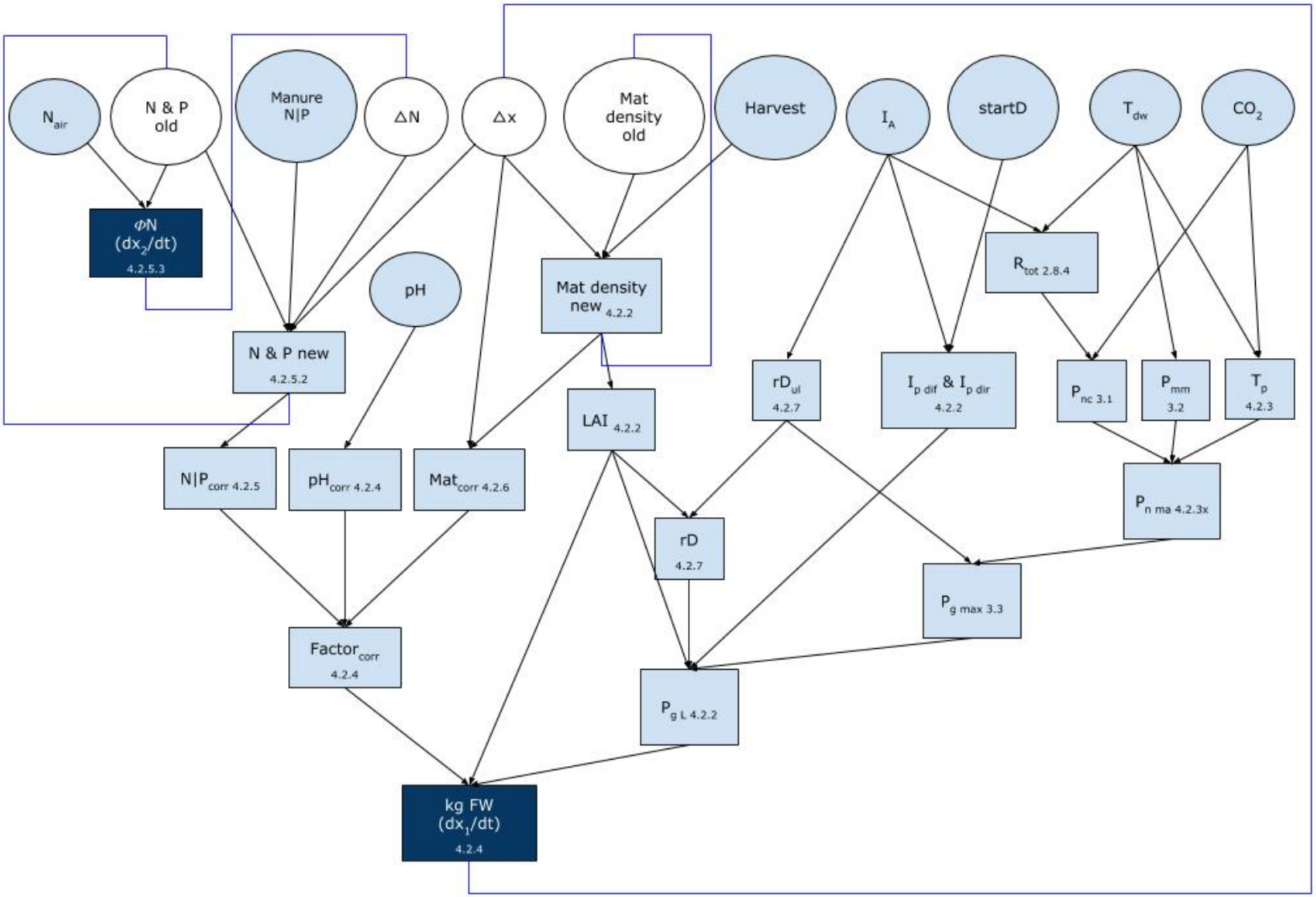

Figure 12. Summary of all processes that are calculated to determine the kg FW duckweed with given inputs (circles).

Table 17. All parameters and variables of paragraphs 4.2 to 4.5.

Mat density			
Mat_{new}	New mat density	eq 4.49	$[g\ FW\ m^{-2}]$
Mat_{old}	Old mat density from previous time step	input	$[g\ FW\ m^{-2}]$
$Harvest(ZB)$	Amount of duckweed harvested at time t	input	$[kg\ FW]$
Δx	Increase in biomass	input	$[kg\ FW]$
TPU			
$V_{c\,max}$	Maximum carboxylation rate	model	$[\mu mol\ m^{-2}\ s^{-1}]$
V_c	Carboxylation rate of RuBp	eq 4.70	$[\mu mol\ m^{-2}\ s^{-1}]$
Foc	Fraction oxygenation and carboxylation	0.21	$[\frac{V_{o\,max}}{V_{c\,max}}]$
α_{TPU}	Fraction gluconate carbon not returned to chloroplast	0.5	$[-]$
CO_{2a}	CO_2 concentration in the air of the greenhouse	input	$[ppm]$
K_{c25}	Michaelis-Menten carboxylation at 25°C	310	$[\mu bar]$
K_{o25}	Michaelis-Menten oxygenation at 25°C	155	$[mbar]$
K_c	Michaelis-Menten carboxylation	eq 10.2	$[\mu bar]$
K_o	Michaelis-Menten oxygenation	eq 10.3	$[mbar]$
E_c	Activation energy K_c	59356	$[J\ mol^{-1}]$
E_o	Activation energy K_o	35948	$[J\ mol^{-1}]$
O	Partial pressure O_2 inside stomata	210	$[mbar]$
M_{CO_2}	Molar mass CO_2	$44*10^{-3}$	$[mg\ \mu mol^{-1}]$
$JtoVc$	Conversion factor J_{max} to $V_{c\,max}$	2.68	$[-]$
Conversion CO_2 to biomass			
$P_{g\,N}$	Net assimilation rate corrected for the pH, Mat density and nutrients	eq 4.72	$[mg\ CO_2\ m^{-2}\ soil\ s^{-1}]$
rD	Total dark respiration	eq 4.83*LAI	$[\mu mol\ CO_2\ m^{-2} soil\ s^{-1}]$
$dFW\ dt^{-1}$	Amount of kg produced biomass per second	eq 4.74	$[kg\ FW\ m^{-2} soil\ s^{-1}]$
c_{cs}	Conversion CO_2 to CH_2O	30/44	$[kg\ CH_2O\ kg^{-1}\ CO_2]$
$ASRQ$	Conversion CH_2O to kg FW	1.2	$[\ kg\ CH_2O\ kg\ DW]$
Modelling nutrients			
C_N	Nitrogen concentration	input	$[mg\ N\ L^{-1}]$
K_N	Constant for inhibition at low C_N	0.95	$[mg\ N\ L^{-1}]$
K_{IN}	Constant for inhibition at elevated C_N	604	$[mg\ N\ L^{-1}]$
C_P	Phosphorus concentration	input	$[mg\ P\ L^{-1}]$
K_P	Constant for inhibition at low C_P	0.31	$[mg\ P\ L^{-1}]$
K_{IP}	Constant for inhibition at elevated C_P	101	$[mg\ P\ L^{-1}]$
N_{corr}	Correction factor at limiting concentrations	eq 4.77	$[-]$
N & P consumption formula			
$N_{conc\,Old}$	Nitrogen concentration from previous integration	input	$[mg\ N\ L^{-1}]$
tNK	Vector with amount and time when thin fraction was added	input	$[L\ thin\ fraction]$
N_{concCL}	Nitrogen concentration thin fraction	4016.6	$[mg\ N\ L^{-1}]$
ΔN_{air}	Amount of ammonia from air to water	model	$[mg\ N\ m^{-2}]$
$N_{content}$	Nitrogen content of duckweed	model	$[\%]$
P_{concCL}	Phosphorus concentration thin faction	634.9	$[mg\ P\ L^{-1}]$

Ammonia mass transfer coefficient			
$C_{m,b}^{g}$	Nitrogen concentration (gas)	4	$[mg\ N\ L^{-1}]$
$C_{m,b}^{l}$	Nitrogen concentration (liquid)	equal C_N	$[mg\ N\ L^{-1}]$
H	Henry constant	eq 2.1	$[liquid/air]$
m_{gl}	Inverse of Henry constant	1/H	$[air/liquid]$
k_l	Mass transfer coefficient liquid	-	$[m\ s^{-1}]$
k_g	Mass transfer coefficient gas	0.0265	$[m\ s^{-1}]$
K	Total mass transfer coefficient	0.0265	$[m\ s^{-1}]$
ϕ_m''	Mass transfer from air to water	eq 4.80	$[mg\ m^{-2}\ s^{-1}]$
Mat density			
D_l	Limited mat density	177	$[g\ DW\ m^{-2}]$
D_o	Current mat density	input	$[g\ DW\ m^{-2}]$
r_i	Intrinsic growth rate	eq 4.81	$[d^{-1}]$
h	Time step Runge-Kutta	0.05	$[d^{-1}]$
Dark respiration			
I_m	Measured irradiation in greenhouse	input	$[W\ m^{-2}]$
ζ	Conversion factor from W m^{-2} to µmol m^{-2} s^{-1}	4.59	$[\mu mol\ J^{-1}]$
$rD_{ul}0$	Dark respiration rate at 0 µmol m^{-2} s^{-1}	1.36	$[\mu mol\ m^{-2}\ leaf\ s^{-1}]$
rD_{ul}	Dark respiration rate	eq 4.83	$[\mu mol\ m^{-2}\ leaf\ s^{-1}]$
Correlation coefficient and sensitivity			
J	Jacobian matrix	eq 4.84	$[-]$
V	Error of model compared with harvested data	-	$[-]$
N	Amount of measurements	-	$[-]$
n_p	Amount of parameters	18	$[-]$
cov	Covariance matrix	eq 4.85	$[-]$
$varP$	Diagonal of covariance matrix	-	$[-]$
$stdp$	Standard deviation	-	$[-]$
cc	Correlation coefficient matrix	eq 4.86	$[-]$
Lasfar's model			
R	Standard growth rate	0.62	$[d^{-1}]$
r_iL	Intrinsic growth rate Lasfar's model	eq 4.87	$[d^{-1}]$
$f(T)$	Correction factor for water temperature	eq 4.88	$[-]$
$g(E)$	Correction factor for photoperiod	eq 4.89	$[-]$
θ_1	Parameter for correction water temperature	0.0025	$[-]^{*2}$
θ_2	Parameter for correction water temperature	0.66	$[-]^{*2}$
T_{op}	Optimal water temperature	26	$[°C]$
θ_3	Parameter for correction photoperiod	0.0073	$[-]^{*2}$
θ_4	Parameter for correction photoperiod	0.65	$[-]^{*2}$
E_{op}	Optimal water temperature	13	$[h]$

[*2] In the research of Lasfar (2007), the values of these parameters are mentioned in the wrong order. In this table the values belong to the correct parameter.

5 Results

5.1 Temperature model

In the previous chapter, the formulas are given to determine the temperature of duckweed (T_{dw}). However, for determining T_{dw} also the roof temperature (T_r), soil temperature (T_s) and stable temperature (T_{st}) had to be calculated. Below the results of the month May are given. In the figures, the temperature is given as a function of time. The fluctuations are caused since temperature changes during day and night. The left figure is less clear, since a lot of temperatures are shown. However, it is given to be aware of all temperature processes that are calculated or measured. The soil temperature is relatively high compared to the temperature in the greenhouse (Figure 13B). This figure compares the soil temperature with the greenhouse temperature. On average the T_s is higher than the T_g. Irradiation of the sun is in an important factor for the relatively high T_s. This irradiation is absorbed by the soil; as a result, the temperature increases. Moreover, little energy of the soil is removed by convection, since the airflow in the greenhouse is relatively low.

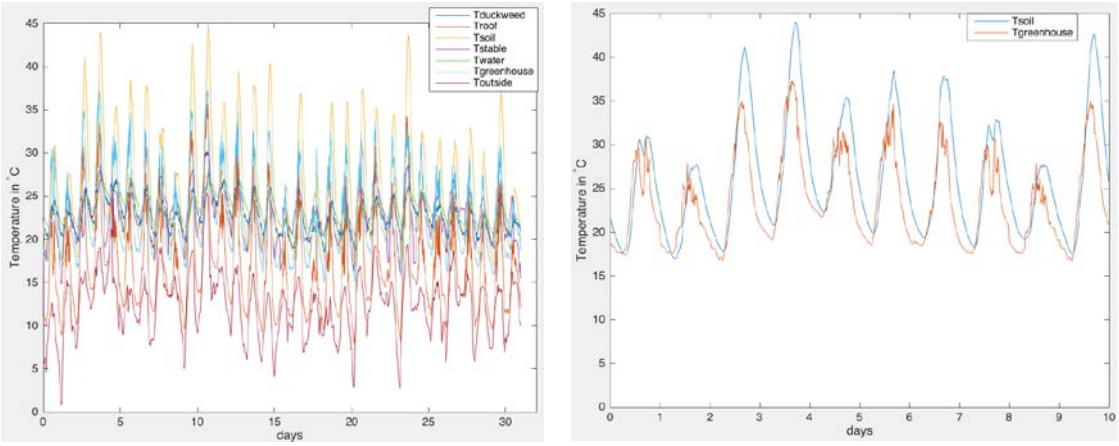

Figure 13A & B. The left image shows all temperature processes in May. Figure B shows the T_s compared with the T_g for the first ten days.

The roof temperature is on average 6.1°C lower than the greenhouse temperature (Figure 14A). Convection from the greenhouse and longwave radiation from the soil and duckweed to the roof increased the T_r. However, a lot of energy is lost by convection to outside and evaporation of water; as a result, T_r is lower than T_g. The temperature of the stable is also calculated to make the energy process complete, this result can be found below. The temperature of the stable is on average lower than the greenhouse temperature, because there is no irradiation from the sun. Moreover, the stable has ventilation with the outside air.

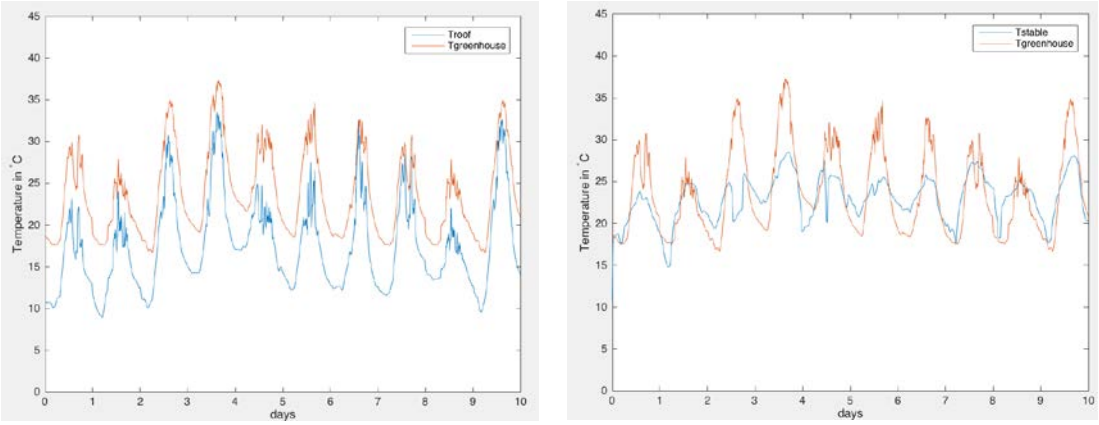

Figure 14A & B. Result of the T_r and T_g in May for the first ten days, clearly the T_r is lower than the T_g. Figure B shows the T_{st} compared with the T_g. On average, the T_{st} is lower than the T_g.

From physics, it is expected that in the months with a lot of radiation, the temperature of duckweed is higher than the water temperature. In Figure 15A the irradiation of the month July to September is given. Obviously, the irradiation in July is generally higher than in the other months. The irradiation in June was even higher; however, at this month, the pond was not covered with duckweed and therefore this data is not taken into account. The difference between T_{dw} and T_w is higher in July than in September and October. This difference might be caused by fact that the greenhouse is on top of a stable. As a result, conduction through the concrete increased the T_w. These temperature comparisons are given in Figure 15B for the first 10 days of July. However, from the graph during daytime the T_{st} is almost similar as T_w and T_{dw}. Consequently, the increase of the T_w by heat conduction through the concrete is relatively low. As a result, it is more likely that the lower temperature of duckweed than water is caused by another process for example evapotranspiration or a low greenhouse temperature in the night.

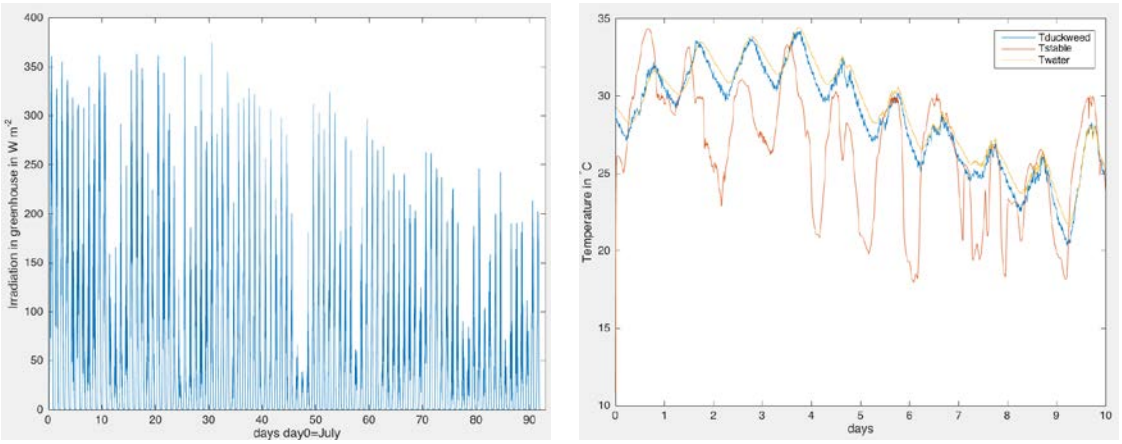

Figure 15A & B. Figure A shows a decreasing irradiation from July to September. (Figure B) Comparison of T_{dw} with T_w and T_{st}.

During the night, the duckweed temperature is much lower than T_w, which is partly caused by a lower greenhouse temperature. In the figures below, the water temperature shows fewer fluctuations than the greenhouse temperature, this is partly because the duckweed performs as an isolation layer. As a result, the water temperature does not fluctuate as much. Moreover, water has a high heat capacity, combined with the volume much energy is needed to increase the water temperature. Despite the fact that the model of the duckweed temperature has a lot of equations, the result shows that the temperature of duckweed does not differ much from the water temperature.

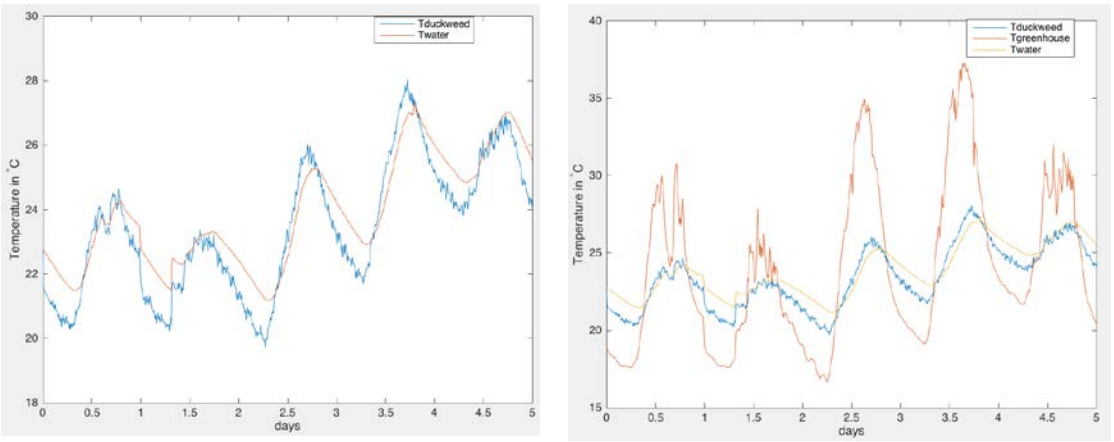

Figure 16A & B. T_{dw} compared with T_w and T_g in May. The water and duckweed temperature are relatively similar and do not fluctuate as much as the temperature of the greenhouse. During the night both T_{dw} and T_g are lower than T_w (B).

Another important process is the evapotranspiration of water by duckweed. In the model, this process is calculated with the Penman-Monteith equation. This model is partly based on the vapour pressure deficit. September and October had duckweed temperatures closer to T_w and relatively high humidity's of 91% or larger. July had a relative humidity of 83%. Calculations of September with a constant RH of 83% resulted in an increased difference between T_{dw} and T_w of 13.6%[3]. In other words, if the relative humidity decreases, the average temperature of duckweed is lower. This indicates that evapotranspiration has much influence on the duckweed temperature. Below the result of the total evaporated water in May is given. For comparisons with literature, the model is also simulated with a higher airflow. This results in an increased evapotranspiration of water.

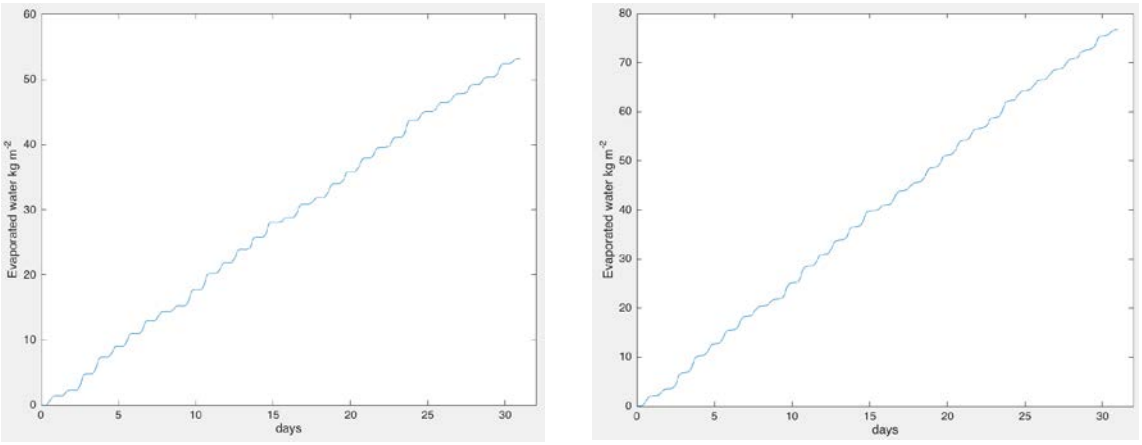

Figure 17A & B. Total evaporation per square meter in May, left result with VwindG=0.09 m s^{-1} and right with VwindG=3.2 m s^{-1}.

5.2 Consumption nutrients and parameter estimation

5.2.1 Nutrient uptake

Before determining the influence of the nutrient concentration on the model, the concentration has to be determined. In the figures on the next page the concentration of N and P in the pond are given as a function of time. The initial nutrient concentration is set to 20 mg N L^{-1} and 10 mg P L^{-1}. Already in one month, all nitrogen was removed. As a result, growth will be strongly reduced, since optimal N concentrations are between 7 and 20 mg N L^{-1} (Caicedo et al., 2000; Lasfar et al., 2007). Different values are also found in literature, but these values are certainly in the optimal range. Moreover, Figure 18A gives the N consumption in the pond calculated with the harvested data from the company. The figure is relatively static due to the fact that only the harvested data was used to determine the nutrient consumption. Figure 18B represents the result from the simulated biomass. Sometimes the concentration increases without adding thin fraction, because dark respiration caused a decrease of the total biomass during night. As a result, less N is taken up by duckweed, which results in a slight increase in the nutrient concentration. From the figures and uptake rates obviously too little thin fraction is added to have optimal nutrient concentrations. Especially the N concentration starts to inhibit photosynthesis early. The yellow and purple lines in Figure 18B at which concentrations growth is inhibited (Lasfar et al., 2007).

3 $\frac{dif_{new}-dif_{old}}{dif_{old}} = \frac{-0.3972+0.3497}{-0.3497}$

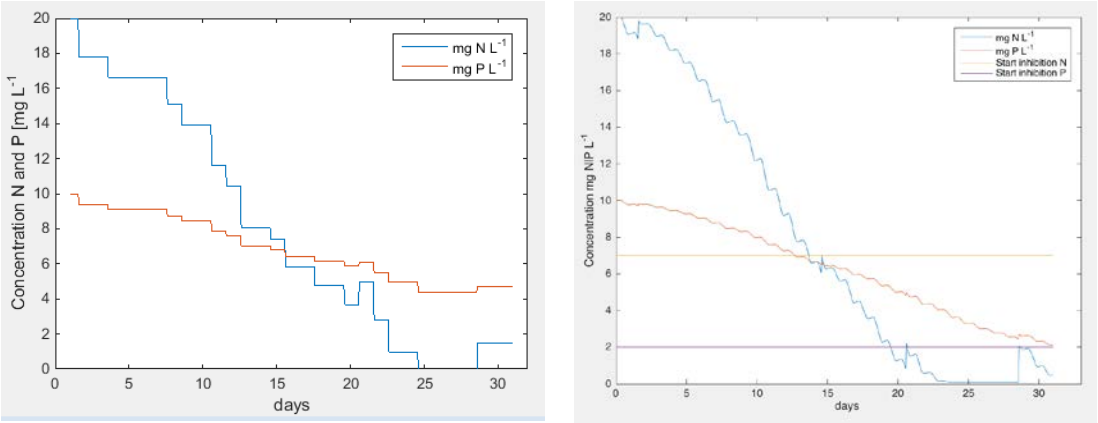

Figure 18A & B. (Left) Static nutrient consumption N and P consumption as function of time. (right) N and P consumption photosynthetic model, both figures are without the influence of ammonia from the air.

According to paragraph 2.2.4 the ammonia from the air can increase the N concentration. The results with assuming a constant NH_3 concentration of 6 ppm in the air are given below. The left figure is with ammonia from air and right without. Both graphs have similar trends, namely the concentration N and P concentrations are decreasing over time. Figure 19A shows more fluctuations and the concentration is generally more than 1 mg N L^{-1}. In contrary to Figure 19B, the concentration decreases faster and after 7 days the concentration becomes almost zero. This result is obtained with a higher mat density, otherwise too much duckweed was harvested and the mat density became zero. A lower concentration in the air would result in faster nitrogen consumption caused by volatilization of ammonia. Dissolving of ammonia clearly results in an increase in N concentration. As a result, growth is still possible despite the fact that the concentrations are not optimal.

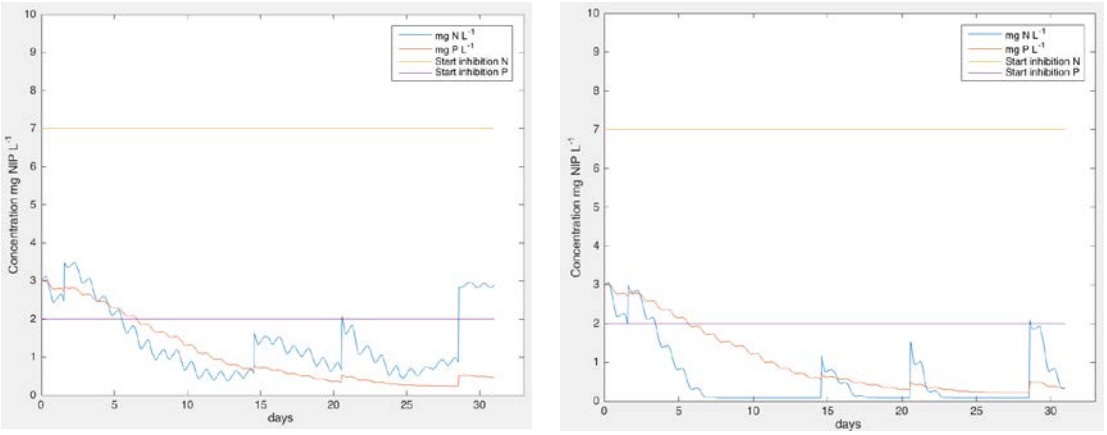

Figure 19A & B. Nitrogen concentration in May as a function of time. Figure A with an ammonia concentration of 6 ppm, and B without ammonia in the air.

5.2.2 Sensitivity and correlation matrix

A sensitivity analysis has been done to determine which parameters are most sensitive and therefore most promising for parameter estimation. From the ECOFERM report it is found that nitrogen was only added by adding thin fraction and trace elements. From the results above the volatilization and nutrient uptake by duckweed resulted in a low N & P concentration. Consequently, the initial concentration can have a large influence on the total produced biomass at the start of the integration. Therefore, the initial concentration is included as a parameter for the sensitivity analysis. On the next page the results of the Jacobian and correlation coefficients are given. The results are from May, simulated with an initial concentration of 3 mg N & P L^{-1} and an initial duckweed density of 296.3 g FW m^{-2}. Due to the fact that the initial density is unknown, the result of a sensitivity analysis with an initial density of 311.1 g FW m^{-2} is also given (see appendix 10.3).

According to the sensitivity matrix on the next page, the most sensitive parameters are T_{opt}, J_{max26}, FullA, JtoVc, Foc and the initial density. T_{opt} is the optimal temperature and J_{max26} the maximum electron transport rate at 26°C. FullA determines at which mat density the LAI is equal to one. JtoVc is a conversion factor for converting the electron transport rate to the carboxylation rate. Foc is the fraction oxygenation and carboxylation. Some of these can be estimated, other parameters have a high correlation. If two parameters have a strong correlation with each other, only one of these parameters can be used for parameter estimation.

From Table 19, T_{opt}, is strongly correlated with FullA. For parameter estimation the parameters with high sensitivity and non-confident prior knowledge are the best option to obtain an accurate result (van Willigenburg and van Ooteghem, 2015). The parameters JtoVc and Foc both have a high sensitivity, but are not used for parameter estimation since the current values are applicable for all C_3 plants. In the next paragraph, only the initial mat density is determined with parameter estimation, because this parameter is sensitive for small changes and the actual value of the initial mat density is unknown.

Table 18. Sensitivity matrix of May with an initial mat density of 296.3 g FW m^{-2}. The bold parameters have the highest sensitivity.

	alpha_TPU	Topt	Initial density	J_max26	Ej	Ec	Eo	Rs	theta	Gamma	r_Dulold	FullA	VwindG	Fp	JtoVc	Foc	Cn	PPM
alpha_TPU	3.94E+09	1.69E+10	-1.07E+10	-1.11E+10	1.77E+09	-5.44E+08	2.14E+08	2.27E+07	-1.37E+09	1.45E+07	2.99E+09	1.11E+10	-1.39E+07	3.75E+09	1.03E+10	6.19E+09	-1.22E+09	-2.22E+09
Topt		8.76E+10	-4.97E+10	-5.12E+10	7.43E+09	-2.32E+09	9.09E+08	9.67E+07	-5.88E+09	6.16E+07	1.26E+10	5.29E+10	-5.92E+07	1.61E+10	4.80E+10	2.72E+10	-5.30E+09	-9.54E+09
Initial density			3.01E+10	3.12E+10	-4.75E+09	1.47E+09	-5.79E+08	-6.14E+07	3.71E+09	-3.91E+07	-8.06E+09	-3.16E+10	3.76E+07	-1.02E+10	-2.90E+10	-1.70E+10	3.33E+09	6.03E+09
J_max26				3.24E+10	-4.95E+09	1.53E+09	-6.03E+08	-6.39E+07	3.87E+09	-4.08E+07	-8.40E+09	-3.28E+10	3.92E+07	-1.06E+10	-3.01E+10	-1.77E+10	3.47E+09	6.28E+09
Ej					8.00E+08	-2.46E+08	9.70E+07	1.03E+07	-6.17E+08	6.54E+06	1.35E+09	4.91E+09	-6.29E+06	1.68E+09	4.53E+09	2.76E+09	-5.52E+08	-1.00E+09
Ec						7.56E+07	-2.98E+07	-3.16E+06	1.90E+08	-2.01E+06	-4.15E+08	-1.52E+09	1.93E+06	-5.18E+08	-1.41E+09	-8.51E+08	1.70E+08	3.08E+08
Eo							1.18E+07	1.25E+06	-7.49E+07	7.94E+05	1.64E+08	5.99E+08	-7.63E+05	2.04E+08	5.53E+08	3.35E+08	-6.70E+07	-1.22E+08
Rs								1.32E+05	-7.93E+06	83967	1.73E+07	6.35E+07	-80689	2.16E+07	5.86E+07	3.55E+07	-7.09E+06	-1.29E+07
theta									4.77E+08	-5.05E+06	-1.04E+09	-3.85E+09	4.86E+06	-1.30E+09	-3.55E+09	-2.14E+09	4.27E+08	7.75E+08
Gamma										53526	1.10E+07	4.05E+07	-51436	1.38E+07	3.74E+07	2.26E+07	-4.52E+06	-8.20E+06
r_Dulold											2.28E+09	8.34E+09	-1.06E+07	2.85E+09	7.71E+09	4.68E+09	-9.32E+08	-1.69E+09
FullA												3.35E+10	-3.89E+07	1.06E+10	3.07E+10	1.78E+10	-3.46E+09	-6.26E+09
VwindG													49428	-1.32E+07	-3.59E+07	-2.17E+07	4.34E+06	7.88E+06
Fp														3.57E+09	9.76E+09	5.89E+09	-1.17E+09	-2.12E+09
JtoVc															2.81E+10	1.64E+10	-3.19E+09	-5.78E+09
Foc																9.79E+09	-1.92E+09	-3.48E+09
Cn																	3.82E+08	6.93E+08
PPM																		1.26E+09

Table 19. Correlation coefficient matrix of May with an initial mat density of 296.3 g FW m^{-2}. The green blocks show a strong positive correlation and the red blocks a strong negative correlation.

	alpha_TPU	Topt	Initial density	J_max26	Ej	Ec	Eo	Rs	theta	Gamma	r_Dulold	FullA	VwindG	Fp	JtoVc	Foc	Cn	PPM
alpha_TPU	1	0.73952	0.43935	-0.48191	0.34487	-0.28865	-0.32853	0.26365	-0.24866	0.24515	0.37652	-0.36042	0.26579	-0.9883	0.2837	-0.32913	0.61838	0.26607
Topt		1	0.39587	-0.54674	0.53405	-0.56278	-0.6006	0.42422	-0.0067943	0.52146	-0.0044204	-0.64614	0.41744	-0.70446	0.50894	-0.4607	0.90959	0.13727
Initial density			1	-0.93516	0.17823	-0.17033	-0.20566	0.071025	-0.034799	-0.000108	0.13636	-0.069734	0.053578	-0.41557	0.065631	-0.41248	0.046474	0.81163
J_max26				1	-0.37485	0.22312	0.29029	-0.10807	0.10842	-0.27582	0.033609	0.33693	-0.10793	0.4426	-0.26225	0.56614	-0.26999	-0.82174
Ej					1	-0.65839	-0.76009	0.65644	0.054225	0.72838	-0.66117	-0.68779	0.6902	-0.29176	0.65239	-0.42264	0.53213	0.22209
Ec						1	0.98777	-0.77671	-0.69232	-0.42445	0.36434	0.36321	-0.73502	0.25387	-0.37801	0.18563	-0.52724	-0.06134
Eo							1	-0.78875	-0.60307	-0.52056	0.42896	0.4704	-0.75937	0.28905	-0.48007	0.25498	-0.5596	-0.1235
Rs								1	0.36138	0.3042	-0.36779	-0.30654	0.99455	-0.24932	0.3548	-0.014506	0.39494	-0.05257
theta									1	-0.078116	-0.20272	0.11773	0.27959	0.26591	-0.023122	0.094568	-0.033731	-0.113
Gamma										1	-0.51178	-0.79365	0.3561	-0.19547	0.72223	-0.52311	0.64685	0.25551
r_Dulold											1	0.40826	-0.39849	-0.46944	-0.43171	0.43678	-0.089695	-0.01620
FullA												1	-0.34328	0.31416	-0.94548	0.54121	-0.64517	-0.10265
VwindG													1	-0.2506	0.38775	-0.034765	0.40149	-0.04010
Fp														1	-0.23345	0.19455	-0.58657	-0.23788
JtoVc															1	-0.52727	0.46215	0.1141
Foc																1	-0.37288	-0.45087
Cn																	1	-0.06404
PPM																		1

5.2.3 Estimation of parameters in May

Which parameters should be estimated is described above. Below the results of the parameters determined with least squares method are given. The figures show the production of duckweed compared to the harvested data. The mat density is estimated two times, one time for the nutrient model based on the Michaelis-Menten equation of Lasfar (2007) and the other one for the average half saturation coefficients mentioned by Landolt (1987) (for Lasfar see equation 4.75, 4.76 and 4.76 and for Landolt equation 10.26, 10.27 and 10.28). The mat density as a function of time is also given. The influence of harvesting is visible in the mat density graph as vertical straight lines in the figure.

Parameter estimation in May results in an initial mat density of 296.3 g FW m^{-2}, which is low compared to the average mat density 350 g FW m^{-2} in Augustus. If the nutrient parameters of Landolt are used, the result is even lower. Obviously, both models can describe the data well and the difference between them is small; however, calculations in the next chapters will be done based on the model of Lasfar, since this model is more recent and the initial mat density is more in agreement with the harvest strategy at the ECOFERM. In the figure below the harvested data (red stars) is compared with the output of the photosynthetic model (PHS).

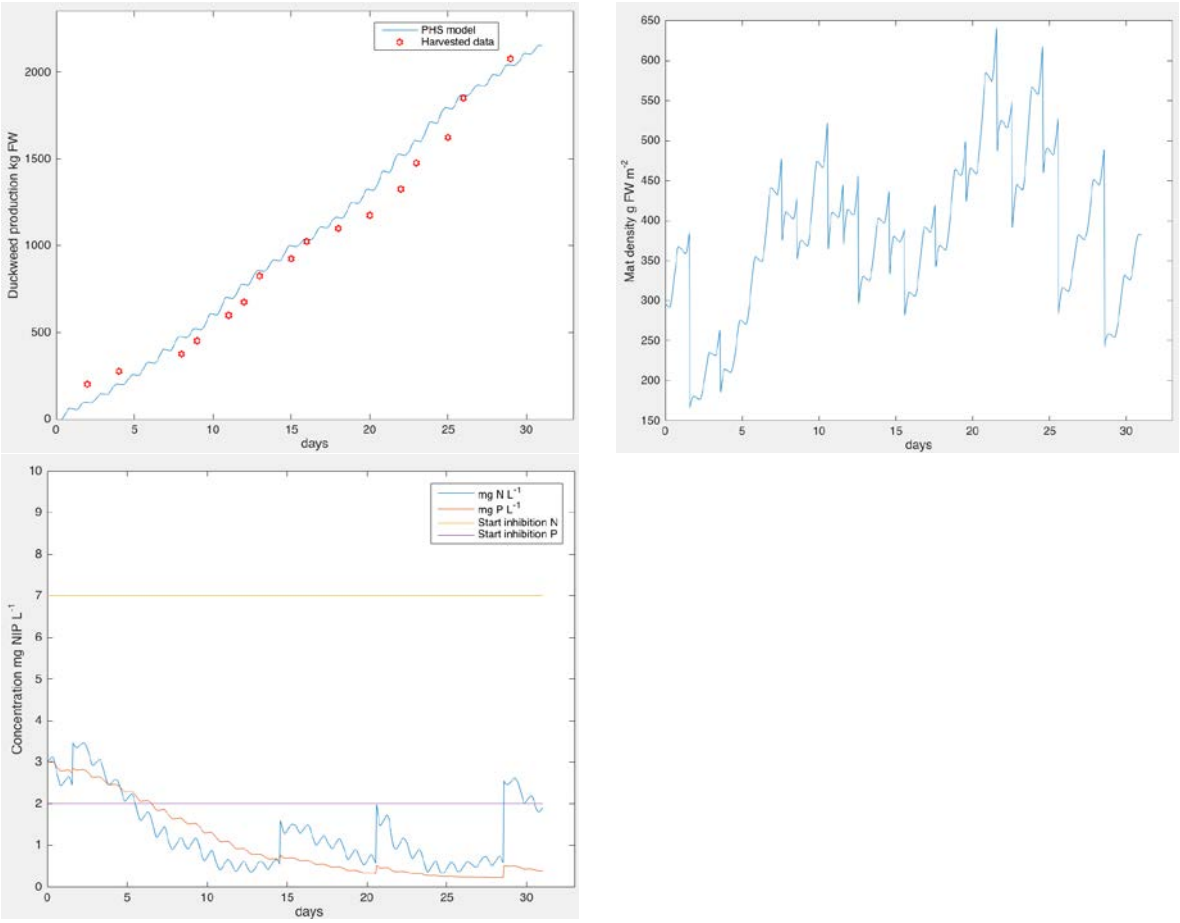

Figure 20A, B & C. Result of May with Lasfar's model initial nutrient concentrations mg N|P L^{-1} (Cn=[N, P] = [3 3]), initial density=296.3 g FW m^{-2} and an deviation error of 3.5%.

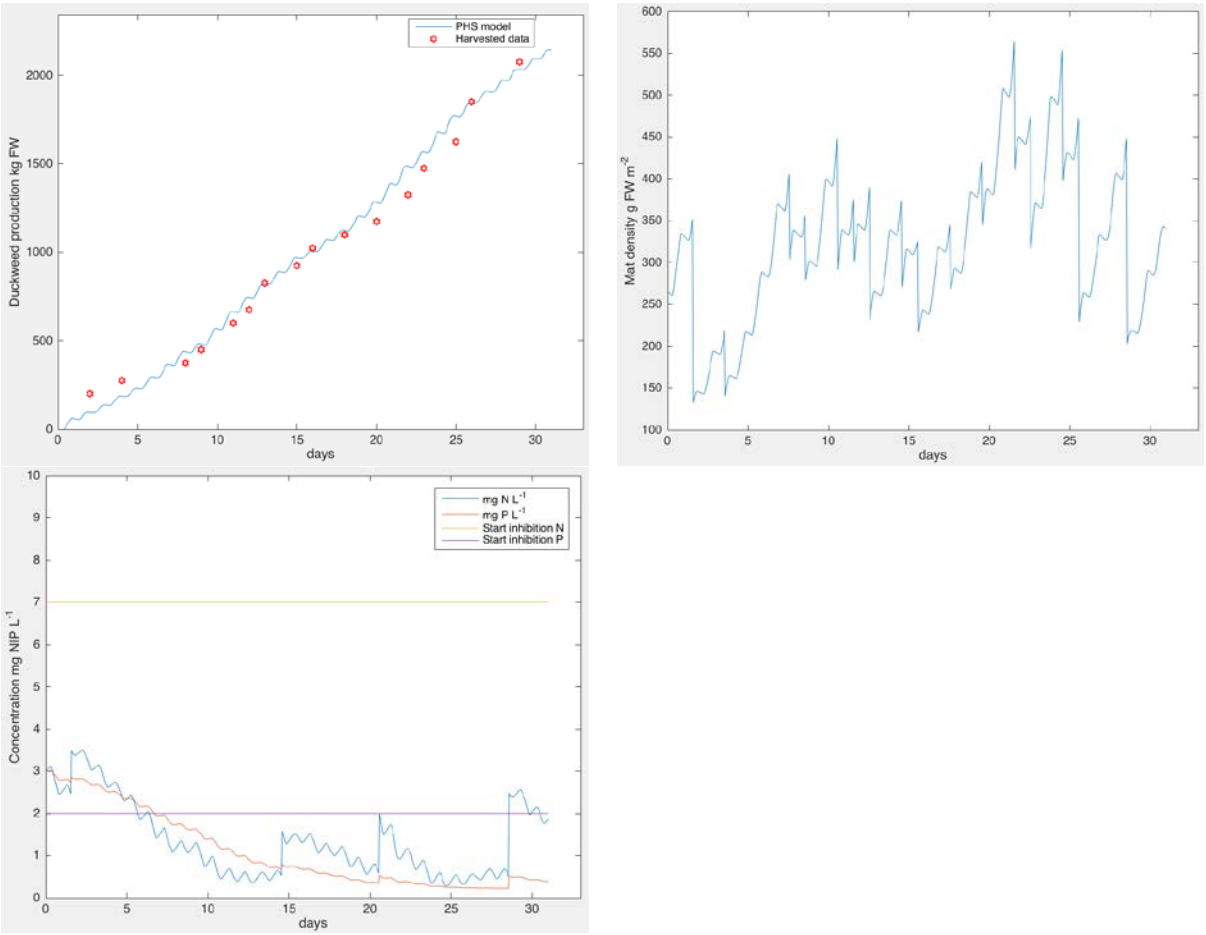

Figure 21A, B & C. Result of May with Landolt's model initial Cn= [3 3], initial density=265.2 g FW m^{-2} and a deviation fit of 3.2%.

5.2.4 Simulations with measured mat density

Unfortunately, the system is sensitive for small changes in the mat density. For example, a simulation with an increase of the initial mat density with 5% gives a monthly production of 3323 kg FW, where in Figure 20A only a production of 2149 kg FW was obtained. Consequently, it seems that estimating the initial mat density removes errors in the system that that are not caused by the initial mat density, but other mechanisms in the model.

A correct model should be able to determine the production from July to September. Only the initial mat density and initial nutrient concentrations should be determined. However, the results above show completely different results for small changes in the initial mat density. Consequently, if the model is simulated once for all months, a small error in the month July will result in a relatively big error for the month Augustus. It is therefore better to estimate the parameters with a known mat density. Moreover, it is unlikely that by only estimating the initial mat density the model can describe the harvested data, because this would assume that the model is perfect and only the initial mat density is an unknown or incorrect parameter. Therefore, the simulation starts at 24 Augustus with the measured mat density of 325 g FW m^{-2} at 9 o'clock. The initial density was chosen a little bit higher than the measured value to prevent a lower mat density by dark respiration. Due to the fact that the mat density is now known, a new sensitivity analysis has been done. This sensitivity analysis can be found in appendix 10.3. Again, T_{opt} is the most sensitive parameter followed by FullA. FullA is estimated, because the exact value is unknown, since literature shows a range between 457 to 620 g FW m^{-2} (Jupsin et al., 2005; Körner and Vermaat, 1998). Furthermore, J_{max26} is also estimated, because the current value is only based on one research and this parameter did not have a correlation with FullA. T_{opt} is not estimated, because it has a correlation with FullA and J_{max26}. Some non-sensitive parameters without correlation could also be added, however this would result in fitting of errors.

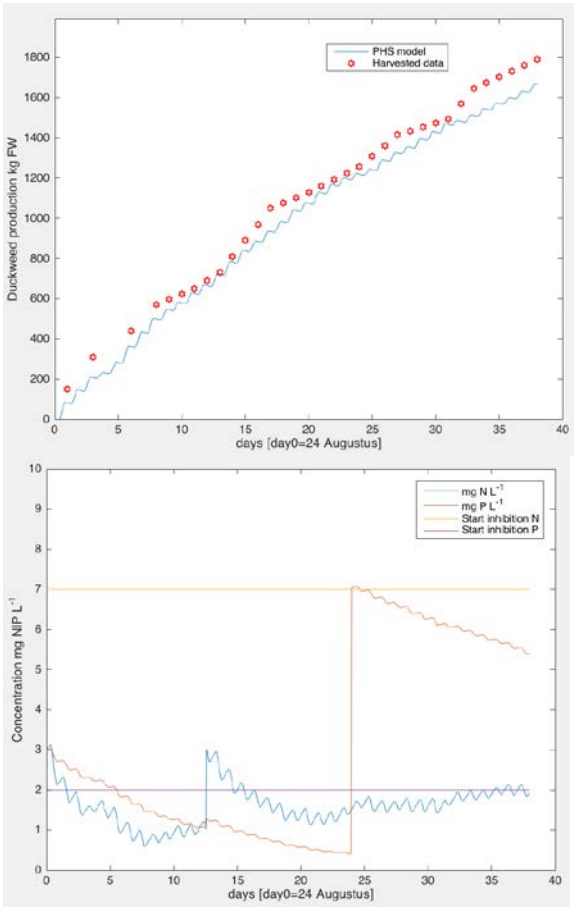

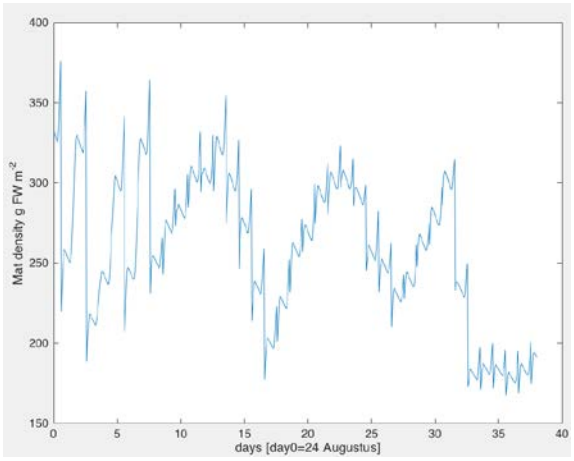

Figure 22A, B & C. Results of estimating FullA for 24 Augustus to 30 September. The first figure shows the production from the model compared with the harvested data. The other figures show the mat density and nutrient concentration as a function of time.

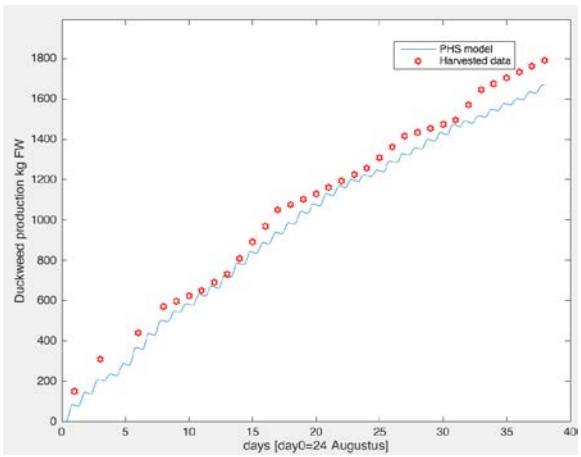

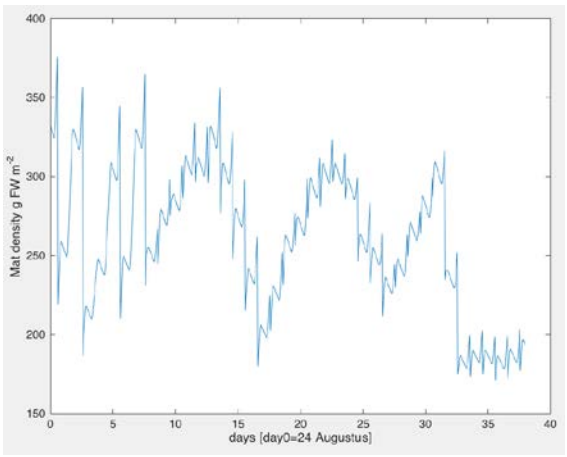

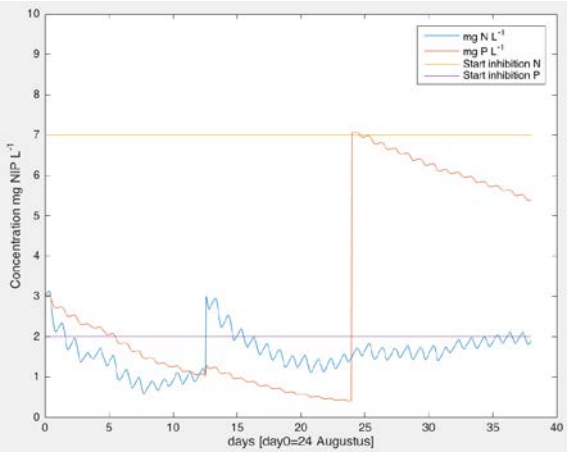

Figure 23A, B & C. Result of estimating both parameters FullA and J_{max26} for 24 Augustus to 30 September. The first figure shows the production from the model compared with the harvested data. The other figures show the mat density and nutrient concentration as a function of time.

The total production in Figure 22 is 133 kg FW lower than according to the harvested data. The model shows almost a straight line; in contrary to the harvested data that shows ups and downs. This is partly caused since the amount of harvested is duckweed is not constant. Consequently, the harvested data shows at day 14 and 31 an increased biomass. Similar to the result in May the effect of harvesting is obviously visible.

After estimating the parameters above, the model should be able to predict the production from July to September, only the initial mat density has to be determined. The month October is not included due to the fact that all duckweed was removed from the pond. Otherwise, parameter estimation will give a wrong result, since the model tries to minimalize the error between harvested and biomass assimilation, but in fact there is no biomass generated since all harvested data is caused by removing all duckweed from the pond. The result is given below, the predicted production is less than the harvested data, but in general the model is in agreement with the harvested data. Moreover, the mat density at day 53 (24 Augustus) is not overestimated.

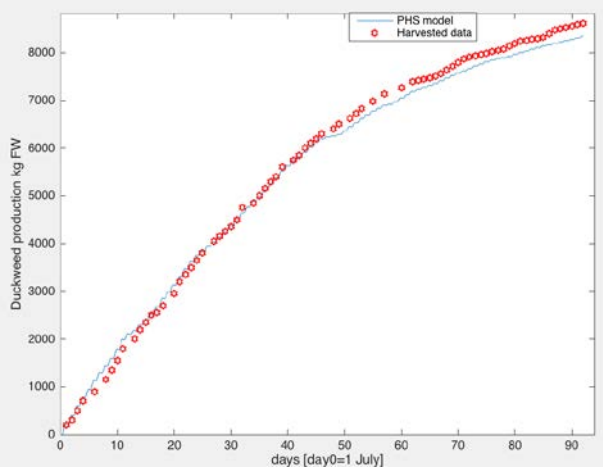

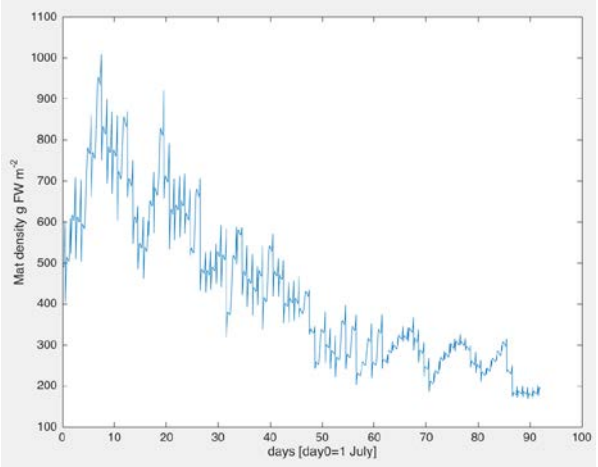

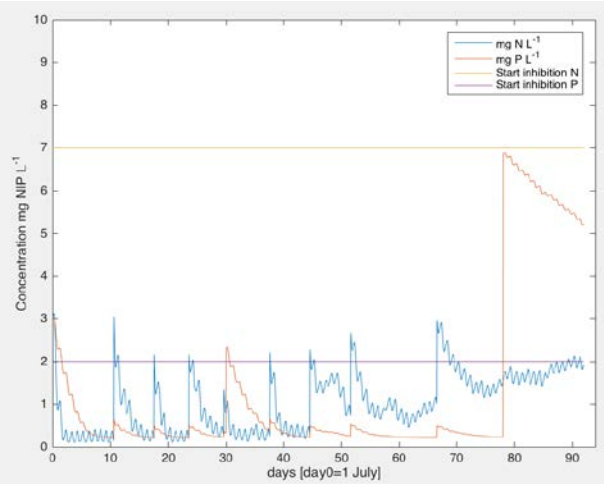

Figure 24A, B & C. Simulation of the model from July to September with only estimating FullA. The result has a deviation fit of 3.1%.

5.3 Results with optimal management

During the production of duckweed a lot of N and P was removed, however according to paragraph 5.2.1 too little thin fraction was added to obtain a maximum production. The model is adapted to maximize N & P uptake and production. Therefore, thin fraction was added when N or P is lower than 9 mg N L^{-1} or 4 mg P L^{-1}. The duckweed is harvested when the optimal mat density is exceeded. To prevent harvesting at every time step, at 2 o'clock the following decision is made; if the current mat density is higher than the optimal mat density, then the difference between current and optimal is harvested. The result below is obtained for 24 Augustus to 30 September. In 38 days, a production of 5.6 kg FW m^{-2} is realised, which is 3 times more compared to the actual harvested data.

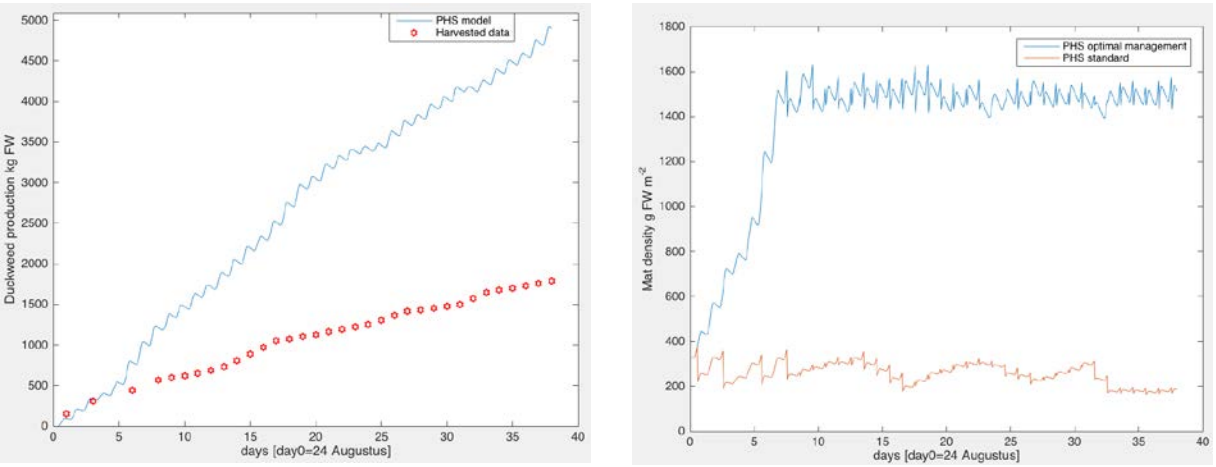

Figure 25A & B. Left the production with optimal management with the same initial mat density as at ECOFERM. Right the mat density as a function of time, with a harvest frequency of one time a day and compared to with and without optimal management.

The problem with current result is that the LAI becomes relatively large, namely at an optimal mat density, the LAI is ±3.0. In contrary, the parameters obtained with the least squares method are determined when the LAI of ±0.75. Consequently, the model is not validated for higher mat densities, in other words there is an uncertainty at these mat densities. From literature, an average growth rate of 0.29 is possible with optimal nutrients and an average light intensity of 179 µmol m^{-2} s^{-1}. From 24 Augustus to 30 September the average light intensity was 168 µmol m^{-2} s^{-1}. Given this growth rate and a harvest frequency of each day it is possible to have a maximum yield of 8.1 kg FW m^{-2} (Frédéric et al., 2006). In other words, the optimal management result is theoretically possible. As expected with an increased production, more thin fraction has to be added to have optimal concentrations. Besides this, the increased concentrations result in a higher volatilization

rate. In Figure 26A the N & P concentrations as a function of time are given. 12.0 m^3 thin fraction needs to be added to guarantee optimal uptake and production. It could be remarked that not only too little thin fraction increased the production, Figure 26B shows that if the company would not have harvested so much at low densities, a much higher production would have been possible.

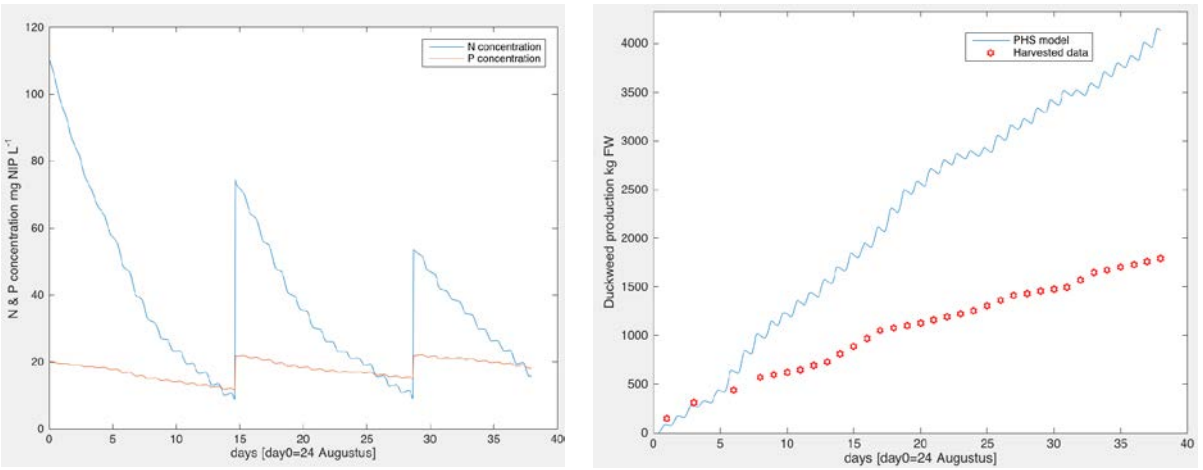

Figure 26A & B. A Nutrient concentration with optimal management as a function of time. B The duckweed production with optimal management and a constant nutrient concentration of 1 mg N|P L^{-1}.

The dark respiration is influenced by the light intensity and the initial value of dark respiration not inhibited by light. Below the fraction of dark respiration divided by the net assimilation rate (F_{net} mg net CO_2) is given. The first peak is caused since the system starts in night. As a result, the light intensity is low, so there is a high dark respiration rate. In the first 15 days the $\frac{rD}{F_{net}}$ is ±20%, however at the end of the simulation this increases to 32%.

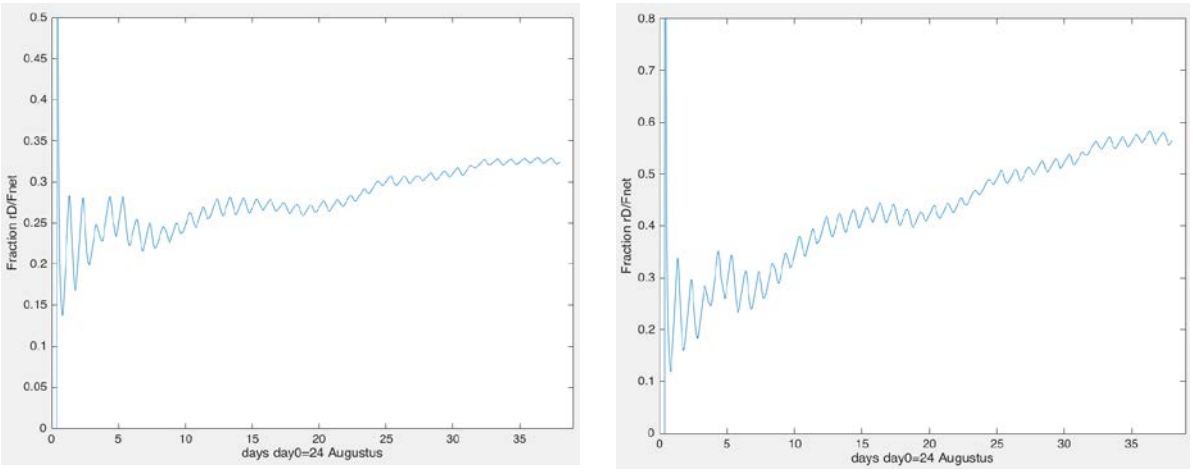

Figure 27A & B. Dark respiration from 24 Augustus to 30 September. In the right figure optimal management is applied with an initial density of 333 g FW m^{-2}. The difference between the two figures is caused by an elevated LAI.

In the previous calculation, the optimal yield was calculated at the measured initial density. On the next page the result is given if at all months optimal management is applied, the initial density was 1500 g FW m^{-2}. The result of the photosynthetic model is compared with Lasfar's model. The intrinsic growth rate is calculated based on the daily photoperiod and water temperature. Combined with equation 4.82, the maximum production with given intrinsic growth rate is calculated and compared to the optimal production of the photosynthetic model.

Table 20. Comparison of optimal production with photosynthetic model compared with the model of Lasfar (equation 4.82) and actual production.

Month	Average T_{dw} [°C]	Average I_A [µmol m^{-2}]	Prod kg FW PH model	Prod kg FW Lasfar's model	Total m^3 thin fraction	Actual m^3 thin fraction	Actual production kg FW
May	22.8	296.4	7914	6366	14.22	0.32	2072
June	25.1	327.6	8847	4538	14.89	[-]	925
July	26.4	308.4	8835	5245	11.95	0.4	4500
Aug.	26.7	260.3	7081	7753	9.71	0.3	2895
Sept.	21.3	155.6	3300	9000	4.10	0.1	1220
Oct.	16.4	95.3	913	5769	2.24	0.05	640

5.4 Simulations compared with literature

Although the results in paragraph 5.2.4 were relatively accurate, it is unknown if the model is in agreement with literature. The model of Frederic (2006) calculates the increase in mat density at given intrinsic growth rate. Unfortunately, the CO_2 concentration in this experiment has not been given. Therefore, it is assumed that the CO_2 concentration is equal to the ambient CO_2 concentration of 400 ppm. Furthermore, the temperature was constant 20°C and the photoperiod was 12.5 h with a light intensity of 342 µmol m^{-2} s^{-1}. With these inputs, the photosynthetic model is simulated and compared with generated biomass based on equation 4.82. Below the results are given; obviously the model cannot describe the production from literature at low CO_2 levels. The model is clearly too sensitive for low CO_2 concentrations.

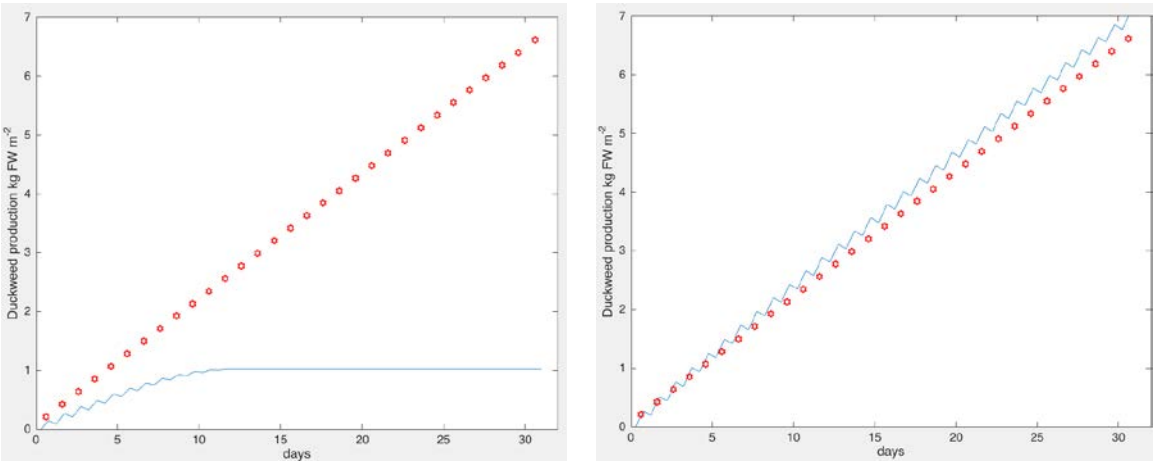

Figure 28A & B. Result with photosynthetic model with an initial mat density of 1467 g FW m^{-2}. Figure A is with a CO_2 level of 400 ppm and B with 1500 ppm.

As mentioned in the literature study in chapter 2, the growth rate of duckweed is not sensitive for elevated CO_2 concentrations. The growth rates as a function of the CO_2 from Table 4 were measured at a room temperature of 25°C with a light intensity of 180 µmol m^{-2} s^{-1} and a photoperiod of 8 hours. The daily maximum production is calculated again by using equation 4.82. The photosynthetic model is simulated with similar inputs and a CO_2 concentrations of 350 and 1500 ppm. The result at an CO_2 concentration of 1500 ppm can be found on next page.

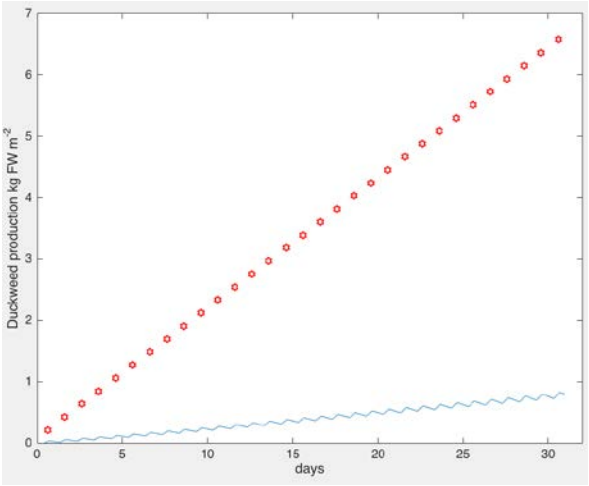

Figure 29. Result of simulation with the inputs of Andersen (1984); 1500 ppm and 8 h photoperiod of 180 µmol m^{-2} s^{-1}.

According to literature an relative growth rate of 0.288 was found at 1500 ppm (Andersen et al., 1985). Without the effect of harvesting, the photosynthetic model calculated a production of 0.79 kg FW m^{-2} at 1500 ppm (Figure 29). Obviously, this production is much lower than theoretically possible. Moreover, the low light conditions increased the dark respiration rate and decreased the assimilation rate. As a result, a low production is calculated. Unfortunately, in the simulations at 350 ppm CO_2 the dark respiration is higher than the net CO_2 assimilation rate. Consequently, the mat density decreased to zero.

5.5 Costs maintaining duckweed

As mentioned in the introduction only the electricity use is taken into account for the economic analysis. The depreciation and labour costs are neglected. The table below shows the average amount of rainfall compared with the amount of evaporated water by duckweed. The evaporated water by duckweed is clearly less; therefore, the cost of water can be neglected.

Table 21. Total evapotranspiration of water by duckweed given for each month.

Month	Evaporated water by duckweed [kg m^{-2}]	Rainfall of water [kg m^{-2}]
May	53.2	62
June	54.6	65
July	54.3	80
Augustus	45.9	72
September	23.7	78
October	13.8	82

The total electricity consumed in 2015 was 2500 kWh (Kroes et al., 2016). Unfortunately, it is unknown which calculations they have done to determine this. On next page a table is given for the energy consumption of each component. The components are similar as mentioned in the report. For the production of duckweed only a blower, conveyor and impeller are needed. The energy consumption of the ventilation is not taken into account, since these costs belongs to the rosé calves and not to the production of duckweed.

Table 22. Summary of energy costs, based on the production of 2015 ([1]('Peekoi', 2016),[2]('123Rollenbaan', 2016), [3](Kroes et al., 2016))

	Energy consumption kWh (source)	Hours per day	Yearly energy costs, € (214 days)
Blower	1.5[1]	1.3	89.3
Conveyor	0.25[2]	1.5	17.2
Impeller	1.08[3]	12	593.5

With an increased production, the electricity costs of the blower and conveyor increase. The production increased with a factor of 2.6. As a result, the total electricity cost at optimal production is €865.7.

5.6 Cattle feed composition and cost

The idea behind growing duckweed is to reduce the manure transport costs and decrease the costs for cattle feed. Yearly the energy cost was €700.0. The table below is based on the feed requirements given in Table 15 and Table 16.

Table 23. Composition of the fodder at current duckweed production compared with the optimal duckweed production.

	Current yield	O.y. PHS model	O.y. Lasfar model
Wheat straw	1.42E+00	3.98E-01	5.64E-01
Duckweed	8.59E+02	2.33E+03	2.44E+03
Grass sil.	9.00E+04	9.00E+04	9.00E+04
Maize sil.	4.50E+05	4.50E+05	4.50E+05
Soy60RC	2.41E+00	6.91E-01	9.57E-01
Potatoes Parings	1.12E+06	1.12E+06	1.12E+06
Turnip flakes	1.79E+06	1.79E+06	1.79E+06
Sugar Beet pulp	1.58E+06	1.59E+06	1.59E+06
Grass sil.	1.03E+06	1.03E+06	1.03E+06
Maize sil.	2.34E+00	6.70E-01	9.05E-01
Total costs	€ 1,189,488	€ 1,189,255	€ 1,189,238
*O.y. =Optimal yield			

With the production of 2015, only € 136.2 is saved on cattle feed. According to the report 1220 L thin fraction was added throughout the year, which means that 18 euro has been saved by lower transportation costs of manure.

Besides the profit of using manure and less soy, there are some subsidies for lower emission of CO_2. In 2006 for each recycled ton CO_2, 30 euros was given; unfortunately, nowadays this has been reduced to 5 euros per ton CO_2. The conversion factor from kg CO_2 to kg FW of duckweed is 9.46. With a production of 14,430 kg FW per year, the production of duckweed gives a subsidy of €7.6 for reducing the greenhouse effect. During cold days it is possible that the heat produced by the rosé calves is used in the greenhouse. Air from the stable is then transported to the greenhouse. However, T_s and T_w are mostly higher than T_{st} (Figure 15B), which means that there is energy transfer from the greenhouse to the stable. Therefore, no CO_2 emission has been reduced by using the heat of the stable from May to October. In the winter energy from the stable will increase the water temperature. However, according to Van den Top (2014) no growth is possible during the winter. In the table on the next page, a comparison is given between current situation and optimal management.

Table 24. Result of economic possibilities with current situation compared with the production when optimal management is applied.

	Current situation (€)	Optimal management (PHS model) (€)
Cattle feed savings	136.2	369.9
CO_2 equivalents	7.6	19.5
Manure (15+0.6*1.05)*m^3	19.1	892.6
Profit	-430.6	416.3

The table above gives the results for the combination of duckweed and rosé calves. In contrary to rosé calves, pigs have less feed requirements. Therefore, the production of duckweed might have more opportunities for pigs than rosé calves. Unfortunately, the solution is non-feasible, because the phosphorus content of pig feed is relatively high. In addition, a simulation with a food composition with sugar beet pulp feed, still results in a non-feasible solution, despite the fact that the phosphorus content of sugar beet pulp is relatively low. It seems that current raw materials have a too high phosphorus content and the constraints are too strict, if the phosphorus constraint is neglected then a feasible solution is found.

6 Discussion

6.1 Temperature model

In paragraph 5.1 the results of the temperature model were given. This model was made to establish the difference between the water and duckweed temperature. In the previous version of the photosynthetic model the crop temperature was assumed to be equal to the water temperature. Consequently, it is important to know if there is big difference between the water and the duckweed temperature. The temperatures of soil, roof and stable temperature cannot be validated, since these variables were not measured. However, comparisons with physics and other temperatures are possible.

The soil temperature (T_s) can be estimated well, namely on average in May T_s-T_g = 2.8°C. In all other months the average difference was 2.0°C. T_g is influenced by all processes in the greenhouse. The high T_s elevated the T_g, but the T_g is decreased by heat loss through convection with T_r, T_{dw} and T_w. It would be strange if T_s<T_g in the middle of the day because there is irradiation from the sun. During the night T_s is also higher than T_g (Figure 13B), which is surprising since in the night the radiation is almost zero. T_g decreases fast enough through heat loss by convection, as a result during the night T_s>T_g. Unfortunately, no measurements of T_s have been done, consequently T_s cannot be validated with data.

Further, the roof temperature (T_r) has been calculated. According to Figure 14A T_r is mostly lower than the T_g. On average in all months the T_g was at least 4.0°C higher than T_r. Although some parameters like C_{Tsky} and V_{windG} had to be estimated and I_{tot} is determined with the transmittance of the roof, the result seems to be theoretically possible. Convection between T_{out} and T_r causes a decrease of T_r. It was also possible to determine I_{tot} given the climate data of De Bilt. However, this would result in highly inaccurate estimations, since the measured irradiation in the greenhouse would differ from the data of De Bilt by time delay or clouds for example. In appendix 10.4, the measured irradiation is converted to the outside radiation and compared with the data of the KNMI. It seems that the transmittance is estimated too high. In other words, the total radiation outside is underestimated. Although this fact, the obtained result is still theoretically possible.

The stable temperature (T_{st}) is determined with the model of Van den Top (2014). According to this research the stable temperature was almost constant, because there is always heat production by rosé calves and the only variable heat transfer is the transfer of cold air from outside the stable. In appendix 10.4, a figure is given with the results of Van den Top. In contrary to his conclusion at day 120 the daily temperature also varied with 8°C. Figure 14B of the temperature model ranges between 18 and 27°C. As a consequence, T_{st} does not differ much compared to the result of Van den Top.

The temperature of duckweed (T_{dw}) is according to literature on average 1 to 3°C higher than the T_w (Landolt and Kandeler, 1987). Furthermore, in open cultures at 5000 lux, T_{dw} is 2°C higher than T_w (Casperson, 1956). In contrary to another research the duckweed temperature is closely related to the temperature 2 cm below or above the fronds (Dale and Gillespie, 1976). According to this experiment, during irradiation T_{dw}, T_w and $T_{air/g}$ were almost the same, and during the night T_{dw} was closely related to the air temperature. This is similar to the result of the simulation (Figure 16B). Only there is a difference between T_g, T_w and T_{dw} at irradiation. Particularly, the greenhouse temperature was much higher at irradiation and lower during the night. This result is in contrary to the results of Landolt, Casperson and Dale. It might be caused by the fact that the soil temperature has a relatively big surface compared to the duckweed pond; 4560 and 880 m^2 respectively. As a result, the T_g is largely determined by the T_s. In the night the result was similar to the experiments of Dale, namely the T_{dw} was lower than the T_w. On average, over the whole months for each simulation, T_{dw} did not often exceed the water temperature. This is probably caused since the original model for evapotranspiration is developed for non-floating plants, therefore some adaptions had to be made, which resulted in an approximation for e.g. the aerodynamic resistance. Consequently, the evapotranspiration might be overestimated.

In Figure 17A, the total amount of evaporated water by duckweed is given; on average 1.72 kg m^{-2} water was evaporated daily. Normally a duckweed pond evaporates 60 to 80% water compared to open water (Al Nozaily, 2000). In a relatively dry climate, daily evaporation was 6 to 10 kg water m^{-2} (Al Nozaily, 2000). In other words, compared to literature less water was evaporate; 1.72 vs 6 kg water m^{-2}. This was partly caused by the fact that there is almost no wind in the greenhouse, increasing VwindG to 3.2 m s^{-1} increased daily water evaporation to 2.48 kg water m^{-2} (Figure 17B). The measurements of Al Nozaily were outside in Yemen and evapotranspiration is climate dependent. As a result, with an average humidity of 47% the VPD was much higher. Consequently, the plants could evaporate water more easily. In January, the relative humidity was 77%, and the evapotranspiration was 3.85 mm (Vwind=3.38 m s^{-1}) (Al Nozaily, 2000), clearly this is closer to our results. Simulation of May with the constant parameters RH=77% and VwindG=3.38 gave 2.33 kg water m^{-2}. Obviously, this is a rough comparison, since irradiation and temperature are different and therefore change the VPD. However, from this comparison it can be concluded that the evapotranspiration is not overestimated.

Another factor why the model is not fully in agreement with the results of Landolt and Dale is partly caused by different climate conditions and through climate data. Specifically, the climate data is not perfect, because water was added to decrease the duckweed temperature; moreover, a part of the pond was covered with a screen to decrease the temperatures during summer. As a result, the energy processes of water and duckweed change. Given all these reasons it is logical that the duckweed temperature is not fully in agreement with literature. The result is partly in accordance with the conclusions of Dale, namely the water and duckweed temperature are related to each other at irradiation. However, the duckweed temperature was in the night more closely related to the water temperature, which is in contrary to the results of Dale. The result was mainly in agreement with literature, therefore it is better to simulate the model with the temperature of duckweed instead of the water temperature. It is possible to simulate the model with the water temperature since the average difference is less than 0.5. However, during the night the difference between the water ad duckweed increases. Therefore, it is favourable to simulate the photosynthetic model with the temperature of duckweed.

6.2 Nutrient consumption rates

Nutrient consumption by duckweed was calculated with the N & P content of newly generated duckweed at a given concentration in the water. A similar method was used in literature (Frédéric et al., 2006). It was possible to calculate the removal rates with different models. However, other methods based on Michaelis-Menten models did not give reliable results or were not nutrient dependent. From 24 Augustus to 30 September the total N & P consumption by duckweed was 1.1 kg N ha^{-1} d^{-1} and 0.3 kg P ha^{-1} d^{-1}. As mentioned in paragraph 2.2, nutrient consumption by duckweed is 1-4.8 kg N ha^{-1} d^{-1} and 0.1-0.6 kg P ha^{-1} d^{-1} (Al-Nozaily et al., 2000). Frederic (2006) obtained consumption rates in the range of 4.8 kg N ha^{-1} d^{-1} and 1.2 kg P ha^{-1} d^{-1}. Compared to this the consumption rate is relatively low. However, this is caused by the fact the N and P content of the fronds is concentration dependent. Moreover, less biomass was produced compared to the results of Frederic. Consequently, the total consumption rates were much lower than in literature. Accurate consumption rates were obtained when the result is compared to the research of Al Nozaily (2002). In other words, current removal rates are theoretically possible.

The N concentration in the water was influenced by the concentration in the air. For simulations a constant concentration of 6 ppm in the air was assumed, which was lower than ammonia concentration in the stable (Koerkamp et al., 1998). However, the bio bed removes an unknown amount of ammonia and therefore a lower concentration is expected. The average mass transfer was $1.3*10^{-3}$ mg N m^{-2} s^{-1}, from the air to the water. Normally at high N concentration only volatilization takes place, however the low concentration in the water at ECOFERM caused a mass transfer from the air to the water. According to literature, mass transfer rates of 108.1 mg N m^{-2} s^{-1} are possible (Ibusuki and Aneja, 1984). The difference originates from the fact that the average value is calculated. Obviously, the current average mass transfer rate is not overestimated and thus theoretically possible.

6.3 Nutrient correction factor

As mentioned in previous chapter, too little nitrogen was added to have optimal growth. The total gross leaf assimilation rate ($P_{g\,L}$) is multiplied with a correction factor to correct the assimilation rate at N deficit conditions. This correction factor was based on Michaelis-Menten models derived from literature. A lot of different models were available and unfortunately the results from these models were not the same. Eventually, two models were compared and the differences between these models are given in appendix 10.4. Clearly, the model of Landolt has a smaller correction factor than Lasfar's. Simulations with both models resulted in a different production, which was mainly caused by the fact that the correction factor determined the initial density. Therefore the result of Landolt's model in Figure 21 was obtained with a lower initial mat density. All simulations were done with the Michaelis-Menten model of Lasfar, since the results with this model were theoretically better. As mentioned in paragraph 2.2.5, non-optimal nutrient concentration causes a decrease in important photosynthetic parameters for example the J_{max}, $V_{c\,max}$ and the activation energies (Bown et al., 2007; Walcroft et al., 1997). Besides these parameters, also the internal resistance and chloroplast CO_2 concentrations are influenced (Warren, 2004). Therefore, it would be better if the parameters of the model were adapted instead of using a correction factor based on the Michaelis-Menten equation. Unfortunately for duckweed species no research has been done, probably because the parameters J_{max} and the $V_{c\,max}$ are hard to measure (Walcroft et al., 1997). Besides this, for macrophytes it is more convenient to measure the nutrient concentrations and then determine the growth rate.

6.4 Dark respiration rate

The result for the dark respiration rate was given in Figure 27. The model was mainly based on the model of Farquhar. According to this model, dark respiration is ±5.8% of net assimilation (Fuhrer, 1983). From other literature at normal O_2 concentrations the percentage loss of all C available in duckweed was 1.7% in light and 3.2% in dark (Filbin and Hough, 1985). Mean dark respiration for *Lemna* gibba is 1.85 and for *Spirodela oligorrhiza* 2.44 mg CO_2 g^{-1} FW h^{-1}. Photosynthesis rates at low light are 13.37 and at 200 µmol 21.00 mg CO_2 g^{-1} FW h^{-1} (Takemoto and Noble, 1986). This means that the dark respiration rate is 13.8% at low light and 8.8% at 200 µmol m^{-2} s^{-1}. Dark respiration was calculated with equation 4.83 based on the results of (Fuhrer, 1983). According to this study at saturating light conditions rD was 7.7% of net assimilation at ambient CO_2 and O_2. In appendix 10.4 a figure of the dark respiration and light intensity is given. The rD/F_{net} ratio decreased for increased light intensities and at the first 5 days the ratio was ±20%. Slowly this increased to 32%, which was caused by an increased LAI and a reduced assimilation rate.

Compared to literature, the model seems to overestimate dark respiration, especially at the last 15 days. The increased ratio is partly caused by the correction factors for pH, mat density and nutrient concentration. Moreover, the light intensity decreased during time (Figure 15A). Consequently, the light dependent dark respiration increased and the produced biomass decreased. Moreover, the rD/F_{net} ratio is determined by integration, as a result the error at low light intensities increases with time. Therefore, the first 20 days are more representative.

Furthermore, an important parameter is the LAI, because the measurements by Furher are done with an unknown mat density. However, in the photosynthetic model the rD is multiplied with the LAI to adapt the respiration for the increasing mat densities. At a higher LAI, the fronds absorb less light, but the dark respiration rate is multiplied with the same factor. Consequently, the respiration increased but the net assimilation rate decreased. The theory mentioned above, was supported by the results of the optimal model. At an optimal nutrient concentration and LAI, the rD/F_{net} ratio reached levels above 50%. Fast growing grass species have in in general a loss of 14 to 30% of the carbon assimilated per day (Van der Werf et al., 1992). Even when duckweed is compared with these species, the dark respiration rate is overestimated at high mat densities. Obviously, a high LAI causes an error in the model. Unfortunately, no measurements were done at high mat density. Therefore, parameters have to be estimated for higher mat densities to reduce this error.

6.5 Photosynthetic model

The photosynthetic model could describe the harvested data in May accurately by estimating the initial mat density. The error was relatively low compared to previous research, namely from 24 Augustus to 30 September the error was 7.4%. In previous research the lowest obtained error was 9% (Rooijakkers, 2016). It is possible that some errors in the model are removed by estimating the parameters. For example, the O_2 concentration in the water was ±59.5 ppm. However already at 20 ppm O_2 the net photosynthesis rate is strongly reduced (Filbin and Hough, 1985). Besides this, some parameters were estimated with standard values and equations. For example, the boundary resistance ($R_{b\ heat}$) is determined with a standard equation. Furthermore, the maximum electron transport is temperature dependent, but the temperature dependency is calculated with a standard formula.

Furthermore, with estimating the initial mat density a small deviation of 5% resulted in a production increase of 50%. Therefore, simulations were done with a known mat density and estimating the maximum electron transport rate at 26°C (J_{max26}) and FullA, which is a parameter that determines at which mat density the LAI is equal to one. However, when both parameters were estimated FullA was 382.4 g FW m^{-2} and consequently outside the range of 457 to 620 g FW m^{-2} (Jupsin et al., 2005; Körner and Vermaat, 1998). Therefore, all other simulations were done with only estimating FullA, because then FullA was 455.4 g FW m^{-2}, which is more in agreement with the value found in literature. From Augustus to September, with only estimating the parameter FullA, an accurate result was obtained, however some errors of the other parameters are fitted in FullA. As a result, for the simulation from July to September at day 53 (24 Augustus) the mat density was not the same as measured. Namely, 325 g FW m^{-2} was measured, but the model calculated a mat density of 273 g FW m^{-2}. Besides this, the initial mat density had to be determined with a number of at least 7 digits behind the comma, otherwise the mat density became zero after 75 days. This error could be reduced if the model was validated for higher mat densities, because then a better relation between the duckweed production, mat density and LAI can be determined.

The model was compared with literature. From this it was obvious that high growth rates are possible at low CO_2 concentrations (Andersen et al., 1985; Björndahl and Nilsen, 1985). Simulations with a low CO_2 concentration did not give accurate results. This was caused by the CO_2 limited rate (P_{nc}), since this variable was relatively low compared to the CO_2 assimilation rate from the P_{mm} and TPU. Consequently, the CO_2 assimilation rate is mainly determined by P_{nc}. P_{nc} is calculated with the CO_2 concentration and the total CO_2 resistance. The total resistance might be overestimated. However, even a lower resistance did not give a better result, because then TPU starts to inhibit the CO_2 assimilation rate. In other words, the resistance is not the problem, but the low CO_2 concentration. Duckweed is not sensitive for different CO_2 concentrations, but obviously the photosynthetic model is sensitive for low CO_2 levels. Therefore, it might be a good option to reduce the effect of the P_{nc} and TPU at low CO_2 levels in the photosynthetic model. Simulations with a low photoperiod of solely 8 hours and a light intensity of 180 µmol m^{-2} s^{-1} did not give an accurate result, partly caused by the high respiration and the photoperiod. The photosynthetic model does not take the effect of the photoperiod into account. As a result, the production will always increase if the light duration increases, however literature shows an optimum of 13 hours (Lasfar et al., 2007). In other words, it seems that the model should be adapted for low CO_2 levels and photoperiods.

6.6 Optimal management

The climate data of ECOFERM was used to determine the production when optimal management was applied. There was a clear difference between the optimal production based on the photosynthetic model and the model of Lasfar. This difference was mainly caused by the fact that the model of Lasfar is determined by the photoperiod, but the photosynthetic model uses the light intensity. The photosynthetic model has problems with calculating the dark respiration, nutrient influence and mat density. Figure 36 in the appendix clearly shows that the photoperiod is the most limiting factor in the model of Lasfar. Unfortunately, this photoperiod is not light intensity

dependent; therefore, the model assumes that the growth rate is not influenced by the light intensity. However, the growth rate of duckweed is obviously light intensity dependent (Docauer, 1983). In other words, both models have their advantages and disadvantages and are not perfect.

The optimal mat density was calculated with the model of Lasfar. Unfortunately, the photosynthetic model is not validated for higher mat densities, since the LAI is mainly lower than 0.95 [4]**.** The photosynthetic model takes the effect of less light on the fronds at higher mat densities into account. The model calculated a higher CO_2 assimilation rate at lower mat densities than according to the optimal mat density from equation 4.82. Despite this fact, no data was available to prevent this error. This error could not be prevented by using the inputs from literature, since the model is sensitive to low CO_2 concentrations. According to paragraph 5.2, a higher yield could be obtained when more thin fraction would be added. The mat density was relatively low 350 g FW m^{-2} compared to an optimal mat density of ±1300 g FW m^{-2}. Although the optimal management models are not perfect, higher yields were certainly possible.

When optimal management was applied, the profit was increased by adding more manure. It is possible to obtain optimal concentrations of N and P with only adding thin fraction. It was assumed that the costs for the trace elements were not significant, since the costs for these elements are not mentioned in the ECOFERM report. However, for a more reliable result these costs should have been added. With optimal management, it was possible to make profit, however this profit does not take into account the depreciation or labour costs. Moreover, it remains a question if it is possible to apply the optimal management in practice. 85% of all electricity costs are determined by the impeller. However, if enough duckweed is harvested an impeller is unnecessary (van der Werf, 2016).

Simulations for pigs did not give a feasible solution due to the fact that the phosphorus content of the feed was too high. Sugar beet pulp has a low phosphorus content; however even with sugar beet pulp, no feasible solution was found. It seems that with current raw materials, it is not possible to have an optimal production. Although, according to literature it is possible to replace 50% of all protein sources by duckweed for sows (Le thi Men et al., 1997). Another research found no difference in weight gain when 10% of pig feed was replaced by duckweed (Gutierrez et al., 2001). In contrary for rosé calves duckweed has to be dried using the heat of a gas turbine or using ultraviolet light. The last one causes a reduced concentration of beta carotene (Skillicorn et al., 1993), beta carotene is used for vitamin A production. At ECOFERM duckweed was not dried, but directly given to the animals, no problems occurred due to low amounts of duckweed were given. Drying is also not a good option, because it will increase the price significantly (Holshof et al., 2009). It is also possible to squeeze or ferment the duckweed. Squeezing is not an good option either due to the fact that there is only a small increase in dry matter percentage and there are losses of valuable products (Hoving et al., 2012). By adding additives, fermentation has more opportunities, but unfortunately current methods are not applicable for silage. Furthermore, according the same research the uptake of fresh duckweed by cows is limited due to the taste and odour (Hoving et al., 2012). In other words, for rosé calves and cows duckweed has to be dried. Besides this, it is expected that only 2% of all concentrate can be replaced by duckweed (Holshof et al., 2009). In other words, duckweed has much more possibilities for pigs than for rosé calves.

[4] Average mat density from July to September is ±431 g FW m^{-2}; $LAI = \frac{431}{455.4} = 0.95$

7 Conclusion

In the previous model, the temperature of the water was used for the temperature of the duckweed in the photosynthetic model. Simulations with all energy processes showed that the temperature of duckweed does not differ much from the temperature of water. This result was partly in agreement with literature. At night the difference between the water and duckweed temperature increased, therefore it is better to do simulations in the photosynthetic model with the temperature of duckweed instead of the water temperature.

The estimated parameters from previous research were compared to literature; clearly previous parameters were in a different range. These parameters are adapted; still some other parameters are determined with standard equations. It is assumed that these equations are correct, however as shown with the formula of the CO_2 compensation point this is not always true. It would be better if these equations were validated for duckweed species.

According to literature study in chapter 2, the most important nutrients were nitrogen and phosphorus. The photosynthetic model is based on optimal concentrations for all nutrients. Current results of the nutrient consumption rates are in range with literature, however too little thin fraction was added to obtain optimal N & P concentrations. Therefore, the model is adapted for nutrient deficit conditions. This adaption is made on a Michaelis-Menten equation of Lasfar. Other models were also available, but did not give a reliable result after estimating the parameters. It would be better if the photosynthetic parameters were adapted instead of using a correction factor. Unfortunately, the change of the parameters at nutrient deficit conditions is currently unknown.

The model is mat density dependent. The results showed clearly that the system is sensitive for small changes in the mat density. As a result, determining the initial mat density for each month would result in fitting of errors. From 24 Augustus to 30 September an accurate prediction of the production is made with a deviation fit of 7.4%. The error from July to September was relatively small; 3.1%. However, it is unlikely that the photosynthetic model is able to predict the production of a different data set without estimating any parameters. Namely, it was not possible to obtain an accurate result from July to September if the estimated parameter for the initial mat density has less than 7 digits behind the comma. To improve the model, the parameters should be determined from a data set with high mat densities.

The model is simulated with parameters from literature; only at high CO_2 concentrations, the model could give an accurate result. Besides, at low light intensities the production was too low compared to literature. Currently the CO_2 sensitivity of the model is a problem, because the growth rate of duckweed does not change for elevated CO_2 concentration. However, the CO_2 limited rate and TPU are CO_2 concentration dependent. As a result, simulations with a low CO_2 concentration did not give an accurate result. Therefore, more research has to be done to improve the model for low CO_2 concentrations.

The possible production with optimal management was determined. Clearly, a much higher yield is obtained in both the optimal photosynthetic model and the optimal model of Lasfar. The increased profits were mainly obtained by adding more thin fraction, instead of the reduced feed costs. If the depreciation and labour costs are taken into account, then it is not possible to cultivate duckweed commercially. Probably a semi-closed loop with duckweed and pigs is more suitable, since it is possible to replace 50% of current soy in the pig feed composition with duckweed. More research is needed for pigs to validate this and calculate the reduced costs by using duckweed.

8 Recommendations

The accuracy of the photosynthetic model can be increased if the correction factor at nutrient deficit conditions is replaced by nutrient dependent activation energies, maximum electron transport rate and carboxylation rate. Moreover, it would be better if the nutrient concentration would be measured, because the nutrient concentration is determined with ammonia from air and nutrient uptake by duckweed. However, also other processes for example denitrification by algae can influence the nutrient concentration, in the model this influence is not taken into account. Furthermore, to validate the model at elevated mat densities, more data is needed. Currently the parameters were only fitted at an LAI of ±0.95. Consequently, the optimal management model had dark respiration rates higher than theoretically possible. Moreover, the mat density should be measured more times, because the model is sensitive to the mat density. As a consequence, the model could only be validated once from 24 Augustus to 30 September.

The disadvantage of the photosynthetic model is the sensitive for the CO_2 concentration. Consequently, the results of the model with low CO_2 levels and inputs from the literature did not give an accurate result. As a result, for further research the CO_2 limited photosynthesis rate (P_{nc}) and the triose phosphate use (TPU) should be adapted or neglected at low CO_2 levels. If this adaption is hard to realise or theoretically not possible, then it might be better to improve the model of Lasfar and extend the model with an equation for the light intensity instead of using the photoperiod. Furthermore, it might be a good idea to implement the effect of the photoperiod in the model, due to the fact that the model assumes that for an increasing light duration the production always increases.

Finally, more research to the requirements of pig feed has to be done. More raw materials have to be added to improve the photosynthetic model. Besides this, the requirements for the maximal phosphorus content should be validated with more literature, since a lot of raw materials have a higher phosphorus content than the permissible concentration. Moreover, more research has to be done to the maximum uptake of duckweed by pigs. Subsequently the profit with and without duckweed needs to be determined.

9 References

'123Rollenbaan'. 2016. Opvoerband. Available at: https://123rollenbaan.nl/rvs-opvoerband-lopendeband-25-cm. Accessed 05-01-2017.

'CBS'. 2016. Overschrijding fosfaatplafond hoger. C. B. v. Statistiek, ed.

'IME'. 2013. How much water is needed to produce food and how much do we waste? Available at: https://www.theguardian.com/news/datablog/2013/jan/10/how-much-water-food-production-waste#data. Accessed 04-01-2017.

'Peekoi'. 2016. Airflow 1.5 kW. Available at: http://www.peekoi.nl/8026614/air-flo-lm-1-5-kw-230-volt-50m-kabel. Accessed 05-01-2017.

'USDA'. 2016. National Nutrient Database for Standard Reference, Soybeans 16108. U. S. D. o. Agriculture, ed.

'WorldofMeters'. 2016. World of Meters.

'Forfarmers'. 2016. Forfarmers. Available at: http://www.forfarmersdml.nl/. Accessed 02-01-2017.

Al-Nozaily, F., G. Alaerts, and S. Veenstra. 2000. Performance of duckweed-covered sewage lagoons—II. Nitrogen and phosphorus balance and plant productivity. *Water Research* 34(10):2734-2741.

Al Nozaily, F. 2000. *Performance and Process Analysis of Duckweed-Covered Sewage Lagoons for High Strength Sewage-the Case of Sana'a, Yemen*. CRC Press.

Allen, R. G., L. S. Pereira, D. Raes, and M. Smith. 1998. Crop evapotranspiration-Guidelines for computing crop water requirements-FAO Irrigation and drainage paper 56. *FAO, Rome* 300(9):D05109.

Andersen, I., C. Dons, S. Nilsen, and M. Haugstad. 1985. Growth, photosynthesis and photorespiration of Lemna gibba: response to variations in CO2 and O2 concentrations and photon flux density. *Photosynthesis research* 6(1):87-96.

Ashby, E., and T. Oxley. 1935. The Interaction of Factors in the Growth of Lemna: VI. An Analysis of the Influence of Light Intensity and Temperature on the Assimilation Rate and the Rate of Frond Multiplication. *Annals of Botany* 49(194):309-336.

Atkeson, F., T. Warren, and G. Anderson. 1934. Water requirements of dairy calves. *Journal of Dairy Science* 17(3):249-256.

Bauer, H., and P. Martha. 1981. The CO 2 Compensation Point of C 3 Plants-A Re-Examination I. Interspecific Variability. *Zeitschrift für Pflanzenphysiologie* 103(5):445-450.

Björndahl, G., and S. Nilsen. 1985. Growth potential of Lemna gibba: Effect of CO 2 enrichment at high photon flux rate. *Aquatic botany* 22(1):79-82.

Bot, G. P. 1983. Greenhouse climate: from physical processes to a dynamic model.

Bowker, D., and P. Denny. 1980. THE SEASONAL SUCCESSION AND DISTRIBUTION OF EPIPHYTIC ALGAE IN THE PHYLLOSPHERE OF LEMNA-MINOR-L. *Archiv Fur Hydrobiologie* 90(1):39-55.

Bown, H. E., M. S. Watt, P. W. Clinton, E. G. Mason, and B. Richardson. 2007. Partititioning concurrent influences of nitrogen and phosphorus supply on photosynthetic model parameters of Pinus radiata. *Tree physiology* 27(3):335-344.

Caicedo, J., N. Van der Steen, O. Arce, and H. Gijzen. 2000. Effect of total ammonia nitrogen concentration and pH on growth rates of duckweed (Spirodela polyrrhiza). *Water Research* 34(15):3829-3835.

Casperson, G. 1956. Warmehaushaltstudien an Wasserpflanzen. *Ber. Deut. Bot.*(69):479-486.

Cedergreen, N., and T. V. Madsen. 2002. Nitrogen uptake by the floating macrophyte Lemna minor. *New Phytologist* 155(2):285-292.

Cheng, J., L. Landesman, B. Bergmann, J. J. Classen, J. Howard, and Y. Yamamoto. 2002. Nutrient removal from swine lagoon liquid by Lemna minor 8627. *Transactions of the ASAE* 45(4):1003.

CVB. 2012. Tabellenboek Veevoeding 2012. CVB, ed. Den Haag: Productschap Diervoeder 2012.

Dale, H., and T. Gillespie. 1976. The influence of floating vascular plants on the diurnal fluctuations of temperature near the water surface in early spring. *Hydrobiologia* 49(3):245-256.

Dasgupta, P. K., and S. Dong. 1986. Solubility of ammonia in liquid water and generation of trace levels of standard gaseous ammonia. *Atmospheric Environment (1967)* 20(3):565-570.

DeBusk, T., J. Ryther, and L. Williams. 1983. Evapotranspiration of Eichhornia crassipes (Mart.) Solms and Lemna minor L. in central Florida: relation to canopy structure and season. *Aquatic Botany* 16(1):31-39.

Docauer, D. 1983. A nutrient basis for the distribution of the Lemnaceae. *Dissertations Abstracts International, B (Sciences and Engineering)* 44(6):1705-1706.

Drexler, J. Z., R. L. Snyder, D. Spano, U. Paw, and K. Tha. 2004. A review of models and micrometeorological methods used to estimate wetland evapotranspiration. *Hydrological Processes* 18(11):2071-2101.

Driever, S. M., E. H. v. Nes, and R. M. M. Roijackers. 2005. Growth limitation of Lemna minor due to high plant density. *Aquatic Botany* 81(3):245-251.

Eshel, A., and S. Beer. 1986. Inorganic carbon assimilation by Spirodela polyrrhiza. *Hydrobiologia* 131(2):149-153.
Evans, J., I. Jakobsen, and E. Ögren. 1993. Photosynthetic light-response curves. *Planta* 189(2):191-200.
Farquhar, G. v., S. v. von Caemmerer, and J. Berry. 1980. A biochemical model of photosynthetic CO2 assimilation in leaves of C3 species. *Planta* 149(1):78-90.
Filbin, G. J., and R. A. Hough. 1985. Photosynthesis, photorespiration, and productivity in Lemna minor Ll. *Limnol. Oceanogr* 30(2):322-334.
Flexas, J., M. Ribas-Carbo, A. DIAZ-ESPEJO, J. GalmES, and H. Medrano. 2008. Mesophyll conductance to CO2: current knowledge and future prospects. *Plant, Cell & Environment* 31(5):602-621.
Frankart, C., P. Eullaffroy, and G. Vernet. 2003. Comparative effects of four herbicides on non-photochemical fluorescence quenching in Lemna minor. *Environmental and Experimental Botany* 49(2):159-168.
Frédéric, M., L. Samir, M. Louise, and A. Abdelkrim. 2006. Comprehensive modeling of mat density effect on duckweed (Lemna minor) growth under controlled eutrophication. *Water research* 40(15):2901-2910.
Fuhrer, J. 1983. LIGHT-INHIBITION OF DARK RESPIRATION IN LEMNA-MINOR-L. *Botanica Helvetica* 93(1):67-75.
Gaastra, P. 1959. Photosynthesis of crop plants as influenced by light, carbon dioxide, temperature, and stomatal diffusion resistance.
Gelder, J. W., and A. Herder. 2012. Soja Barometer 2012.
Genty, B., J.-M. Briantais, and N. R. Baker. 1989. The relationship between the quantum yield of photosynthetic electron transport and quenching of chlorophyll fluorescence. *Biochimica et Biophysica Acta (BBA)-General Subjects* 990(1):87-92.
Goudriaan, J., and H. Van Laar. 1994. *Modelling potential crop growth processes: textbook with exercises*. Springer Science & Business Media.
Gutierrez, K., L. Sangines, F. Perez, and L. Martinez. 2001. Studies on the potential of the aquatic plant Lemna gibba for pig feeding. *Cuban Journal of Agricultural Science* 35(4):343-348.
Gwaze, F. R., and M. Mwale. 2015. The Prospect of Duckweed in Pig Nutrition: A Review. *Journal of Agricultural Science* 7(11):189.
Hatew, B. 2015. Low emission feed: opportunities to mitigate enteric methane production of dairy cows. Wageningen University.
Heldt, H.-W., and B. Piechulla. 2011a. 6 - The Calvin cycle catalyzes photosynthetic CO2 assimilation. In *Plant Biochemistry (Fourth Edition)*, 163-191. San Diego: Academic Press.
Heldt, H.-W., and B. Piechulla. 2011b. 7 - Phosphoglycolate formed by the oxygenase activity of RubisCO is recycled in the photorespiratory pathway. In *Plant Biochemistry (Fourth Edition)*, 193-209. San Diego: Academic Press.
Heldt, H.-W., and B. Piechulla. 2011c. 8 - Photosynthesis implies the consumption of water. In *Plant Biochemistry (Fourth Edition)*, 211-239. San Diego: Academic Press.
Hikosaka, K., K. Ishikawa, A. Borjigidai, O. Muller, and Y. Onoda. 2006. Temperature acclimation of photosynthesis: mechanisms involved in the changes in temperature dependence of photosynthetic rate. *Journal of experimental botany* 57(2):291-302.
Holshof, G., I. Hoving, and E. T. H. M. Peeters. 2009. *Eendenkroos: van afval tot veevoer*. Wageningen UR Livestock Research.
Hoving, I., G. Holshof, and M. Timmerman. 2012. Effluentzuivering met eendenkroos= Effluent polishing with duck weed. Wageningen UR Livestock Research.
Ibusuki, T., and V. P. Aneja. 1984. Mass transfer of NH 3 into water at environmental concentrations. *Chemical Engineering Science* 39(7):1143-1155.
Ilahi, W. F. F. 2009. Evapotranspiration Models in Greenhouse.
Ingemarsson, B., L. Johansson, and C. M. Larsson. 1984. Photosynthesis and nitrogen utilization in exponentially growing nitrogen-limited cultures of Lemna gibba. *Physiologia plantarum* 62(3):363-369.
Jupsin, H., H. Richard, and J. Vasel. 2005. Contribution of floating macrophytes (Lemna sp.) to pond modelization. *Water Science and Technology* 51(12):283-289.
Koerkamp, P. G., J. Metz, G. Uenk, V. Phillips, M. Holden, R. Sneath, J. Short, R. White, J. Hartung, and J. Seedorf. 1998. Concentrations and emissions of ammonia in livestock buildings in Northern Europe. *Journal of Agricultural Engineering Research* 70(1):79-95.
Körner, S., and J. Vermaat. 1998. The relative importance of Lemna gibba L., bacteria and algae for the nitrogen and phosphorus removal in duckweed-covered domestic wastewater. *Water Research* 32(12):3651-3661.

Krishna, K. B., and C. Polprasert. 2008. An integrated kinetic model for organic and nutrient removal by duckweed-based wastewater treatment (DUBWAT) system. *ecological engineering* 34(3):243-250.
Kroes, K., s. Huurman, C. d. Visser, G. Hemke, J. Liere, and N. v. d. Top. 2016. De ECOFERM Kringloopboerderij in de praktijk.
Kromer, S. 1995. Respiration during photosynthesis. *Annual review of plant biology* 46(1):45-70.
Laisk, A., and F. Loreto. 1996. Determining photosynthetic parameters from leaf CO2 exchange and chlorophyll fluorescence (ribulose-1, 5-bisphosphate carboxylase/oxygenase specificity factor, dark respiration in the light, excitation distribution between photosystems, alternative electron transport rate, and mesophyll diffusion resistance. *Plant Physiology* 110(3):903-912.
Landolt, E., and R. Kandeler. 1987. Biosystematic investigations in the family of duckweeds (Lemnaceae)(vol. 4). *The family of Lemnaceae-a monographic study* 2:211-234.
Lasfar, S., F. Monette, L. Millette, and A. Azzouz. 2007. Intrinsic growth rate: a new approach to evaluate the effects of temperature, photoperiod and phosphorus–nitrogen concentrations on duckweed growth under controlled eutrophication. *Water research* 41(11):2333-2340.
Le thi Men, B. H. V., M. T. Chinh, and T. Preston. 1997. Effect of dietary protein level and duckweed (Lemna spp) on reproductive performance of pigs fed a diet of ensiled cassava root or cassava root meal. *Livestock Research for Rural Development* 9(1).
Lee, C. g., T. D. Fletcher, and G. Sun. 2009. Nitrogen removal in constructed wetland systems. *Engineering in Life Sciences* 9(1):11-22.
Loats, K., R. Noble, and B. Takemoto. 1981. Photosynthesis under Low-Level SO2 and CO2 Enhancement Conditions in Three Duckweed Species. *Botanical Gazette*:305-310.
Mangat, B., W. Levin, and R. Bidwell. 1974. The extent of dark respiration in illuminated leaves and its control by ATP levels. *Canadian Journal of Botany* 52(4):673-681.
Müller, P., X.-P. Li, and K. K. Niyogi. 2001. Non-photochemical quenching. A response to excess light energy. *Plant physiology* 125(4):1558-1566.
Nolan, W. G., and R. M. Smillie. 1976. Multi-temperature effects on Hill reaction activity of barley chloroplasts. *Biochimica et Biophysica Acta (BBA)-Bioenergetics* 440(3):461-475.
Ritchie, R. J., and N. Mekjinda. 2016. Arsenic toxicity in the water weed Wolffia arrhiza measured using Pulse Amplitude Modulation Fluorometry (PAM) measurements of photosynthesis. *Ecotoxicology and Environmental Safety* 132:178-185.
Rooijakkers, P. 2016. Photosynthesis model to predict duckweed growth at the Ecoferm greenhouse.
Rusoff, L. L., E. W. Blakeney Jr, and D. D. Culley Jr. 1980. Duckweeds (Lemnaceae family): a potential source of protein and amino acids. *Journal of Agricultural and Food Chemistry* 28(4):848-850.
Sage, R. F. 1990. A model describing the regulation of ribulose-1, 5-bisphosphate carboxylase, electron transport, and triose phosphate use in response to light intensity and CO2 in C3 plants. *Plant Physiology* 94(4):1728-1734.
Sander, R. 1999. Compilation of Henry's law constants for inorganic and organic species of potential importance in environmental chemistry. Max-Planck Institute of Chemistry, Air Chemistry Department Mainz, Germany.
Sharkey, T. D., C. J. Bernacchi, G. D. Farquhar, and E. L. Singsaas. 2007. Fitting photosynthetic carbon dioxide response curves for C3 leaves. *Plant, Cell & Environment* 30(9):1035-1040.
Shelp, B. J., and D. T. Canvin. 1980. Utilization of exogenous inorganic carbon species in photosynthesis by Chlorella pyrenoidosa. *Plant physiology* 65(5):774-779.
Skillicorn, P., W. Spira, and W. Journey. 1993. A New Aquatic Farming System for Developing Countries. *The World Bank Group*.
Takemoto, B., and R. Noble. 1986. Differential sensitivity of duckweeds (Lemnaceae) to sulphite. I. Carbon assimilation and frond replication rate as factors influencing sulphite phytotoxicity under low and high irradiance. *New phytologist*:525-539.
Tuomisto, H. L., and M. J. Teixeira de Mattos. 2011. Environmental impacts of cultured meat production. *Environmental science & technology* 45(14):6117-6123.
Ullrich-Eberius, C., A. Novacky, and A. Van Bel. 1984. Phosphate uptake inLemna gibba G1: energetics and kinetics. *Planta* 161(1):46-52.
Valdés-Gómez, H., S. Ortega-Farías, and M. Argote. 2009. Evaluation of water requirements for a greenhouse tomato crop using the Priestley-Taylor method.
van 't Ooster, A. 2016. Building Physics and Climate Engineering. *FTE-25303*.
van der Werf, A., R. Welschen, and H. Lambers. 1992. Respiratory losses increase with decreasing inherent growth rate of a species and with decreasing nitrate supply: a search for explanations for these observations. *Molecular, biochemical and physiological aspects of plant respiration*:421-432.
van der Werf, A. 2016. Personal conversation requirements cultivation of duckweed.
van Ooteghem, R. 2016. Physical Transport Phenomena. *BCT-22803*.

van Ooteghem, R. J. C. 2007. Optimal control design for a solar greenhouse. *IFAC Proceedings Volumes* 43(26):304-309.
van Willigenburg, L., and R. van Ooteghem. 2015. reader Modelling Dynamic Systems.
von Caemmerer, S. 2000. *Biochemical models of leaf photosynthesis*. Csiro publishing.
Walcroft, A., D. Whitehead, W. Silvester, and F. Kelliher. 1997. The response of photosynthetic model parameters to temperature and nitrogen concentration in Pinus radiata D. Don. *Plant, Cell & Environment* 20(11):1338-1348.
Wang, X., J. D. Lewis, D. T. Tissue, J. R. Seemann, and K. L. Griffin. 2001. Effects of elevated atmospheric CO2 concentration on leaf dark respiration of Xanthium strumarium in light and in darkness. *Proceedings of the National Academy of Sciences* 98(5):2479-2484.
Warren, C. R. 2004. The photosynthetic limitation posed by internal conductance to CO2 movement is increased by nutrient supply. *Journal of Experimental Botany* 55(406):2313-2321.
Weiss, J., H. Liebert, and W. Braune. 2000. Influence of microcystin-RR on growth and photosynthetic capacity of the duckweed Lemna minor L. *Journal of Applied Botany* 74(3/4):100-105.
Wendeou, S. P. H., M. P. Aina, M. Crapper, E. Adjovi, and D. Mama. 2013. Influence of Salinity on Duckweed Growth and Duckweed Based Wastewater Treatment System. *Journal of Water Resource and Protection* 5(10):993.
Wertenbroek, N., E. Kannekens, M. Steenaert, and M. Ordeman. 2013. *Zakboek varkens Belangrijke Informatie voor de varkenshouderij*. Boehringer Ingelheim.
Whiteman, P., and D. Koller. 1967. Species characteristics in whole plant resistances to water vapour and CO2 diffusion. *Journal of Applied Ecology*:363-377.
Willmer, C. M., and M. Fricker. 1996. *Stomata*. Chapman & Hall.
Wostrikoff, K., and D. B. Stern. 2009. Chapter 9 - Rubisco. In *The Chlamydomonas Sourcebook (Second Edition)*, 303-332. London: Academic Press.
Xu, J., and G. Shen. 2011. Effects of harvest regime and water depth on nutrient recovery from swine wastewater by growing Spirodela oligorrhiza. *Water Environment Research* 83(11):2049-2056.
Yang, J. T., A. L. Preiser, Z. Li, S. E. Weise, and T. D. Sharkey. 2016. Triose phosphate use limitation of photosynthesis: short-term and long-term effects. *Planta* 243(3):687-698.
Zhang, K., Y.-P. Chen, T.-T. Zhang, Y. Zhao, Y. Shen, L. Huang, X. Gao, and J.-S. Guo. 2014. The logistic growth of duckweed (Lemna minor) and kinetics of ammonium uptake. *Environmental technology* 35(5):562-567.
Zimmo, O., N. Van der Steen, and H. Gijzen. 2004. Nitrogen mass balance across pilot-scale algae and duckweed-based wastewater stabilisation ponds. *Water Research* 38(4):913-920.

10 Appendix

10.1 Appendix literature chapter

Table 25. Composition of a Hutner 1/5 solution (Landolt and Kandeler, 1987).

Substance	mg L^{-1}
NH_4NO_3	40
K_2HPO_4	80
$Ca(NO_3)_2$*4 H_2O	40
$MgSO_4$*7H_2O	100
$FeSO_4$*7H_2O	5
$MnSO_4$*7H_2O	3
$ZnSO_4$*7H_2O	13
H_3BO_3	3
Na_2MoO_4*2H_2O	5
$CuSO_4$*5H_2O	0.8
$CoSO_4$*7H_2O	0.2
Na_2 salt of EDTA	100

The following carbohydrates cannot be used by *Lemnaceae* species; ethanol, glycerol, mannitol, inuline, starch, lactose, arabinose, ribose, tartrate, succinate, acetate, citrate, malonic acid, oxalic acid, glucuronic acid, and glutamic acid.

Below the equations for Figure 1 (N consumption rate by duckweed) can be found (Zhang, 2014); x is the ammonium concentration.

$$y = \frac{\left(0.082 * \frac{x}{1.877 + x}\right)}{18.04} * 14 \qquad [mg\ N\ m^{-2}\ h^{-1}] \qquad 10.1$$

Table 26. Parameters for calculation CO_2 compensation point calculation (Farquhar et al., 1980).

K_c	Michaelis-Menten constant for CO_2	460	$[\mu bar]$
K_o	Michaelis-Menten constant for O_2	330	$[mbar]$
k_c	Turnover number of RuP_2 carboxylase	2.5	$[s^{-1}]$
k_o	Turnover number of RUP_2 oxygenase	0.525	$[s^{-1}]$
O	Partial pressure of O_2	210	$[mbar]$
R_d	Dark respiration (Fuhrer, 1983)	min=0.34;max=1.36	$[\mu mol\ m^{-2} s^{-1}]$
$V_{c\,max26}$	Maximum carboxylation rate	23.8	$[\mu mol\ m^{-2} s^{-1}]$

Table 27. Parameters for calculating the mesophyll resistance. Some values might be different then Table 26, due to this model is based on a different research (van Ooteghem, 2007).

K_{c25}	Michaelis-Menten constant for CO_2	310	$[\mu bar]$
K_{o25}	Michaelis-Menten constant for O_2	155	$[mbar]$
K_c	Michaelis-Menten carboxylation	eq 10.2	$[\mu bar]$
K_o	Michaelis-Menten oxygenation	eq 10.3	$[mbar]$
K_m	Effective Michaelis-Menten constant	eq 10.4	$[\mu bar]$
E_c	Activation energy K_c	59356	$[J\ mol^{-1}]$
E_o	Activation energy K_o	35948	$[J\ mol^{-1}]$
E_{vc}	Activation energy $V_{c\,max}$	58520	$[J\ mol^{-1}]$
O	Partial pressure of O_2	210	$[mbar]$
$\rho CO_2 T$	Density of CO_2	eq 3.2	$[kg\ m^{-3}]$
$V_{c\,max26}$	Maximum carboxylation rate at 26	23.8	$[\mu mol\ m^{-2}\ [leaf]\ s^{-1}]$
$V_{c\,max}$	Maximum carboxylaton rate at given T	eq 10.5	$[\mu mol\ m^{-2}\ [leaf]\ s^{-1}]$
R_m	Mesophyll resistance	eq 10.6	$[s\ m^{-1}]$

Below all equations are given to calculate the mesophyll resistance.

$$K_c = K_{c25} * e^{E_c * X} \quad [\mu bar] \quad 10.2$$

$$K_o = K_{o25} * e^{E_o * X} \quad [mbar] \quad 10.3$$

$$K_m = K_c * (1 + \frac{O}{K_o}) \quad [\mu bar] \quad 10.4$$

$$V_{c\,max} = V_{c\,max26} * e^{E_{vc} * X} \quad [\mu mol\ m^{-2} s^{-1}] \quad 10.5$$

$$R_m = \frac{K_m}{V_{c\,max}} * \frac{\rho CO_2 T}{MCO_2} + 15 \quad [s\ m^{-1}] \quad 10.6$$

10.2 Appendix theory model

Table 28. Formulas to calculate the fictive emission of a clear sky and the vapour pressure outside.

$E_{sky\,clear} = 0.53 + 6 * 10^{-3} * \sqrt{poH_2O}$	Fictive emission coefficient of clear sky	$[-]$	10.7
$poH_2O = poH_2Os * RH_{out}$	Vapour pressure outside	$[Pa]$	10.8

Below the formulas are given for determining the diffuse fraction. I_o is in this case the measured outdoor radiation. Otherwise the τ_{atm} could not be calculated due to the fact that for determining the outside radiation f_{par} is needed eq. 10.12. If the sinB is smaller than 0.001, only diffuse radiation is possible, because then the position of the sun is too low to cause direct radiation.

Table 29. Formulas to determine the diffuse fraction f_{difpar}.

$Solar_C = 1367 * (1 + 0.033 * \cos\left(2\pi * \frac{dayN}{365}\right))$	Solar radiation at outer layer of atmosphere	$[W\ m^{-2}\ soil]$	10.9
$\tau_{atm} = \frac{I_o}{solar_C + sinB}$	Transmittance of atmosphere	$[-]$	10.10
$f_{difpar} = 1$ $or\ if\ sinB > 1 * 10^{-3}$ $f_{difpar} = \min(f_{dif} * (1 + 0.35 * f_{clear}), 1)$	Fraction diffuse PAR in total radiation	$[-]$	10.11

The table below is a summary to determine the direct and diffuse radiation inside and outside the greenhouse. I_{PO} is PAR outside greenhouse. Normally the outside radiation is converted to PAR, however I_{PO} is calculated with equation 10.12 and 10.13, as a result f_{par} was not needed.

Table 30. Calculation of the diffuse ($I_{P\,dif}$) and direct ($I_{P\,dir}$) radiation inside the greenhouse.

$I_o = \frac{I_A}{f_{par} * \tau_{dirR}}$	Radiation outside, I_A is measured radiation in greenhouse.	$[W\ m^{-2}\ soil]$	10.12
$I_{PO} = f_{par} * I_o$	PAR outside greenhouse	$[W\ m^{-2}\ soil]$	10.13
$I_{P\,difO} = f_{difpar} * I_{PO}$	Diffuse PAR outside	$[W\ m^{-2}\ soil]$	10.14
$I_{PdirO} = I_{pO} - I_{P\,difO}$	Direct PAR outside	$[W\ m^{-2}\ soil]$	10.15
$I_{P\,dif} = \tau_{difR} * I_{P\,difO}$	Diffuse PAR inside	$[W\ m^{-2}\ soil]$	10.16
$I_{P\,dir} = \tau_{dirR} * I_{P\,dirO}$	Direct PAR inside	$[W\ m^{-2}\ soil]$	10.17

To convert the direct and diffuse radiation outside to the irradiation inside the greenhouse I_{pdif} and I_{Pdir} are multiplied with the transmittance coefficients below.

$\tau_{difR} = 0.59$	Transmittance of the roof for diffuse radiation	$[-]$	10.18
$\tau_{dirR} = 0.85 * \left(1 - e^{-0.083 * \frac{360}{2\pi} * \beta_{sun}}\right)$	Transmittance of the roof for direct radiation	$[-]$	10.19

Table 31. Formulas for reflection, transmittance and fraction sunlit leaf area.

$\beta_{dif} = \frac{1-\sqrt{1-s}}{1+\sqrt{1-s}}$	Diffuse reflection by canopy	[−]	10.20
$\beta_{dir} = \frac{2}{1+\frac{k_{difBL}}{k_{dirBL}}} * \beta_{dif}$	Direct reflection by canopy	[−]	10.21
$\tau_{dif} = e^{-k_{dif}*LAI_l}$	Diffuse transmittance	[−]	10.22
$\tau_{dir} = e^{-k_{dir}*LAI_l}$	Direct transmittance	[−]	10.23
$\tau_{dirBL} = e^{-k_{dirBL}*LAI_l}$	Direct transmittance for black leaves	[−]	10.24
$f_{sla} = \tau_{dirBL}$	Fraction sunlit leaf area, in other words which part of the fronds is in the sun.	[−]	10.25

Table 32. All variables and parameters for the leaf area index light correction.

Leaf area index light correction variables and parameters			
LAI	Fraction of A_{pond} covered by duckweed	eq 4.50	[−]
LAI_l	LAI at given layer depth l_1	eq 4.51	[−]
$P_{g\,sun}$	Gross leaf assimilation rate sunlit fronds	eq 4.52	$[mg\ CO2\ m^{-2}\ leaf]$
$P_{g\,shd}$	Gross leaf assimilation rate shaded fronds	eq 4.53	$[mg\ CO2\ m^{-2}\ leaf]$
$P_{g\,l}$	Total leaf assimilation rate	eq 4.54	$[mg\ CO2\ m^{-2}\ leaf]$
X_g	Layer depth correction values	[0.11,0.5,0.89]	[−]
W_g	Weighing factors	[0.28,0.44,0.28]	[−]
l_1	First counter for canopy depth	[1,2,3]	[−]
l_2	Second counter for sunlit leaves	[1,2,3]	[−]
$I_{A\,sun}$	Total irradiation sunlit fronds at layer depth l_1 and light correct l_2	eq 4.55	$[W\ m^{-2}\ leaf]$
$I_{A\,shade}$	Total irradiation shaded fronds at layer depth l_1	eq 4.56	$[W\ m^{-2}\ leaf]$
$I_{A\,dif}$	Diffuse radiation at leaf layer l_1	eq 4.57	$[W\ m^{-2}\ leaf]$
$I_{A\,tdir}$	Total direct radiation at leaf layer l_1	eq 4.58	$[W\ m^{-2}\ leaf]$
$I_{A\,dir}$	Direct radiation at leaf layer l_1	eq 4.59	$[W\ m^{-2}\ leaf]$
$I_{A\,ppd}$	Direct flux leaves perpendicular on direct beam	eq 4.60	$[W\ m^{-2}\ leaf]$
$I_{P\,dif}$	Diffuse light in greenhouse	eq 4.61	$[W\ m^{-2}\ soil]$
$I_{P\,dir}$	Direct light in greenhouse	eq 4.62	$[W\ m^{-2}\ soil]$
$Solar_C$	Solar radiation at outer layer of atmosphere	eq 10.9	$[W\ m^{-2}]$
τ_{atm}	Transmittance of atmosphere	eq 10.10	[−]
$fdifpar$	Fraction diffuse par in total radiation	eq 10.11	[−]
I_O	Radiation outside, I_A is measured radiation in greenhouse.	eq 10.12	$[W\ m^{-2}\ soil]$
I_{PO}	PAR outside greenhouse	eq 10.13	$[W\ m^{-2}\ soil]$
$I_{P\,difO}$	Diffuse PAR outside	eq 10.14	$[W\ m^{-2}\ soil]$
$I_{P\,dirO}$	Direct PAR outside	eq 10.15	$[W\ m^{-2}\ soil]$
$I_{P\,dif}$	Diffuse PAR inside	eq 10.16	$[W\ m^{-2}\ soil]$
$I_{P\,dir}$	Direct PAR inside	eq 10.17	$[W\ m^{-2}\ soil]$
τ_{difR}	Transmittance of the roof for diffuse radiation	0.59	[−]

τ_{dirR}	Transmittance of the roof for direct radiation	eq 10.19	$[-]$
β_{dif}	Diffuse reflection by canopy	eq 10.20	$[-]$
β_{dir}	Direct reflection by canopy	eq 10.21	$[-]$
τ_{dif}	Diffuse transmittance layer depth dependent	eq 10.22	$[-]$
τ_{dir}	Direct transmittance layer depth dependent	eq 10.23	$[-]$
τ_{dirBL}	Direct transmittance for black leaves layer depth dependent	eq 10.24	$[-]$
f_{sla}	Fraction sunlit leaf area, in other words which part of the fronds is in the sun. Layer depth dependent	eq 10.25	$[-]$
s	Scattering coefficient	0.15	$[-]$
k_{difBL}	Diffuse extinction coefficient black leaves	0.8	$[-]$
k_{dif}	Diffuse extinction coefficient	eq 4.63	$[-]$
k_{dirBL}	Direct extinction coefficient black leaves	eq 4.65	$[-]$
k_{dir}	Direct extinction coefficient	eq 4.64	$[-]$
slo	Specific leaf orientation	0.5	$[-]$
SOL_{hr}	Solar Time of the day corrected for Middle European Time	eq 4.67	$[h]$
$sinB$	Sine of solar elevation	eq 4.68	$[-]$
B_{sun}	Elevation of the sun	$\sin^{-1}$(sinB)	$[rad]$
δ_{sun}	Solar declination angle between horizontal plane and sun	eq 4.66	[°]
Lat	Latitude ECOFERM	52.26	[°]
$Long$	Longitude ECOFERM	5.78	[°]

10.3 Appendix results

Table 33. Figures of T_{dw} vs T_w for all months.

May	June
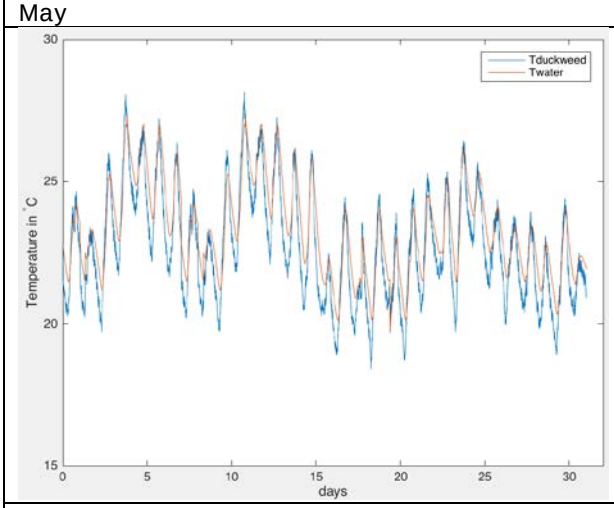	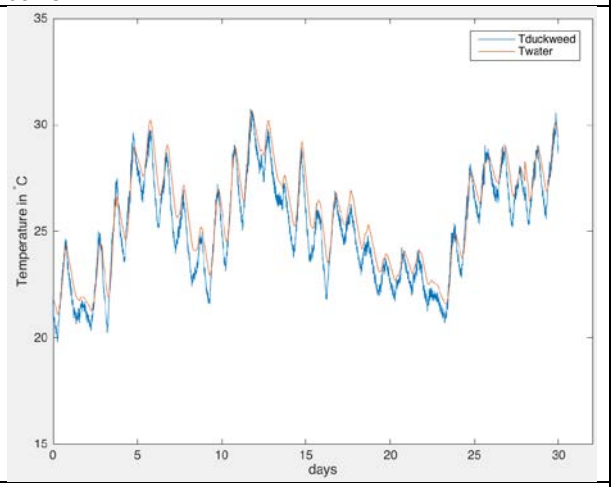
July	Augustus
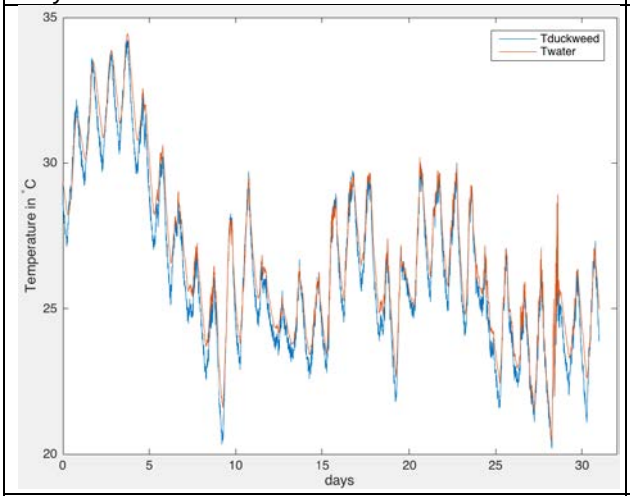	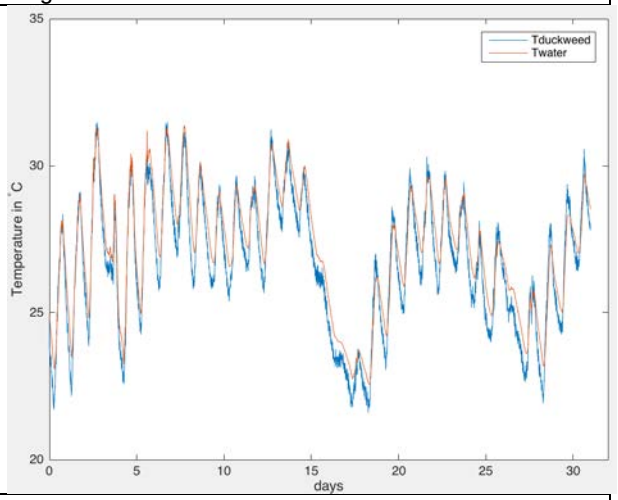
September	October
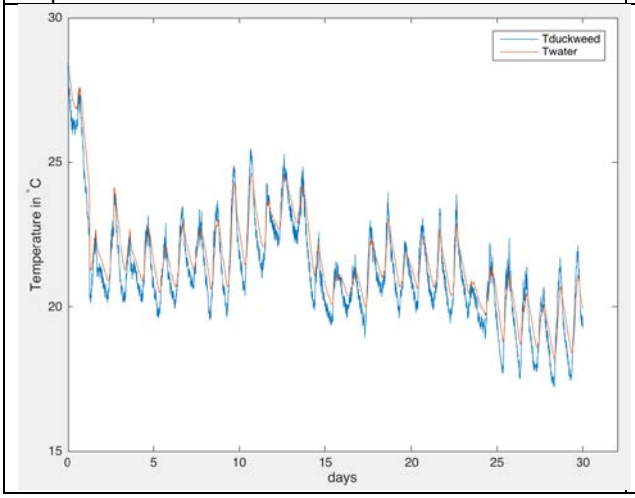	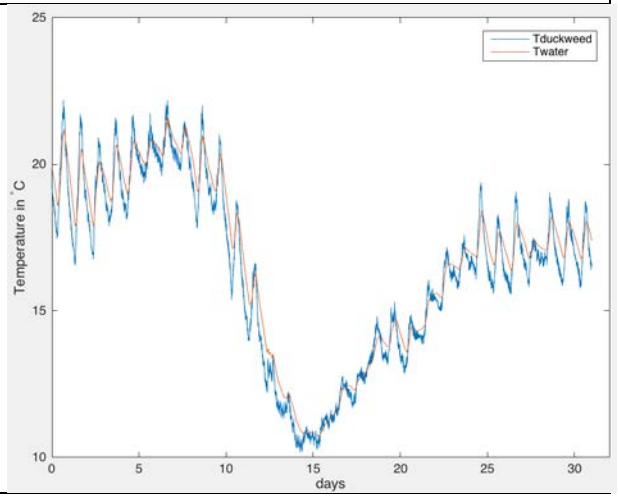

Table 34. Result of sensitivity analysis with an initial density of 311.1 g FW m^{-2}.

	alpha_TPU	Topt	Initial density	J_max26	Ej	Ec	Eo	Rs	theta	Gamma	r_Dulold	FullA	VwindG	Fp	JtoVc	Foc	Cn	PPM
alpha_TPU	1.17E+09	1.36E+10	-3.28E+09	-3.68E+09	5.00E+08	-1.67E+08	6.46E+07	6.52E+06	-4.19E+08	4.66E+06	8.47E+08	8.51E+09	-4.01E+06	1.19E+09	6.82E+09	2.07E+09	-3.50E+08	-7.05E+08
Topt		1.63E+11	-3.98E+10	-4.43E+10	5.78E+09	-1.94E+09	7.49E+08	7.59E+07	-4.89E+09	5.40E+07	9.82E+09	9.77E+10	-4.67E+07	1.37E+10	7.79E+10	2.39E+10	-4.11E+09	-8.23E+09
Initial density			9.97E+09	1.11E+10	-1.40E+09	4.70E+08	-1.81E+08	-1.84E+07	1.19E+09	-1.31E+07	-2.37E+09	-2.35E+10	1.13E+07	-3.30E+09	-1.86E+10	-5.74E+09	1.00E+09	2.01E+09
J_max26				1.24E+10	-1.57E+09	5.27E+08	-2.03E+08	-2.06E+07	1.33E+09	-1.46E+07	-2.66E+09	-2.64E+10	1.27E+07	-3.71E+09	-2.09E+10	-6.44E+09	1.12E+09	2.25E+09
Ej					2.13E+08	-7.13E+07	2.75E+07	2.78E+06	-1.78E+08	1.98E+06	3.61E+08	3.63E+09	-1.71E+06	5.05E+08	2.91E+09	8.80E+08	-1.49E+08	-3.01E+08
Ec						2.39E+07	-9.22E+06	-9.30E+05	5.98E+07	-6.64E+05	-1.21E+08	-1.21E+09	5.72E+05	-1.69E+08	-9.71E+08	-2.95E+08	4.99E+07	1.01E+08
Eo							3.56E+06	3.60E+05	-2.31E+07	2.57E+05	4.67E+07	4.69E+08	-2.21E+05	6.53E+07	3.76E+08	1.14E+08	-1.93E+07	-3.89E+07
Rs								36305	-2.33E+06	25911	4.71E+06	4.72E+07	-22314	6.59E+06	3.78E+07	1.15E+07	-1.95E+06	-3.93E+06
theta									1.50E+08	-1.66E+06	-3.02E+08	-3.03E+09	1.43E+06	-4.23E+08	-2.42E+09	-7.37E+08	1.25E+08	2.53E+08
Gamma										18507	3.37E+06	3.38E+07	-15927	4.71E+06	2.71E+07	8.21E+06	-1.39E+06	-2.80E+06
r_Dulold											6.12E+08	6.14E+09	-2.90E+06	8.56E+08	4.93E+09	1.49E+09	-2.53E+08	-5.10E+08
FullA												6.18E+10	-2.90E+07	8.60E+09	4.97E+10	1.50E+10	-2.53E+09	-5.11E+09
VwindG													13715	-4.05E+06	-2.32E+07	-7.06E+06	1.20E+06	2.42E+06
Fp														1.20E+09	6.90E+09	2.09E+09	-3.53E+08	-7.12E+08
JtoVc															4.00E+10	1.20E+10	-2.02E+09	-4.08E+09
Foc																3.64E+09	-6.15E+08	-1.24E+09
Cn																	1.05E+08	2.11E+08
PPM																		4.26E+08

Table 35. Correlation coefficient of May with an initial density of 311.1 g FW m^{-2}.

	alpha_TPU	Topt	Initial density	J_max26	Ej	Ec	Eo	Rs	theta	Gamma	r_Dulold	FullA	VwindG	Fp	JtoVc	Foc	Cn	PPM
alpha_TPU	1	0.27334	-0.094303	0.25501	0.17454	0.27907	0.18959	0.093582	-0.098576	-0.17867	0.11749	0.14903	0.19929	-0.0080983	-0.38795	-0.74351	0.41173	-0.13534
Topt		1	0.53528	-0.46987	-0.097167	-0.097306	-0.053283	-0.011408	-0.46968	0.03631	-0.43841	-0.34675	0.11869	-0.39044	0.13594	0.18346	0.80441	0.2957
Initial density			1	-0.95601	-0.24124	0.086748	0.14135	-0.022624	-0.32902	-0.020434	-0.46136	-0.483	0.037311	-0.091321	0.26548	0.22036	-0.03105	0.85271
J_max26				1	0.3042	0.0015959	-0.093191	0.061447	0.23997	0.00057554	0.52453	0.6528	0.063052	-0.043054	-0.46148	-0.26428	0.047222	-0.90169
Ej					1	-0.23282	-0.54845	-0.28605	-0.067659	0.26981	0.17091	0.40134	0.3733	-0.27073	-0.46253	0.017964	0.015297	-0.33585
Ec						1	0.93927	-0.5228	-0.59159	0.084393	0.10158	0.081618	0.33923	-0.22655	0.040831	-0.19248	-0.19523	-0.0004783
Eo							1	-0.34334	-0.46655	-0.025792	0.027594	-0.092714	0.1521	-0.08043	0.21619	-0.19732	-0.16521	0.10207
Rs								1	0.72051	-0.37528	0.088029	-0.05293	-0.36906	0.3594	-0.058774	-0.29053	-0.0008927	0.0091366
theta									1	-0.17341	0.15953	-0.077692	-0.5832	0.65736	0.038472	-0.41476	-0.31497	-0.1076
Gamma										1	-0.098029	-0.093176	0.27365	-0.47804	0.10098	0.24259	0.012325	0.026027
r_Dulold											1	0.41939	0.16999	-0.12037	-0.31744	-0.15409	-0.20469	-0.48197
FullA												1	0.24859	-0.24171	-0.83083	0.040078	-0.17435	-0.58298
VwindG													1	-0.40857	-0.41229	0.13368	0.10823	-0.060927
Fp														1	0.076313	-0.5613	-0.31012	0.20015
JtoVc															1	0.17321	0.021954	0.32755
Foc																1	0.018888	0.071954
Cn																	1	-0.12905
PPM																		1

Table 36. Result of sensitivity analysis with a known mat density from 24 Augustus to 30.

	alpha_TPU	Topt	Initial density	J_max26	Ej	Ec	Eo	Rs	theta	Gamma	r_Dulold	FullA	VwindG	Fp	JtoVc	Foc	Cn	PPM
alpha_TPU	4.00E+06	1.05E+08	-6.19E+07	-2.10E+07	-1.25E+06	6.54E+05	-2.14E+05	41931	-2.34E+06	23856	4.10E+06	2.54E+07	-25751	5.50E+06	1.73E+07	6.68E+06	-2.35E+06	-1.24E+06
Topt		2.75E+09	-1.61E+09	-5.50E+08	-3.27E+07	1.71E+07	-5.61E+06	1.10E+06	-6.12E+07	6.24E+05	1.07E+08	6.64E+08	-6.74E+05	1.44E+08	4.52E+08	1.75E+08	-6.15E+07	-3.24E+07
Initial density			9.67E+08	3.25E+08	1.93E+07	-1.01E+07	3.31E+06	-6.49E+05	3.62E+07	-3.69E+05	-6.35E+07	-3.92E+08	3.98E+05	-8.50E+07	-2.67E+08	-1.03E+08	3.63E+07	1.93E+07
J_max26				1.10E+08	6.56E+06	-3.44E+06	1.13E+06	-2.20E+05	1.23E+07	-1.25E+05	-2.16E+07	-1.33E+08	1.35E+05	-2.89E+07	-9.09E+07	-3.51E+07	1.23E+07	6.54E+06
Ej					3.90E+05	-2.04E+05	66965	-13091	7.30E+05	-7450.3	-1.28E+06	-7.92E+06	8039.4	-1.72E+06	-5.40E+06	-2.08E+06	7.34E+05	3.88E+05
Ec						1.07E+05	-35073	6857.5	-3.82E+05	3902.6	6.71E+05	4.15E+06	-4211.4	8.99E+05	2.83E+06	1.09E+06	-3.84E+05	-2.03E+05
Eo							11488	-2246.2	1.25E+05	-1278.3	-2.20E+05	-1.36E+06	1379.4	-2.95E+05	-9.27E+05	-3.58E+05	1.26E+05	66586
Rs								439.9	-24530	250.22	43040	2.66E+05	-270.16	57659	1.81E+05	69996	-24629	-13046
theta									1.37E+06	-13953	-2.40E+06	-1.48E+07	15064	-3.22E+06	-1.01E+07	-3.90E+06	1.37E+06	7.28E+05
Gamma										142.35	24486	1.51E+05	-153.67	32805	1.03E+05	39824	-14013	-7418.5
r_Dulold											4.21E+06	2.60E+07	-26432	5.64E+06	1.77E+07	6.85E+06	-2.41E+06	-1.28E+06
FullA												1.61E+08	-1.63E+05	3.49E+07	1.10E+08	4.23E+07	-1.49E+07	-7.89E+06
VwindG													165.91	-35410	-1.11E+05	-42987	15125	8011.8
Fp														7.56E+06	2.38E+07	9.18E+06	-3.23E+06	-1.71E+06
JtoVc															7.48E+07	2.89E+07	-1.02E+07	-5.38E+06
Foc																1.11E+07	-3.92E+06	-2.08E+06
Cn																	1.38E+06	7.30E+05
PPM																		3.88E+05

Table 37. Correlation coefficient from 24 Augustus to 30 September.

	alpha_TPU	Topt	Initial density	J_max26	Ej	Ec	Eo	Rs	theta	Gamma	r_Dulold	FullA	VwindG	Fp	JtoVc	Foc	Cn	PPM
alpha_TPU	1	-0.31873	0.029396	0.60167	0.66163	-0.43886	-0.55763	0.71629	0.12391	-0.3204	-0.12621	-0.10576	0.70909	0.54881	0.09068	-0.94454	-0.032453	0.26096
Topt		1	0.098935	-0.55092	-0.39649	0.41042	0.4863	-0.40587	-0.080537	0.20742	-0.36768	-0.44798	-0.40559	0.23187	-0.20672	0.32516	-0.32331	-0.34642
Initial density			1	-0.049851	0.068424	0.0058664	-0.022388	0.020969	0.012578	0.0048594	-0.04637	-0.033443	0.020109	0.044954	0.00028351	-0.033829	0.058337	-0.01270
J_max26				1	0.37205	-0.41626	-0.47359	0.3447	-0.40077	-0.19645	-0.29371	-0.27104	0.34281	0.41218	0.082441	-0.39861	0.14697	0.26339
Ej					1	-0.23423	-0.47057	0.68082	0.054249	-0.39972	-0.084414	-0.096146	0.67566	0.50771	-0.17122	-0.5808	-0.17789	0.49783
Ec						1	0.96682	-0.27327	-0.17462	0.3126	-0.047389	-0.12045	-0.26687	-0.31833	-0.12291	0.42074	-0.25871	-0.0691
Eo							1	-0.41228	-0.18648	0.4018	-0.046535	-0.10857	-0.40501	-0.40212	-0.073309	0.52524	-0.19492	-0.17503
Rs								1	-0.032115	0.019599	-0.17339	-0.062833	0.99986	0.27464	0.18762	-0.6914	0.26716	0.60042
theta									1	-0.51443	0.81309	0.7723	-0.042897	-0.23116	-0.0068161	-0.37367	-0.16178	-0.44048
Gamma										1	-0.47924	-0.37906	0.033842	-0.34101	0.49678	0.30289	0.31413	0.08479
r_Dulold											1	0.96262	-0.17952	-0.6067	-0.069732	-0.097349	-0.034663	-0.34796
FullA												1	-0.068128	-0.66632	-0.0067029	-0.117	0.21606	-0.1922
VwindG													1	0.26749	0.19342	-0.68386	0.27006	0.60321
Fp														1	-0.21006	-0.35942	-0.32408	0.17822
JtoVc															1	-0.25376	0.27894	-0.28581
Foc																1	0.032803	-0.08982
Cn																	1	0.44798
PPM																		1

Table 38. Table of the results of each month obtained with optimal management of the photosynthetic model.

May

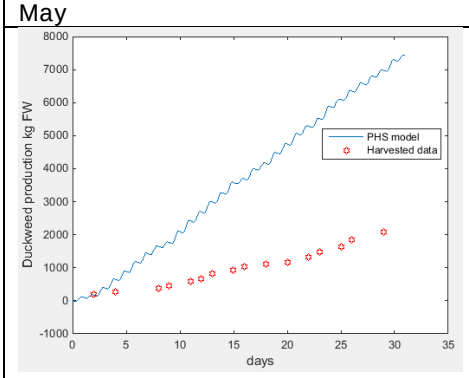

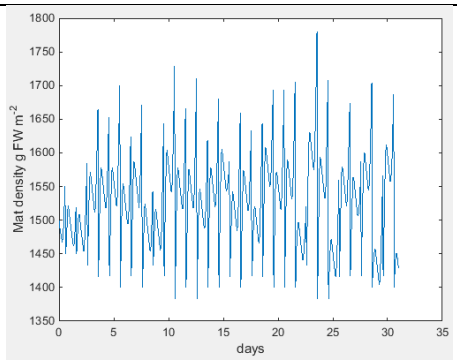

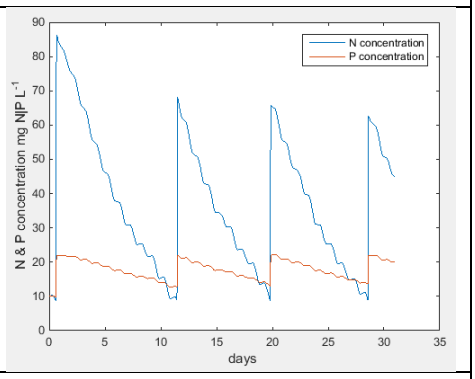

June

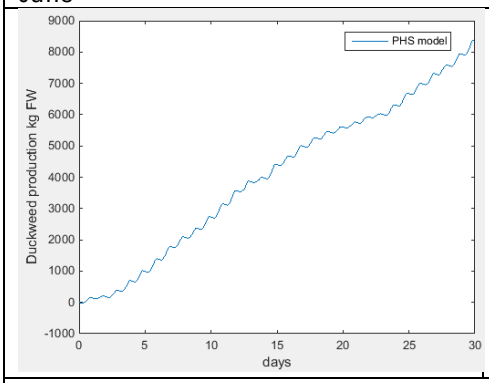

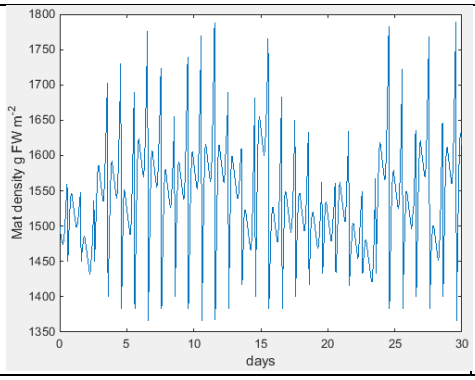

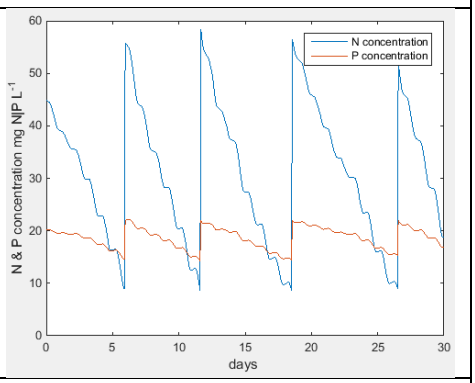

July

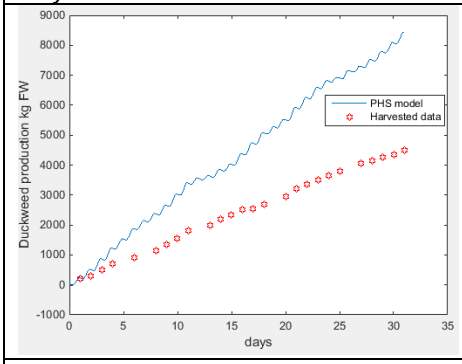

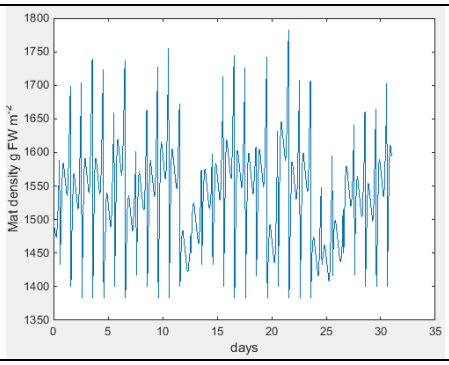

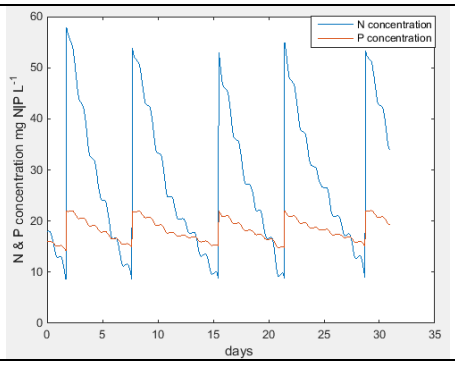

Augustus

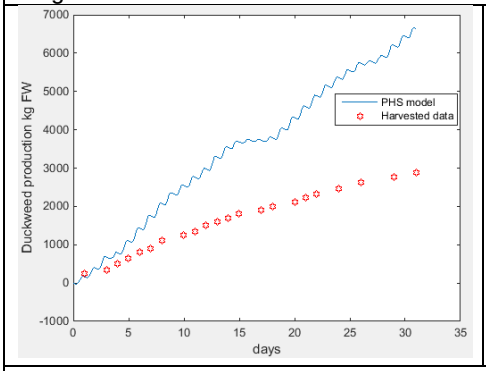

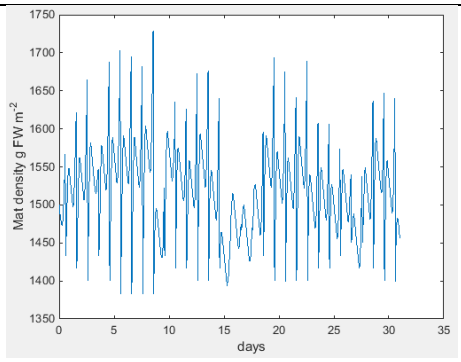

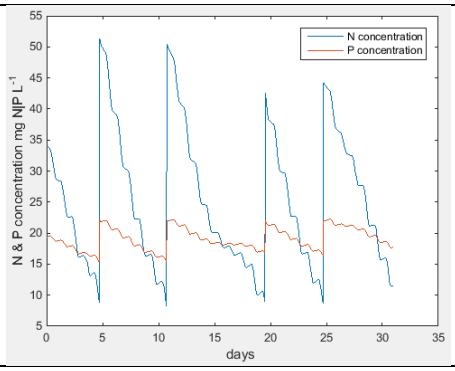

September

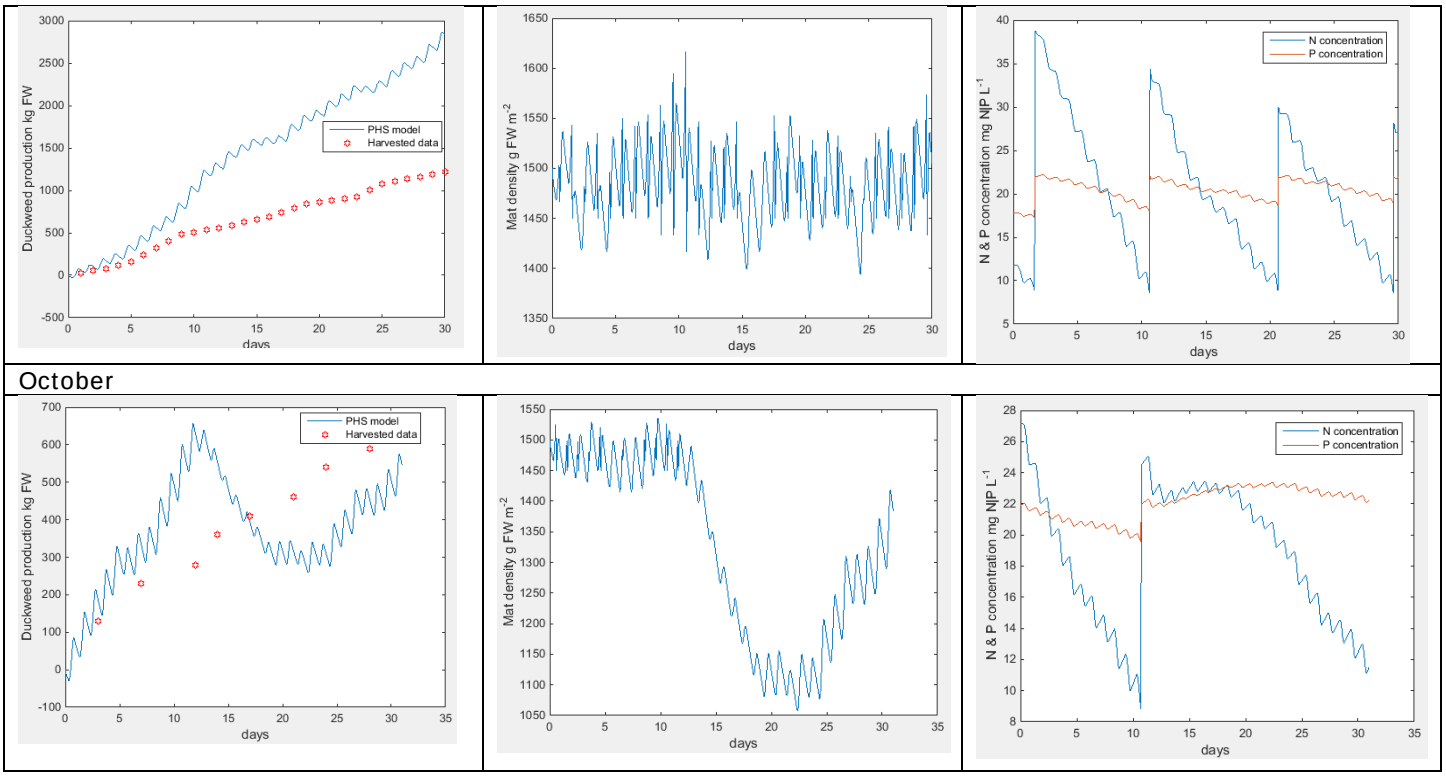

Below the equations are given to determine nutrient correction factor if the model of Landolt (1987) was used.

$$r_n = A_n * \frac{C_n}{K_n + C_p} \qquad [d^{-1}] \qquad 10.26$$

$$r_p = A_p * \frac{C_p}{K_p + C_p} \qquad [d^{-1}] \qquad 10.27$$

$$N_{corr} = \min\left(\frac{e^{r_n}}{e^{r_n max}}, \frac{e^{r_p}}{e^{r_p max}}\right) \qquad [-] \qquad 10.28$$

Table 39. Parameters for determining the nutrient correction factor based on Landolts (1987) research.

A_n	Growth rate factor	0.36	$[d^{-1}]$
C_N	Nitrogen concentration	input	$[mg\ N\ L^{-1}]$
K_N	Constant for inhibition at low C_N	0.95	$[mg\ N\ L^{-1}]$
$r_n max$	Growth rate at optimal N concentration	0.36	$[d^{-1}]$
A_p	Growth rate factor	0.36	$[-]$
C_p	Phosphorus concentration	input	$[mg\ P\ L^{-1}]$
K_P	Constant for inhibition at low C_P	0.31	$[mg\ P\ L^{-1}]$
$r_p max$	Growth rate at optimal P concentration	0.36	$[d^{-1}]$
N_{corr}	Correction factor at limiting concentrations	eq 4.77	$[-]$

10.4 Appendix discussion

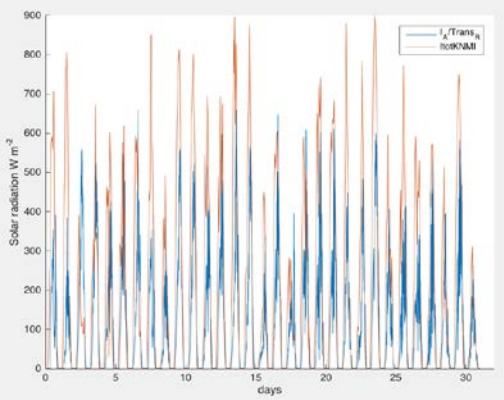

Figure 30. Comparison of measured light intensity at ECOFERM and De Bilt.

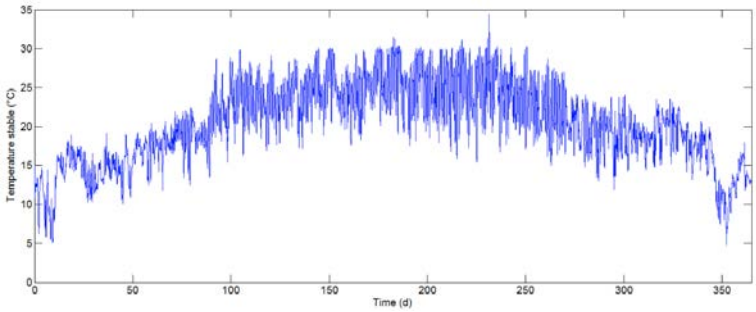

Figure 31. Simulated stable temperature of Van den Top (2014).

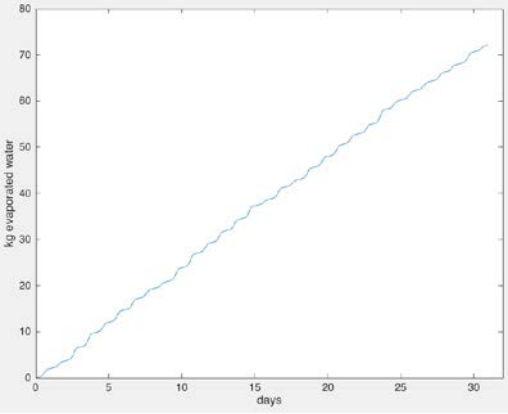

Figure 32. Evaporation in May with VwindG=3.38, RH was constant 77% (2.33 kg water m^{-2}).

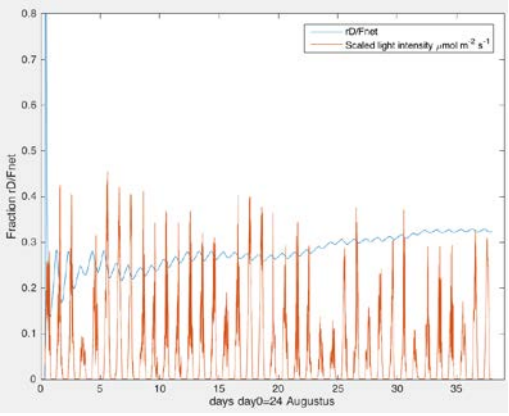

Figure 33. Dark respiration fraction and the influence of the light intensity. At high irradiance, the fraction decreased.

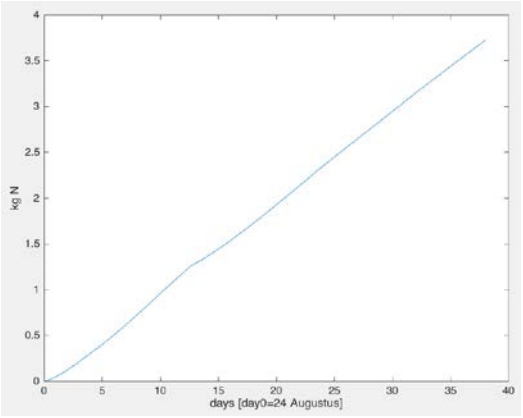

Figure 34. Total kg N obtained from the air.

Calculation mass transfer rate based on literature at a concentration difference of 5 mg L^{-1} NH_3.

$$J = -K\left(C_g - HC_l\right) * \frac{1000}{17.03} * 14$$

K	0.0265	$[m\ s^{-1}]$
C_g	6	$[mg\ NH_3\ L^{-1}]$
C_l	1	$[mg\ NH_3\ L^{-1}]$
H	1.04	$[-]$
J	108.1	$[mg\ N\ m^{-2}\ s^{-1}]$

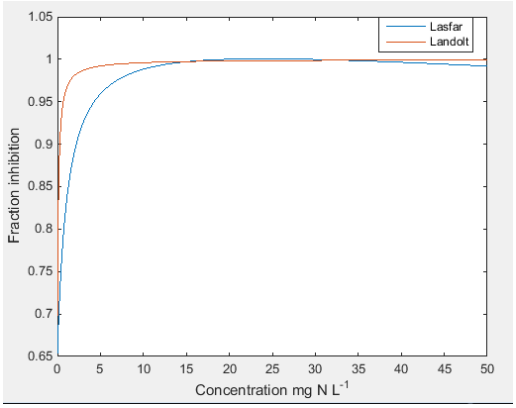

Figure 35. Comparison the correction factor based on Lasfar's or Landolt's model at given N concentration.

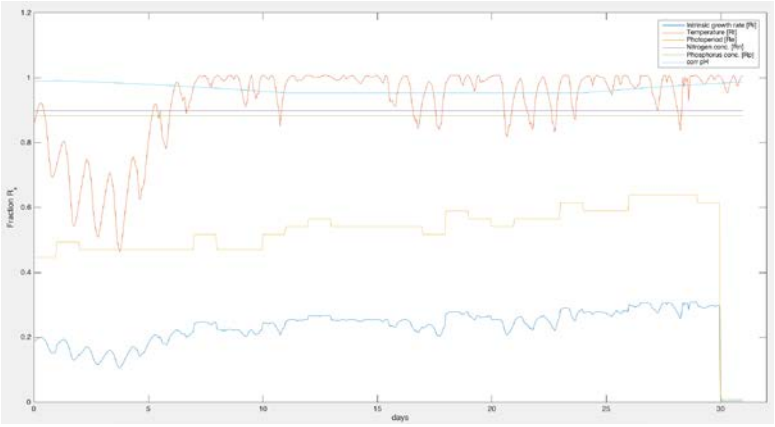

Figure 36. Correction factors of the month July, obviously the photoperiod (yellow) is the most limiting factor for optimal production.

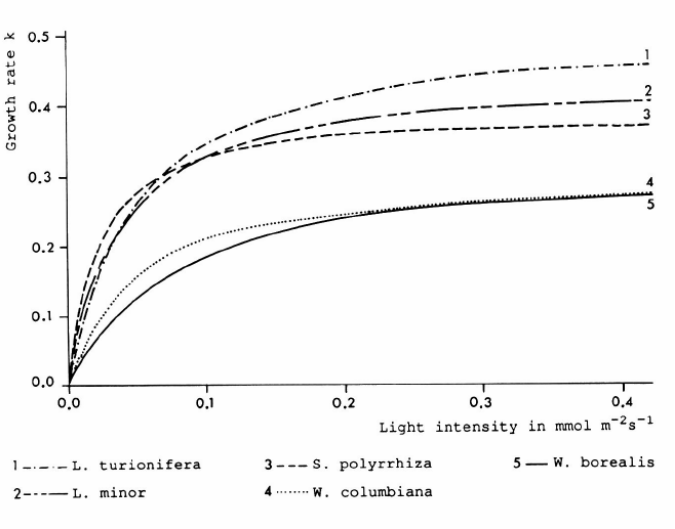

Figure 37. Growth rate as a function of the light intensity, obviously the growth rate is light intensity dependent (Docauer, 1983).